Layered structure of the subducting oceanic plates; implications for the intraplate seismic zones.(Dissertation_全文)

AUTHOR(S):

Ohkura, Takahiro

主論文

Layered structure of the subducting oceanic plates; implications for the intraplate seismic zones.

Takahiro Ohkura

School of Earth Sciences,
Faculty of Integrated Human Studies,
Kyoto University

Abstract

Distinct later phases are frequently observed on seismograms at the seismic stations of Kyoto University, which are located in the Chubu, Kinki, Chugoku districts, for events occurring in subduction zones of the Japan Islands. To investigate origins of such later phases, an analysis of apparent velocity, a three-dimensional ray tracing and a three-dimensional Gaussian Beam method were applied with taking into account three-dimensional structure of the subducting slabs.

First, a conspicuous phase between P and S waves is analyzed, which is frequently observed at the seismic stations in central Honshu on seismograms for events deeper than 50 km that occur on the upper seismic plane of the double seismic zone beneath the northeastern and central Japan arc. The observed phase is dominant in the vertical components of seismograms and has an apparent velocity almost equal to, or slightly larger than, that of the initial P arrivals. The travel time lapse between the first and later arrivals is about 9 seconds. From these features, the phase is interpreted as SP, which was reflected and converted from S to P wave at a boundary inside the subducting oceanic plate. The inferred boundary is located 40km beneath the upper seismic plane. This suggests that the boundary corresponds to a chemical boundary between the upper layer of basalt and harzburgite and an

underlying layer of lherzolite and pyrolite. Our results also suggests that this boundary should be sharp enough to reflect seismic waves. Furthermore, this boundary exists around the lower seismic plane within the double seismic zone. It is possible that the layered structure forms the double seismic zone due to the stress concentration associated with unbending of the upper layer of plate.

Next, a distinct pair of later P and S phases for earthquakes shallower than 60 km occurring in the vicinity of the west Seto Inland Sea are investigated. These later phases are frequently observed at the seismic stations in the Kinki, Chugoku and Shikoku districts. The observed phases are dominant in all three components with an apparent velocity almost equal to the P and S velocity of the lower crust. From these characteristics, the phases are interpreted as waves which travel through the lower crust horizontally near the receivers. These features can be explained if the so-called upper mantle earthquakes take place within a low velocity oceanic crust overlying the high-velocity oceanic plate, and if this oceanic crust is in contact with the continental lower crust between the sources and the receivers. Travel times and synthetic waveforms were calculated using a three-dimensional ray tracing method and a three-dimensional Gaussian-beam method. The calculated travel times and amplitude of the later phases are in good accordance with the observed values. Thus, we can conclude that in the subducting oceanic crust a gabbroic phase remains without transformation to

eclogitic phase to depths of about 60 km. Similar later phases are observed in the Chugoku district from the upper mantle earthquakes beneath the Shikoku district. This suggests that no mantle wedge exists between the overriding continental crust and the subducting oceanic crust beneath Shikoku.

Table of contents

Preface

This thesis is composed of two main parts. In the first part, a relation between velocity structure and the double seismic zone inside the subducting Pacific plate will be discussed. In the second part, structure of the upper part of the Philippine Sea plate subducting beneath southwest Japan will be discussed in connection with its seismic layer.

Beneath the Japan Islands, the Pacific plate and the Philippine Sea plate are being subducted. These two plates cause many earthquakes in Japan. Seismograms of these earthquakes are recorded by the seismic network of Kyoto University which are located in the Kinki, Chugoku and Chubu districts, central and western Japan (Disaster Prevention Research Institute, 1986). The seismic network of Kyoto University is composed of 30 stations with a spatial coverage of 3 and 1.5 degrees, in the E-W and N-S directions, respectively. Since July 1985, waveform data have been stored on digital magnetic tapes at the Disaster Prevention Research Institute. To use waveform data effectively, the author made a computer program which displays waveforms assembled in order of epicentral distance. With this program, the network has a function of a large aperture seismic array and it become easy to find any later phases

on waveforms.

Using this program, two kinds of later phases were detected. One is a conspicuous phase appearing on seismograms for events on the upper seismic plane of the deep seismic zone within the Pacific plate in the Tohoku and Kanto districts, and the other is a distinct pair of later P and S phases for earthquakes shallower than 60 km occurring in the vicinity of the Sea of Iyo (Iyo-Nada) and Bungo channel.

As to the subducting Pacific plate, tomographic studies of travel time yield a higher velocity for the subducting plates than the surrounding mantle (e.g. Hirahara, 1977; Zhao and Hasegawa 1993). The discontinuity between the descending plate and overlying asthenosphere were determined using later arrivals converted at the upper boundary (e.g. Okada, 1971; Matsuzawa et al., 1986; Matsuzawa et al., 1990). However, little is known about the internal structure within the subducting plate, although it is important for the understanding of the processes of its origin and evolution. Furthermore, the internal structure of the plate may effect the cause of the double seismic zone.

In the first part of this thesis, the author intends to show that the conspicuous phase appearing on seismograms for events on the upper seismic plane is the SP wave reflected and converted from S to P at a boundary inside the slab. In addition, we interpret this boundary to coincide with the lower seismic plane of the double seismic zone beneath the Tohoku and Kanto Districts (Hasegawa et al.,1978; Tsumura, 1973).

Regarding to the Philippine Sea plate subducting to southwest Japan, Kimura and Okano (1992), using travel time analysis of the initial P-wave for the upper mantle earthquakes, showed that there is no oceanic crust beneath Shikoku and that the said events occur in the high velocity mantle.

On the other hand, Fukao et al (1983) , Hori et al. (1985) and Hori (1990) concluded that a low-velocity oceanic crust exists at the top of the Philippine Sea plate down to a depth of 60 km in the Kanto, Tokai, and Kinki districts, central and southwest Honshu from an analysis of a clear pair of P and S later arrivals on the seismograms for the upper mantle earthquakes. In and around Shikoku, such an analysis of the later phases as Fukao et al. (1983) was done by Oda et al (1990) but only one station's data was used.

In the second part of this thesis, the author reports that later phases are observed widely in the Kinki, Chugoku, and Shikoku districts on the seismograms of the upper mantle earthquakes in the west Seto Inland Sea. And the author reexamines the presence of the low-velocity oceanic crust taking a three-dimensional configuration of the subducting Philippine Sea plate into account. In addition, the author, by analysis of a later phase, makes it clear that the oceanic crust subducts beneath Shikoku as a part of the Philippine Sea plate and that so-called upper mantle earthquakes beneath Shikoku also occur inside the oceanic crust.

Part 1

The two layered structure of a subducting oceanic plate

1.1 Introduction

It is well known that the Pacific plate subducts beneath the Japan Islands. Tomographic studies of travel time yield a higher velocity for the subducting plate than the surrounding mantle (e.g. Hirahara, 1977; Zhao and Hasegawa, 1993). The discontinuity between the descending plate and the overlying asthenosphere was determined using later arrivals converted at the upper boundary (Okada, 1971; Matsuzawa et al., 1986; Matsuzawa et al., 1990).

However, little is known about the internal structure within the subducting plate, although it is important for understanding the processes of its origin and evolution. In oceanic regions, a two-layered plate model was proposed based on several long-range explosion seismology experiments (Shimamura and Asada, 1976; Shimamura et al., 1983). Travel-time residuals of P and S waves from deep earthquakes nearby were also used to apply geophysical constraints to the lateral heterogeneity of subduction zones. Suyehiro and Sacks (1979) modeled a two-layered structure of the subducting plate based on the spatial distribution of observed and calculated residual data. Iidaka and Mizoue(1991), proposed a two layered slab model with a P-wave velocity of J-B +1.5% for the upper layer and J-B +2.5% for the lower layer using a remarkable high frequency later phase and the distribution of the travel-time residuals.

Recently, seismic stations in Japan have accumulated digitally recorded seismograms. In this paper, we propose that a conspicuous phase appearing on seismograms for events on the upper seismic plane of the deep seismic zone in the Tohoku (Northeastern Honshu) and Kanto (Central Honshu) districts is the SP wave reflected and converted from S to P at a boundary inside the slab. In addition, we interpret that this boundary coincides with the lower seismic plane of the double seismic zone beneath the Tohoku and Kanto districts (Hasegawa et al.,1978; Tsumura, 1973).

1. 2 Later phases

Beneath the Japan Islands, many earthquakes occur along the interface of the subducting Pacific Plate (Fig. 1-1). Seismograms of these earthquakes are recorded by seismic networks of Kyoto University which are located in the Kinki, Chugoku and Chubu districts, central and western Japan (Disaster Prevention Research Institute, 1986). The seismic network of Kyoto University is composed of 30 stations with a spatial coverage of 3 and 1.5 degrees, in the E-W and N-S directions, respectively (Fig. 1-1). These stations are equipped with 1-s high-sensitivity velocity seismometers. Since July 1985, waveform data have been stored on digital magnetic tapes at the Disaster Prevention

Research Institute (DPRI) with a sampling rate of 100 points/sec. We analyzed seismograms of about 400 earthquakes from the area between 34.5°N to 42°N latitudes, located approximately 300~1000 km away from the network. These earthquakes occurred at depths shallower than 200 km and were recorded from July 1985, when the digital recording system was completed at DPRI, through December 1988. In Fig. 1-2, epicentral distribution of events used in this study is shown.

In our analysis, we used precise hypocenter data obtained by the Observation Center for Prediction of Earthquakes and Volcanic Eruptions of Tohoku University and the Natural Research Institute for Earth Science and Disaster Prevention (NIED). Both institutes have dense seismic networks using highly sensitive seismometers covering the Tohoku and Kanto districts (Hasegawa et al., 1983 : Ishida, 1984). The high precision of these data enabled us to check whether the hypocenters are located on the upper or the lower seismic plane of the subducting slab.

Fig. 1-3 is an example of seismograms for an intermediate-depth earthquake located in the upper seismic plane of the double seismic zone off the Kanto district. In these seismograms, a clear phase is seen after the initial P wave arrival. This type of later phase is observed in seismic events located in the Kanto to Tohoku district, 300~1000 km away from the networks (Fig. 1-4). The observed phase, hereafter referred to as the X phase, is dominant in the vertical components. Its apparent velocity is

almost equal to or slightly larger than that of the initial P phase. Fig. 1-5 is another example of seismograms with the X phase for an event located in the upper seismic plane of the double seismic zone beneath the Tohoku district. The X phase is observed for earthquakes occurring at depths of 50 to 200 km, located in the upper seismic plane. Fig. 1-6 shows particle motions of the P and X phases observed at the AZJ station located in the Chubu district. This figure shows that the direction of wave approach of the X phase is approximately the same as that of the P phase. Fig. 1-7 shows the relation between the focal depth and travel time difference between the P and later phases. This figure shows that the travel time difference is almost constant (8~10 seconds) and is independent of focal depth. These observations show that the origin of the later phase exists near the sources. Possible interpretations for this phase are as follows, (Fig. 1-8)

(a) P-reflected P at a boundary below the source,

(b) S-converted P at a boundary above the source,

(c) S-reflected P at the surface of the earth,

(d) S-reflected and converted P at a boundary below the source.

If the X phase is the P-to-P reflected phase at a boundary below the source (case (a), Fig. 1-8a), its apparent velocity is expected to be much larger than that of the initial P phase. However, our observations suggest otherwise. Thus, we exclude this phase (Fig. 1-8a) as a possible candidate for the X phase.

We can also exclude the S-to-P phase (case (b), Fig. 1-8b) refracted and converted at the upper boundary of the descending oceanic plate (UBP) found by Matsuzawa et al. (1990) based on the following arguments. In the Tohoku region, the upper boundary of the subducting plate is located just, within 10 km, above the upper seismic plane (Matsuzawa et al.1986). Hence, the observed X-P delays of 8-10 s are too long for the S-to-P phase which is converted at UBP from an intermediate-depth earthquake occurring on the upper seismic plane. Fig. 1-9 is an example of waveforms from such an intermediate-depth event occurring on the lower seismic plane. On these seismograms, clear arrivals are seen 6-8 s after the initial P phase. Furthermore, we note that the apparent velocity of this phase is lower than that of the initial P phase. Therefore, it can be interpreted as an S-to-P phase refracted and converted at UBP, and is different from the X phase observed in this study.

Umino et al. (1995) identified an sP phase from nearby earthquakes off northern Tohoku which is reflected and converted at the ocean bottom (case (c), Fig. 1-8c), with a delay time of 11-21 s after the P phase. Such events are mostly shallower than 40 km and located near the Japan trench. Fig. 1-10 is an example of this depth phase recorded at our DPRI network. However, the X phase can be observed on seismograms for events at depths down to 200 km, much deeper than those studied by Umino et al. (1995). This fact rejects the hypothesis that

the X phase is a depth phase like sP or pP (Fig. 1-8c) in that the delay time of the depth phase varies widely over a range of 10 s depending on hypocentral depths. As shown in Fig. 1-7, the X phase's delay time is almost uniform (8-10 s) throughout the events. We thus conclude that the X phase is not a depth phase like the sP or pP. We interpret the X phase as an SP phase, reflected and converted from S to P wave at a boundary below the sources as shown in Fig. 1-8d.

1.3 Ray tracing

To determine the location of the discontinuity beneath the sources, a three-dimensional ray tracing method was applied. We first constructed a three-dimensional velocity model for this method. The configuration of the upper boundary of the Pacific plate is determined from the distribution of deep earthquakes (Yoshii, 1979). The lower boundary of the slab is set to be 110 km below its upper boundary (Fig. 1-11). Since the dip angle of the slab is almost 30° beneath the Tohoku district (Hasegawa et al., 1978), its thickness is estimated to be about 100 km. This thickness is based on the thickness of high velocity zone obtained by Hirahara (1977). We also assumed the velocity discontinuity inside the slab. To determine its location, we constructed some models varying the location of the discontinuity. First, we assumed the velocity

discontinuity to be located 40 km below UBP. For the seismic velocities of the slab, we assigned the seismic velocity to the upper layer above the discontinuity and the lower layer below it to be 2% and 8% higher than the J-B model, respectively, where the J-B is the seismic velocity model by Jeffreys and Bullen (1940).

We also assigned a velocity 2% lower than the J-B to the overlying asthenosphere. The interface boundaries and the velocity structure were determined with interpolation of the cubic spline function. The Q_p values (P-wave attenuation) of the subducting Pacific plate, the mantle wedge and crust were assumed to be 2000, 400, and 1000, respectively, after Sacks and Okada (1974). The ratio of Q_p to Q_s was assumed to be 2.25 (Knopoff,1964). The density (ρ) was assumed using the following formula (Birch, 1961): $Vp = -1.87+3.05\rho(g/cm^3)$ when mean atomic weight is equal to 21. The Philippine Sea plate is neglected in this model because of its thin width.

In the model mentioned above, we calculated the theoretical waveforms by means of a program using three-dimensional Gaussian-beam method (Cerveny, 1985; Sekiguchi, 1992). In the first step, travel times were calculated for shooting points A, B, and C (Fig. 1-12). These points were selected to locate at even intervals in studied area from the northern end to the southern end. Matsuzawa et al. (1986) showed that UBP is located just above the upper seismic plane of the double seismic

zone. Therefore, the shooting points are located 5-10 km below UBP. The results of these calculations are shown in Fig. 1-13. The calculated travel time differences between initial P and later arrivals all fall around 8 seconds, but these values are somewhat smaller than the observed values of 10 s. Therefore, it can be concluded that the actual interface is located deeper than the initial assumption. In the next step, we assumed that the velocity discontinuity is located 50 km below UBP.

With the model above, we calculated synthetic waveforms for points B and C. Figs. 1-14 and 1-15 show the calculated waveforms for cases B and C, respectively. The assumed radiation patterns of each sources are also shown in Figs. 1-14 and 1-15, respectively. A thrust type and a down-dip compression type of mechanism were selected, respectively, which are typical mechanisms at their depth. Travel time differences between initial P and later arrivals fall around 10 seconds. These results show that the interface is considered to be located 40~50 km bellow UBP, equivalent to 30~40 km below the upper plane of the double seismic zone.

However, Fig. 1-14 clearly shows that the calculated amplitudes of the later arrivals are much smaller than those observed. Fig. 1-15 shows the synthetic waveforms for case C. The synthetic amplitudes are much smaller than the observed amplitudes. Fig. 1-16 shows that the results of a calculation for an extreme case where the velocity of the lower layer is 12 % higher than that of the J-B model. These results

indicate that the velocity contrast of 10 % between the upper and lower layers is still insufficient to generate the amplitudes comparable to those observed.

1.4 Discussion

The results of our calculations clearly show that the Gaussian Beam method leads to a small S-to-P wave amplitudes even assuming a 10 % velocity contrast between the upper and lower layers of the slab. In order to explain the large amplitude of the observed X phase, we need a much larger velocity contrast between the two layers. However, such high velocity contrasts have been found neither in the interiors of the subducting Pacific plate by inversion of travel time (e.g. Hirahara,1977, Zhao and Hasegawa 1993), nor in the oceanic plates by long-range refraction surveys (Shimamura and Asada, 1976; Shimamura et al., 1983). As shown in Fig. 1-4, the X phase is found in only 10 % of the earthquakes analyzed in this study. This suggests that the X phase is not always generated with an observable amplitude from events on the upper seismic plane. Therefore, a large velocity contrast is not necessary over the interface. Thus, the observed large amplitude of the X phase could be due to other conditions, which are described below.

First, we examined the effect of the radiation pattern of the event. We calculated waveforms for case B by slightly changing the

radiation pattern. As shown in Fig. 1-17, amplitudes of the later arrivals for this radiation pattern are significantly larger than those in the previous calculations. It is highly possible that the radiation patterns of the events are major factor in making the amplitude of the X phase large enough to be observable.

Next, we examined the effect of inhomogeneity of the interface to the amplitude of later arrivals. For this purpose, we considered an interface inside the slab with a sine curve undulation (Fig. 1-18). At first, we assumed an undulation with a wavelength of 200 km. Fig. 1-19 shows the results when the peak to trough distance is 6 km. The shooting point of ray-tracing is located above the trough of the undulation. The waveform was calculated for case B and the same radiation pattern for Fig. 1-12 was used. As shown in Fig. 1-19, the amplitudes of the later arrivals are about five times of that in the model with a flat interface due to the focusing effect of rays. Therefore, if some kind of inhomogeneity exists at the slab interfaces, the focusing effect of the rays may make the amplitude of the X phase large enough to be observed, although the change of the radiation pattern seems to more effective.

Our study shows that the thickness of the upper layer is about 35~45 km and its interface exists at depths of 50~150 km. On the other hand, Iidaka and Mizoue (1991) proposed a two layered slab model with an upper layer thickness of 30 km. In their study, a remarkably high frequency later phase and distribution of the travel-time residuals from

earthquakes deeper than 300 km were used. And the interface which they found exists in the depth range of 250~400 km. It is possible that both interfaces are the same and that a velocity discontinuity exists in the depth ranges 50~400 km in the subducting Pacific plate. The thickness of the upper layer obtained in this study is almost equal to that obtained by oceanic long-range explosion seismological experiments (Shimamura and Asada, 1976; Shimamura et al., 1983). Ringwood (1982) suggested that the oceanic lithosphere has a chemically and petrologically zoned structure: the upper layers of basalt and harzburgite, about 36 km thick in total, underlain by the lower layers of lherzolite and pyrolite. The thickness is almost equal to the upper layers which we estimated in this study. However, in this structure, velocity difference between basalt layer and harzburgite layer is large, thickness of basalt layer is too thin to yield travel time lapse between the initial P and the X phases. Irifune and Ringwood (1993) showed that density difference between harzburgite and pyrolite is 0.05 - 0.08 g/cm^3 in the depth range of 220 km - 350 km. Adapting Birch's law, this value corresponds to a 2 - 5 % of velocity difference. The density and velocity differences could account for the boundary which generates the X phase. Therefore, it is highly possible that the boundary we found is a chemical boundary proposed by Ringwood (1982). Furthermore, our results show that this boundary is sharp enough to reflect high frequency seismic waves. The boundary of chemical zonation is formed by melting and

differentiation at mid-oceanic ridges (Ringwood, 1982). However, Ringwood (1991) showed that the thickness of the upper layer is 12 - 27 km, which is a little thinner than the value we obtained in this study. Further chemical and petrological studies are required to determine the accurate thickness of the upper layer and to check the sharpness of the boundary.

In this study, we found a velocity discontinuity within the subducting Pacific plate. This discontinuity is located 40~50 km below the UBP. On the other hand, the double-planed structure of the deep seismic zone has been observed in the depth range 70~150 km beneath Japan Arc (Tsumura, 1973; Hasegawa et al., 1978; Suzuki et al., 1983; Ishida, 1984). The planes are almost parallel and 30~40 km apart. Since the upper plane is just below the UBP (Matsuzawa et al., 1990), our results show that the depth of a velocity discontinuity is almost equal to, or slightly deeper than, that of the lower seismic plane. The cause of the double seismic zone has been discussed by many researchers: stresses associated with phase changes (Veith, 1974; Kao and Liu, 1995), unbending of the slabs (e.g. Engdhal and Scholtz, 1977; Tsukahara, 1980; Kawakatsu, 1986), sagging of the plate (Sleep, 1979), and thermo-elastic stresses (Hamaguchi et al. ,1983). Nevertheless, a chemical discontinuity has not been taken into account for the mechanisms of the double seismic zone. Ringwood (1982) discussed that the chemical zonation may correspond to the mechanical zonation. Suzuki and Kasahara (1996)

analyzed focal mechanisms of large events in the lower seismic zone and concluded that the descending slab consists of two layers, a seismic, brittle upper layer and an aseismic, ductile lower layer. Our results show that this boundary is also reflective and that the chemical zonation and the mechanical zonation coincide. We conclude that this structure forms the double seismic zone due to the stress concentration at the discontinuity associated with unbending of the upper layer of plate (Fig. 1-20).

1.5 Concluding remarks of part 1

In the Kinki, Chugoku and Chubu districts, central and western Japan, a conspicuous phase is frequently observed between P and S waves in seismograms. These events occur on the upper seismic plane of the double seismic zones beneath the Tohoku and Kanto districts. This phase is interpreted as an SP wave, reflected and converted from S to P wave at a boundary located 40~50 km below the upper boundary of the subducting plate. This indicates that the subducting Pacific plate has a layered structure with an upper layer with a thickness of about 40 km. This structure corresponds to the chemical zonation formed at the mid oceanic ridge as proposed by Ringwood (1982). Our results show that the interface is sharp enough to reflect high frequency seismic waves.

Furthermore, this velocity discontinuity is located just below the lower seismic plane of the double seismic zone in the region, suggesting that the chemical zonation and mechanical zonation coincide with each other.

Part 2

Structure of the upper part of the Philippine Sea plate estimated by later phases of the upper mantle earthquakes in and around Shikoku, Japan

2.1 Introduction

Upper mantle earthquakes deeper than 30 km take place in the vicinity of Iyo-Nada (the Sea of Iyo) and the Bungo channel in southwest Japan (Fig. 2-1). In this region and to the south of it, seismic activity suggests the existence of a plane dipping WNW (e.g. Miura et al., 1991). This activity is considered to occur in association with the subduction of the Philippine Sea plate. On the other hand, beneath Shikoku island, there is another seismic zone dipping to N22°W (Okano et al., 1985). The general trend of isodepth contours of the upper mantle earthquakes changes its strike near the west Seto Inland Sea (See Fig. 2-2).

Shiono (1974), by using travel time analysis, indicated the presence of a high velocity Philippine Sea plate beneath Shikoku. Nakanishi (1980), employing ScSp phases, found a dipping discontinuity in the upper mantle beneath Shikoku and identified it as the upper boundary of the Philippine Sea plate. Hirahara (1981), by applying three-dimensional inversion of travel time data, found a high-velocity zone corresponding to the subduction of the Philippine Sea plate beneath the Shikoku and Kyushu islands. The Philippine Sea plate is considered to exist continuously beneath Shikoku and Kyushu and to be convexed beneath the western part of Shikoku (e.g. Shiono and Mikumo, 1975; Imagawa et al., 1985).

Oda et al. (1990) found a clear pair of P and S later arrivals on

the seismograms of the upper mantle earthquakes in the west Seto Inland Sea recorded at a station in the Chugoku district. The apparent velocities of these phases are significantly lower than those of the initial P and S arrivals. They interpreted these phases as guided waves traveling through a low-velocity oceanic crust overlying the high-velocity Philippine Sea plate. These later phases are similar to those observed for the upper mantle earthquakes in the Kinki and Tokai districts (Fukao et al., 1983; Hori et al., 1985). Based on these observations, Hori (1990) concluded that a low-velocity oceanic crust exists down to a depth of 60 km along the entire subduction zone on the northern boundary of the Philippine Sea plate.

However, Kimura and Okano (1992), using travel time analysis of the initial P-waves, showed that there is no oceanic crust beneath Shikoku and that these events occur in the high velocity mantle. In addition, Shiono (1974) reported that a later phase is observed in Shikoku with a higher apparent velocity than that reported by Oda et al. (1990) and concluded that the earthquakes occurred just above the interface between the continental and the oceanic plates. These two studies indicate that the structure beneath Shikoku is somewhat different from surrounding areas.

In the present study, we report that later phases are observed on the seismograms widely throughout the Kinki, Chugoku, and Shikoku districts for upper mantle earthquakes in the west Seto Inland Sea. And

we reexamine the presence of the low-velocity oceanic crust by a three-dimensional ray tracing method and a three-dimensional Gaussian beam method. In the calculations we take a three-dimensional configuration of the subducting Philippine Sea plate into account, whereas Oda et al. (1990) adopted a two-dimensional ray tracing method for the calculation of travel times of the initial and later phases. In addition, we reveal that the oceanic crust subducts beneath Shikoku as a part of the Philippine Sea plate and that the so-called upper mantle earthquakes occur inside the oceanic crust by analysis of a later phase from those earthquakes.

2.2 Later phases

2.2.1 Later phases observed at stations in the Chugoku district for events beneath the west Seto inland sea

In this section, we investigate seismograms of 30 upper mantle earthquakes occurring beneath the west Seto Inland Sea from August 1983 through March, 1988. Fig. 2-2 shows the distribution of epicenters for the earthquakes used in this study. We used precise hypocentral data obtained by the Shiraki Microearthquake Observatory, University of Tokyo (Table 1). This observatory has seismic stations around the studied area (Asano et al., 1986).

We analyzed seismograms at 10 stations of the Tottori

Microearthquake Observatory (TMO) of Kyoto University (Fig. 2-2). These stations are equipped with 3-component seismometers. QMT and TRT stations, are equipped with velocity-sensitive seismometers with a natural frequency of 0.1 Hz. All other stations are equipped with velocity-sensitive seismometers with a natural frequency of 1 Hz. All waveform data since July 1985 are stored on digital magnetic tapes at a rate of 100 samples per second. Before then, waveform data were stored on analog magnetic tapes. We digitized these analog data at a rate of 200 samples per second.

Prominent later phases are observed in the seismograms at the stations of TMO from the upper mantle earthquakes occurring beneath the west Seto Inland Sea. Fig. 2-3 is an example of the seismograms of the later phases. The depth of this earthquake is 41 km. A pair of P and S later phases (hereafter referred to as Xp and Xs, respectively), are obvious in these seismograms. The Xp and Xs have larger amplitudes than the initial phases on all three components. The initial P is very small and the initial S wave is often too small to be observed. Fig. 2-4 shows seismograms assembled in order of their epicentral distance for the same earthquake in Fig. 2-3. The initial P phase has an apparent velocity of 7.8 km/s. The Xp and Xs have velocities of 6.7 km/s and 3.8 km/s, respectively.

However, in the seismograms for events deeper than 60 km, the later phase is not observed. An example of such seismograms is shown in

Fig. 2-5 for an earthquake at a depth of 74 km. The initial P and S from the deep events have clear onsets unlike those from shallower events. The apparent velocities of P and S phases are 8.0 km/s and 4.7 km/s, respectively. The later phases can be observed for 20 earthquakes out of the 30 which we investigated. All of these earthquakes are shallower than 60 km. The later phases are not observed for 10 earthquakes. Many of these earthquakes occurred a depths below 60 km. The later phases are not observed only for 2 earthquake which occurred shallower than 60 km, as shown in Fig. 2-6.

Fig. 2-7 is a plot of composite travel times of the initial and later phases. Apparent velocities for each event were obtained by least squares fitting to the arrival time. We obtained 8.0 km/s and 4.7 km/s as the average velocities of the initial P and S phases, and 6.8 km/s and 4.0 km/s as the average velocities of the the Xp and Xs. These values are almost equal to the P and S wave velocities for the continental lower crust. For the earthquakes whose later phases are not observable, the apparent velocities of P and S waves are 8.2 km/s and 4.7 km/s, respectively.

Oda et al. (1990) found a clear pair of P and S later phases in the seismograms of upper mantle earthquakes in the west Seto Inland Sea. The apparent velocities of the Xp and Xs are almost the same as these single-station apparent velocities shown in Oda et al. (1990). They interpreted that these phases as guided by an oceanic crust overlying the high-velocity Philippine Sea plate as shown in Fig. 2-8a.

According to Hori et al. (1985), it is possible to interpret these later phases as waves which traveled through a step-like structure shown in Fig. 2-8b. In this case, station-common apparent velocity should be equal to the velocity of the mantle, but not of the lower crust. It can be seen from Fig. 2-7 that the travel times of the Xp and Xs are aligned. This indicates both event-common and station-common apparent velocities are almost equal to the seismic velocity for the lower crust. Therefore, we can exclude the model shown in Fig. 2-8b.

If the Moho discontinuity is as deep as 60 km and earthquakes take place in the lower crust (Fig. 2-8c), we would be able to observe the Pg and Sg with the same apparent velocities as the Xp and Xs. Also their station-common and event-common apparent velocities should be the same. However, refraction experiments using explosion-source conducted in southwest Japan (e.g. Ito et al., 1982) have revealed that the Moho discontinuity is much shallower than 60 km. Therefore we can reject the model with a thick crust.

An S to P converted phase at the Moho discontinuity is a candidate for the later arrivals of P (Fig. 2-8d) . However, the later arrivals of S can not be generated by this model. Therefore, we can also exclude this model as an explanation of the Xp and Xs.

Therefore, the Xp and Xs are considered to be guided waves through an oceanic crust overlying the high-velocity Philippine Sea plate and that earthquakes take place in the oceanic crust as shown in Fukao

et al. (1983), Hori et al. (1985), Oda et al. (1990), and Hori (1990).

2.2.2 Later phases observed at the stations in Shikoku for the events beneath the west Seto inland sea

In this section, we investigate seismograms of 25 earthquakes beneath the west Seto Inland Sea. These were all included in section 2.2.1. We analyzed seismograms recorded at the Kochi Earthquake Observatory (KEO) of Kochi University. The station distribution of KEO is shown in Fig. 2-2. These stations are also equipped with velocity seismometers with a natural frequency of 1 Hz. Waveform data were originally stored on analog magnetic tapes, and were digitized at a rate of 100 samples per second.

Fig. 2-9 is an example of three component seismograms for an upper mantle earthquake recorded at the stations of KEO. In these seismograms, clear phases are observed after the P and S arrivals.

The later phases are observed for 20 earthquakes with a depth shallower than 60 km at KEO. However, the later phases were not observed for two earthquakes with depths shallower than 60 km at TMO. The later phases were not observed for the remaining 5 earthquakes neither at KEO nor at TMO. These earthquakes occurred at depths below 60 km (Fig. 2-10).

Fig. 2-11 is a plot of composite travel times of the initial and later phases. The apparent velocities for each event were obtained by least squares fitting to the arrival time data. For the average apparent velocities of the initial P and S phases, we obtained a value of 8.1 km/s and 4.9 km/s, respectively. The apparent velocities of the Xp and the Xs were 6.7 km/s and 3.7 km/s, respectively. These values are almost the same as the apparent velocities of later phases observed in TMO networks shown in the previous section. Therefore, the later phases are thought to be waves which traveled through the oceanic crust and then through the continental crust. This indicates that the oceanic and the continental crust are in contact between the sources and the observation network, that is in the western part of the Shikoku island.

2.2.3 Later phases observed in the Chugoku districts for the events beneath Shikoku

To examine the location of the upper mantle earthquakes beneath Shikoku island, we investigated seismograms of 26 earthquakes. These earthquakes occurred beneath Shikoku island from August 1983 through December 1988, and are claimed to be upper mantle earthquakes (Kimura and Okano, 1991). We used precise hypocentral data obtained by KEO (Table 2). We analyzed seismograms recorded at

TMO and DPRI of Kyoto University.

Fig. 2-12 is an example of seismograms recorded at the stations of TMO for an earthquake located beneath Shikoku island with a depth of 32 km. In these seismograms, we can clearly identify a pair of P and S later arrivals. The amplitudes of the initial S phases are extremely small and it is very difficult to detect the onset. We can see that the Xp and Xs phases have apparent velocities of 6.8 and 4.0 km/s, respectively. These values are almost the same as those of the later phases mentioned in the previous section. Fig. 2-13 shows the epicentral distribution of events associated with the later phases. Fig. 2-14 are seismograms recorded at the same stations for an earthquake occurring in the continental upper crust with a depth of 12.4 km beneath Shikoku. We can also find a later arrival of S phase in these seismograms. However, we note that the apparent velocity of the later arrival is about 3.5 km/s. This value is almost the same as the seismic velocity for the continental upper crust and is significantly lower than that of the later phase from the upper mantle earthquakes. Because this event occurred in the continental upper crust, the apparent velocity of the later phase is almost equal to the seismic velocity for the continental upper crust. The velocities of the Xp and Xs are also considered to represent the seismic velocities of the region where this earthquake took place. Therefore, we can conclude that these earthquakes occurred not in the mantle but in the continental lower crust or in the oceanic crust.

2.3 Ray tracing

2.3.1 Cases from the west Seto inland sea to the Chugoku district

In this section, we calculate synthetic seismograms in order to obtain a structure that can account for the observed travel times and apparent velocities of the initial and later phases. Hori et al. (1985) and Oda et al. (1990) explained travel times of the initial and later phases using a two-dimensional ray tracing method. However, in this study, we use a three-dimensional ray tracing method because the Xp and Xs are observed widely in the Chugoku and Kinki districts where the Philippine Sea plate is believed to be a convex structure beneath the west Seto Inland Sea.

In constructing the model for the three-dimensional ray tracing, we must take into consideration the shape of the Philippine Sea plate. The upper boundary of the upper mantle earthquakes in the studied area were obtained by Miura et al. (1991), Okano et al. (1985), and Mizoue et al. (1983). We defined the shape of Philippine Sea plate by connecting these contours smoothly (Fig. 2-15a). Broken lines indicate imaginary isodepth lines. Although no earthquake occurs at these depths, these isodepth lines are necessary for our computer program of the three-dimensional ray tracing. In practice, these assumptions have no effect on the ray paths from source to the stations of TMO or KEO. As stated in

the previous section, the upper mantle earthquakes take place in the oceanic crust. Therefore, we assume that the upper boundary of the oceanic crust is 2 km above the isodepth line of the seismic zone, ant that the lower boundary of the oceanic crust is located 10 km below the upper boundary. This means that the oceanic crust has a thickness of 8.7 km where the Philippine Sea plate subducts with a dip angle of 30°. It is also assumed that the Philippine Sea plate has an infinite thickness. This assumption has no effect on the ray paths from focal region to the stations of TMO or KEO.

In Fig. 2-15b, the P wave velocity of crust and mantle used in the calculations are also shown. The continental crust consists of the surface layer, the upper crust, and the lower crust. The Moho discontinuity is 38 km deep. This structure is based on Hashizume et al. (1966) and is considered to represent the average structure in the Chugoku district. In this model, the oceanic crust overlies the lower crust between the sources and TMO stations, as shown in Fig. 2-15c. It is assumed that the mantle has the same velocity as the J-B model, the P wave velocity in the plate is 4 % higher than the J-B model, and that the oceanic crust has the same velocity as the lower crust. Throughout all the layers, Vp/Vs is assumed to be 1.73. Q values are listed in Table 3. Density (ρ) of each layer is given by the following formula: $Vp=-1.87 + 3.05\rho(g/cm^3)$ (Birch, 1961). We made ray tracing according to this model.

At first, we made ray tracing simulations with assuming that the hypocenter is located at A in Fig. 2-15a with a depth of 45 km. This source is located in the oceanic crust. After the ray tracing, it appeared that the initial phase is the wave that is emitted downward and traveled horizontally in the plate. It can be explained that the later phase is the wave that travels into the continental lower crust from the oceanic crust. The later phase travels directly or reflects once at the upper or lower boundary of the oceanic crust. Fig. 2-15c is a schematic illustration of ray paths of the initial and the later phases. Fig. 2-16 shows the calculated travel times of the initial and later phases which arrive in the Tottori region. Observed travel times for events with a depth of 40~50km are also plotted in this figure. It can be seen from this figure that the calculated travel times have good accordance with the observed travel times.

Next, we calculated the synthetic waveforms by the Gaussian-beam method (Cerveny, 1985; Sekiguchi, 1992). In this calculation, a normal type of mechanism was selected, which have a T-axis parallel to a direction of T-axes in this region shown in Shiono (1977). The result is shown in Fig. 2-17 with an assumed radiation pattern. This figure shows that the later phase has a larger amplitude than the initial phase, which agrees well with observation. We calculated synthetic waveforms assuming another radiation pattern, and the result is shown in Fig. 2-18. This figure also shows that the later phase has a larger amplitude than

the initial phase.

In the next step, we made ray tracing for the hypocenter at B (Fig. 2-15a) with a depth of 54 km, which is also located in the oceanic crust. Fig. 2-19 shows synthetic waveforms at the stations of TMO calculated by means of Gaussian-beam method. An assumed radiation pattern in this figure is the same pattern as that in Fig. 2-17. Obviously, for P and S waves, the later phases have a larger amplitude than that of the initial phases at all stations. We also calculated the synthetic waveforms assuming another radiation pattern, and the result is shown in Fig. 2-20. The later phase has a larger amplitude than that of the initial phase at most stations. These also show good agreement with observation.

2.3.2 Cases from the west Seto inland sea to Shikoku

In order to explain travel times of the initial and later arrivals P and S waves, a three-dimensional ray tracing method was applied. The configuration of the Philippine Sea Plate is the same as that used in the previous section and the oceanic crust has the same thickness as that in the previous model. However, to the velocity of the mantle and the crust in and around Shikoku, we adopted OKM model according to Okano et al. (1986). This model was obtained by an travel time analysis of the initial P

phase from the events in the Chugoku district. In this model, no distinct velocity discontinuity exists between the upper and the lower crust as shown in Fig. 2-21a.

In the first step, we made ray tracing simulation in the case of A. The source is at a depth of 45 km and exists in the oceanic crust. It can be explained that the later phase is the wave that travels in the oceanic crust and in the lower crust and passes through the contact interface between these two crusts. A schematic cross section between the focal region and the stations is shown in Fig. 2-21b. Calculated travel times of the initial and later phases are shown in Fig. 2-22. Observed travel times from all the events with a depth of 40~50km are also plotted in this figure. It can be seen from fig. 2-22 that the calculated travel times have good accordance with the observed travel times. Next, in this model, we make ray tracing simulation for hypocenter located at B (Fig. 2-15a) with a depth of 54 km. This source is also located in the oceanic crust. It can be seen from Fig. 2-23 that calculated and observed travel times have good accordance. This result shows that with oceanic crust beneath Shikoku the travel times of the initial and the later arrivals can be explained.

2.4 Discussion

In the previous sections, we constructed a quantitative three-dimensional model that accounts for the observed travel times and

amplitude of the initial and the later phases. A low velocity oceanic crust lies at the top of the subducting Philippine Sea plate beneath the west Seto Inland sea. Almost all upper mantle earthquakes shallower than 60 km take place in the oceanic crust. The oceanic crust is in contact with the continental lower crust beneath the western part of Shikoku. The later phases travel in the oceanic and continental lower crust along the contact interface between these two crusts.

We examine the earthquakes whose later phases were not observed at the stations of TMO. Among the 30 earthquakes in the present study, 10 earthquakes did not display later phases at the stations of TMO. Among the 10 earthquakes, 2 events (Eq.9 and Eq.20 in Fig. 2-24) are shallower than 60 km and the later phases were observed at the stations of KEO. Because there is no lower crust in contact with the oceanic crust between the northern part of Iyo-Nada and the Tottori region, the later phases of these earthquakes are not observed in Tottori region. In particular, Eq.9 took place in the northern part of the focal region. From this area to the Tottori region, the focal depths become deeper. Therefore, the oceanic crust is in contact with the mantle, and not with the continental crust (Fig. 2-25a). This is thought to be the reason why later phases are not observed in Tottori region for these earthquakes. However, from this point to the Kochi region, the focal depths become shallower. It is possible that the waves travel in the oceanic crust and the lower crust and appear as later phases in the

Kochi region because the oceanic crust is in contact with the lower crust beneath the western part of Shikoku (Fig. 2-25b).

The later phases are not observed in either Tottori or Kochi region for earthquakes deeper than 60 km. This depth is the same as the value reported in Hori et al. (1985). There are two alternative explanations for the absence of the later phases for earthquakes deeper than 60 km. First, basalt may transform into eclogite at a depth of 60 km so that the subducting oceanic crust would not be a low-velocity zone at greater depths. Second, although the untransformed oceanic crust may extend further down below 60 km, earthquakes at greater depths occur outside of it. However, no distinct discontinuity in distribution of hypocenters can be seen in the profile which was shown in Miura et al. (1991), it is unlikely that earthquakes deeper than 60 km occur outside of the oceanic crust. Furthermore, Hurukawa and Imoto (1992), employing focal mechanism data, concluded that the basalt/eclogite transition takes place at depths shallower than 50 km in the Philippine Sea plate beneath the Kanto district, central Japan. Hurukawa and Imoto (1993) found a non double-couple earthquake with a depth of 57 km in the subducting oceanic crust overlying the Philippine Sea plate. They concluded that this event was probably caused by sudden basalt/eclogite transformation. These results also suggest that the subducting oceanic crust would not be a low-velocity zone at depths greater than 60 km. However, from our analysis of the later phases, we can conclude that the oceanic crust

descending into the mantle remains basaltic at least down to the depth of 60 km. As mentioned before, this depth agrees well with the depth reported in Hori (1990). This depth is characteristic for the Philippine Sea plate subducting in Southwest Japan.

Shiono (1974) reported that the P arrivals with a high apparent velocity of about 9 km/s are observed in the southern Shikoku region for earthquakes in the Bungo channel, being followed by a later phase with a normal velocity of 8 km/s arriving 0.5-1.0 second later. In order to explain these arrivals and apparent velocities, Shiono (1974) concluded that earthquakes in the Bungo channel occurred just above the interface between the continental and the oceanic plates. Shiono (1974) obtained the apparent velocity by array analysis of data from three non-telemetered stations. Therefore, the apparent velocity obtained may have a large error due to the lack of timing accuracy. Furthermore, as shown in the previous sections, the so-called uppermost mantle earthquakes occurred in the oceanic crust in the west Seto Inland Sea (including the Bungo channel), and the oceanic crust comes in contact with the continental crust in the western part of Shikoku island. It is probable that the later phase observed in Shiono (1974) is identical to that in this study.

Kimura and Okano (1991, 1992), from travel time analysis of initial P-waves, concluded that the uppermost mantle earthquakes were located in the mantle with a P-wave velocity of 7.8 km/s. In their model,

the Moho discontinuity exists above the uppermost mantle earthquakes and dips to N22°W as shown in Fig. 2-26a. However, if these events occurred in the mantle, the later phases with an apparent velocity smaller than that of the initial phase should not be observed at the stations of TMO . As shown in section 2.2.3, prominent later arrivals are observed in the seismograms at the stations of TMO for the so-called uppermost mantle earthquakes occurring beneath Shikoku. This implies that these events occur not in the mantle, but in the lower crust or in the oceanic crust. Yoshii et al. (1973), using the artificial seismic source, showed the presence of the layer with a P-wave velocity of 6.8 km on the high velocity plate to the south of Shikoku. This layer, dipping to the north, is considered to be the oceanic crust. It is highly possible that the oceanic crust subducts beneath Shikoku island and that the so-called upper mantle earthquakes beneath Shikoku occur inside of the oceanic crust. Nakanishi (1980) found a dipping interface located just above seismic zone beneath Shikoku using a ScSp phase. It is considered that this interface correspond to the upper plane of the oceanic crust.

Although focal depths become deeper from Shikoku towards the stations of TMO, the later phases are observed at the stations of TMO for earthquakes beneath Shikoku as stated in section 2.2.3. Fig. 2-2 indicates that isodepth beneath DOI, located in northern Shikoku, is about 40 km. Since the depth of the Moho discontinuity in the Chugoku district is 38 km (Hashizume et al., 1966), it is considered that the subducting oceanic

crust is still in contact with the lower crust beneath the northern part of Shikoku, and has not undergone basalt/eclogite transition. This structure can account for the later phases at the stations of TMO for earthquakes beneath Shikoku as shown in Fig. 2-26b. As shown in Sacks (1983), there is no mantle wedge in contact with the subducted oceanic crust beneath Shikoku, because the continental crust is in contact with the oceanic crust.

Fig. 2-27 shows the region where the subducting oceanic crust is in contact with the continental crust which is revealed in this study. In this figure, the locations where high-Mg andesites (HMA) were produced at 13-15 Ma are also shown (after Tatsumi et al., 1997). According to Tatsumi et al. (1997), HMA magma is produced when the partial melting of the subducted sediments on the surface of the Philippine Sea plate occurs and the melt reacts with the overlying mantle wedge peridotite during ascent. In other words, the mantle wedge as well as the sediment layer is necessary for the generation of HMA magmas. Where the oceanic crust is in contact with the continental crust, there is no mantle wedge above the oceanic crust. Therefore, no HMA is found south of the solid line in Fig. 2-27, although partial melting of the sediments should also occur in this region as suggested in Tatsumi et al. (1997).

Morris (1995) indicated that melting of the oceanic crust overlying the Philippine Sea plate can explain the chemistry of at least

two of the volcanoes on the Quaternary volcanic front in the Chugoku district. When subduction of a young and hot plate occurs at a shallow angle, melting of the oceanic crust occurs with the amphibole-eclogite transformation. Although there is no seismicity corresponding to the subduction of the Philippine Sea plate, the result of travel time inversion shows the existence of a high velocity zone beneath the Chugoku district (Hirahara, 1981). Furthermore, our result shows that the oceanic crust is subducting beneath the northern part of Shikoku without accompanying basalt/eclogite transformation. Therefore, it is possible that the Philippine Sea plate is subducting aseismically beneath the Chugoku district and melting of the oceanic crust caused volcanic activity in the Chugoku district.

2.5 Concluding remarks of part 2

In the Chugoku, Kinki and Shikoku districts, prominent later phases are frequently observed after P and S phases in the seismograms of upper mantle earthquakes in the vicinity of the west Seto Inland Sea. These phases are dominant in three components and have apparent velocities smaller than the initial P and S waves. These feature can be explained if these later phases are regarded as seismic waves guided by the subducted oceanic crust at the top of the Philippine Sea plate and if

the upper mantle earthquakes take place within the low velocity oceanic crust. These imply that the oceanic crust is in contact with the continental crust in the western part of Shikoku. We applied a three-dimensional ray tracing and a three-dimensional Gaussian-beam method, and have shown that this model accounts for the travel times and amplitudes of the initial and later phases.

The later phases are observed for events shallower than 60 km. This indicates that the subducting oceanic crust remains in a gabbroic phase without transformation to eclogitic phase at depths down to 60 km. This depth is characteristic of the northern boundary of the Philippine Sea plate.

Prominent later arrivals are also observed at the stations in the Chugoku and Kinki districts from the so-called upper mantle earthquakes beneath the Shikoku island. These apparent velocities are almost the same as the velocities of the oceanic crust. This shows that these events occur not in the mantle, but in the subducting oceanic crust. We conclude that the oceanic crust is in contact with the continental crust and there is no mantle wedge between the overriding continental crust and the subducted oceanic crust beneath Shikoku.

Summary of Conclusions

The conclusions obtained throughout the Part 1 and Part are summarized as follows.

1) The subducting Pacific plate beneath the Kanto and Tohoku districts has a layered structure with an upper layer of about 40 km thickness. The internal discontinuity is sharp enough to reflect high frequency seismic waves. Therefore in the Kinki, Chugoku and Chubu districts, we can observe SP wave, reflected and converted from S to P wave at the discontinuity.

2) This structure corresponds to the chemical zonation because of melting and differentiation forming at the mid oceanic ridge.

3) This velocity discontinuity almost coincides with the lower seismic plane of the double seismic zone in the region. It is possible that layered structure forms the double seismic zone because of the stress concentration at the discontinuity associated with unbending of the upper layer of plate.

4) In and around Shikoku, so-called upper mantle earthquakes take place in the low velocity oceanic crust at the top of subducting Philippine Sea plate.

5) The subducting oceanic crust remains in a gabbroic phase without transformation to eclogitic rocks at depths down to 60 km. This depth

is characteristic to the northern boundary of the Philippine Sea plate.

6) The oceanic crust at the top of the Philippine Sea plate contacts with the continental crust in the western and central part of Shikoku. Therefore, in the Chugoku, Kinki and Shikoku districts, prominent later phases are frequently observed after P and S phases in the seismograms of so-called upper mantle earthquakes in and around Shikoku.

7) Beneath Shikoku, there is no mantle wedge between the overriding continental crust and the subducted oceanic plate.

Acknowledgments

I would like to express my gratitude to Prof. Masataka Ando for critically reading of this manuscript and giving many valuable suggestions.

I also wish to express my gratitude to Profs. Kazuo Oike and Yoshiyuki Tatsumi who encouraged me patiently.

I also express my special thanks to Dr. Shoji Sekiguchi who provided me with a program of three-dimensional Gaussian beam method.

I am grateful to Prof. Shozo Kimura who allowed us to use the seismic records and hypocenter data at Kochi Seismological Observatory of Kochi University. And I also thank Prof. Akira Hasegawa of Tohoku University, Mr. Katsumi Miura of the University of Tokyo, and the Kanto-Tokai group of NIED who provided us with hypocenter data. Thanks are due to Dr. Takuo Shibutani and Mr. Setsuro Nakao who helped me to examine the seismic records of Tottori Microearthquake Observatory of Kyoto University.

Discussions with Drs. Satoshi Kaneshima, Fumiaki Takeuchi, Yoshitsugu Furukawa, Hajime Shimoda, Naoto Ishikawa and Mamoru Nakamura were very useful for improving this manuscript.

Some figures were produced by DCL-DENNOU library. I thank

Dr. Satoshi Sakai for managing it.

References

Asano, S., Miura, K., Inoue, Y. , Miura, R., Ishiketa, T. and Yoshii, T., 1986. Recent Seismic Activity in Chugoku District and its Vicinity, Western Japan as Revealed by the Telemetering Network of Shiraki Micro-Earthquake Observatory. *Zisin (J. Seismol. Soc. Jpn), Ser.2, 39*: 229-240 (in Japanese with English Abstract).

Birch, F., 1961. The Velocity of compressional waves in rocks to 10 kilobars, 2. *J. Geophys. Res., 66*: 2199-2224

Cerveny, V., 1985. The application of ray tracing to the numerical modeling of seismic wave fields in complex structures. in *Seismic Shear waves, Handbook of Geophysical Exploration, Section I, Seismic Exploration, Vol.15*, ed.by G.P.Dohr, pp1-124 Geophysical Press, London

Disaster Prevention Research Institute, 1986. Seismic wave automatic processing system at Disaster Prevention Research Institute, Kyoto University. *Report of the Coordinating Committee for the Earthquake Prediction, 35*: 431-436 (in Japanese)

Engdahl, E. R. and Scholz, C.H., 1977. A double Benioff zone beneath the central Aleutians; an unbending of the lithosphere. *Geophys. Res. Let. 4*: 473-476

Fukao, Y., Hori, S. and Ukawa, M., 1983. A seismological constraint on the

depth of basalt-eclogite transition in a subducting oceanic crust. *Nature, 303*: 413-415

Hamaguchi, H. , Goto, K. and Suzuki, Z. , 1983. Double-planed structure of intermediate-depth seismic zone and thermal stress in the descending plate. *J. Phys. Earth, 31*: 329-347

Hasegawa, A., Umino, N. and Takagi, A., 1978. Double-planed deep seismic zone and upper-mantle structure in the Northeastern Japan Arc. *Geophys. J. Roy. astr. Soc., 54*: 281-296

Hasegawa, A., Umino, N., Takagi, A. , Suzuki, S. , Motoya, Y. , Kameda, S., Tanaka, K. and Sawada, Y. ,1983. Spatial distribution of earthquakes beneath Hokkaido and northern Honshu, Japan . *Zisin (J. Seismol. Soc. Jpn), Ser2, 39*: 381-395 (in Japanese with English abstract)

Hashizume, M., Kawamoto, O., Asano, S. , Muramatsu, I. , Tamaki, I. and Murauchi, S., 1966. Crustal Structure in the Western Part of Japan Derived from the Observation of the First and the Second Kurayoshi and the Hanabusa Explosions. Part 2. Crustal Structure in the Western Part of Japan. *Bull. Earthq. Res. Inst. Univ. Tokyo, 44*: 2109-2120

Hirahara, K., 1977. A large scale seismic structure under the Japan islands and the Sea of Japan. *J. Phys. Earth, 25*: 393-417.

Hirahara, K., 1981. Three Dimensional Seismic Structure beneath Southwest Japan: The Subducting Philippine Sea Plate. *Tectonophysics, 79*: 1-44

Hori, S., Inoue, H., Fukao, Y. and Ukawa, M., 1985. Seismic detection of the untransformed 'basaltic' oceanic crust subducting into the mantle. *Geophys. J. R. astr. Soc., 83*: 169-197

Hori, S., 1990. Seismic waves guided by untransformed oceanic crust subducting into the mantle: the case of the Kanto district, central Japan. *Tectonophysics, 176*: 355-376

Hurukawa, N. and Imoto, M., 1992. Subducting oceanic crusts of the Philippine Sea and Pacific plates and weak-zone-normal compression in the Kanto District, Japan. *Geophys. Jour. Int, 109*: 639-652

Hurukawa, N. and Imoto, M., 1993. A non double-couple earthquake in a subducting oceanic crust of the Philippine Sea Plate. *J. Phys. Earth, 41*: 257-269

Iidaka, T. and Mizoue, M., 1991. P-wave velocity structure inside the subducting Pacific plate beneath the Japan region. *Phys. Earth Planet. Inter., 66*: 203-213

Imagawa, K., Hirahara, K. and Mikumo, T., 1985. Source Mechanisms of Subcrustal Earthquakes around the Northeastern Kyushu Region, Southwestern Japan, and their Tectonic Implications. *J. Phys. Earth, 33*: 257-277

Irifune, T. and Ringwood, A.E., 1993. Phase transformations in subducted oceanic crust and buoyancy relationships at depths of 600-800 km in the mantle. *Earth and Planet. Sci. Let., 117*: 101-110

Ishida, M., 1984. The spatial distribution of earthquake hypocenters and the three-dimensional velocity structure in the Kanto-Tokai District, Japan. *J. Phys. Earth, 32*: 399-422

Ito, K., Yoshii, T., Asano, S., Sasaki, Y. and Ikami, A., 1982. Crustal Structure of Shikoku, Southwestern Japan as Derived from Seismic Observations of the Iejima and the Torigatayama Explosions. *Zisin (J. Seismol. Soc. Jpn), Ser.2, 35*: 377-391 (in Japanese with English Abstract)

Jeffreys, H. and Bullen, K. E., 1940. Seismological Table. *Brit. Assoc. Gray-Milne Trust*

Kao. H and Liu, L., 1995. A hypothesis for the seismogenesis of a double seismic zone. *Geophys. Jour. Int, 123*: 71-84.

Kawakatsu, H., 1986. Double seismic zones; kinematics. *J. Geophys. Res., 91*: 4811-4825.

Kimura, S. and Okano, K., 1991. The lower crust and the Moho discontinuity in Shikoku, Southwest Japan. *Research Report of Kochi University, Natural Science Ser.,40*: 49-61 (in Japanese with English Abstract)

Kimura, S. and Okano, K., 1992. Characteristics of Earthquakes Occurring in the Uppermost Mantle in Shikoku, Southwest Japan. *The memoirs of the faculty of science Kochi University Ser B, 13*: 1-12 (in Japanese with English Abstract)

Knopoff, L., 1964. Q. *Reviews of Geophysics, 2*: 625-660

Matsuzawa, T., Umino, N., Hasegawa, A. and Takagi, A., 1986. Upper mantle velocity structure estimated from PS-converted wave beneath the north-eastern Japan Arc. *Geophys. J. R. astr. Soc., 86*: 767-787

Matsuzawa, T., Kono, T. , Hasegawa, A. and Takagi, A., 1990. Subducting plate boundary beneath the northeastern Japan arc estimated from SP converted waves. *Tectonophysics, 181*: 123-131

Miura, K., Tsukuda, T., Miura, R., Inoue, Y. and Asano, S., 1991. Deep Seismic Zone in the Western Part of the Seto Naikai (Seto Inland Sea) and its Surrounding Regions, Southwestern Japan. *Bull. Earthq. Res. Inst. Univ. Tokyo, 66*: 553-570 (in Japanese with English Abstract).

Mizoue, M., Nakamura, M. , Seto, N. and Ishiketa, Y., 1983. Three-layered Distribution of Microearthquakes in Relation to Focal Mechanism Variation in the Kii Peninsula, Southwestern Honshu, Japan. *Bull. Earthq. Res. Inst. Univ. Tokyo, 58*: 287-310

Morris, P. A., 1995. Slab melting as an explanation of Quaternary volcanism and aseismicity in southwest Japan. *Geology, 23*: 395-398

Nakanishi, I., 1980. Precursors to ScS Phase and Dipping Interfaces in the Upper Mantle beneath Southwestern Japan. *Tectonophysics, 69*: 1-35

Oda, H., Tanaka, T. and Seya, K., 1990. Subducting oceanic crust on the Philippine Sea plate in Southwest Japan. *Tectonophysics, 172*: 175-

189

Okada, H., 1971. Forerunners of ScS Waves from Nearby Deep Earthquakes and Upper Mantle Structure in Hokkaido. *Zisin (J. Seismol. Soc. Jpn), Ser2, 24*: 228-239 (in Japanese with English Abstract)

Okano, K., Kimura, S., Konomi, T. and Nakamura, M., 1985. The focal Distribution of Earthquake in Shikoku and Its Surrounding Regions. *Zisin (J. Seismol. Soc. Jpn), Ser.2, 38*: 93-103 (in Japanese with English Abstract)

Okano, K., Kimura, S. and Konomi, T., 1986. The Conrad Discontinuity and the P Wave Velocity of the lower crust in Shikoku and its surrounding regions. *J. Phys. Earth, 34*: 531-542

Ringwood, A. E., 1982. Phase transformations and differentiation in subducted lithosphere; implications for mantle dynamics, basalt petrogenesis, and crustal evolution. *Journal of Geology, 90*, 611-643.

Ringwood, A. E., 1991. Phase transformations and their bearing on the constitution and dynamics of the mantle. *Geochim. Cosmochim. Acta, 55*, 2083-2110.

Sacks, I.S. and Okada, H. , 1974. A Comparison of the anelasticity structure beneath western South America and Japan. *Phys. Earth Planet. Inter., 9*: 211-219

Sacks, I. S., 1983. The Subduction of Young Lithosphere. *J. Geophys. Res., 88*: 3355-3366

Sekiguchi, S., 1992. Amplitude distribution of seismic waves for laterally heterogeneous structure including a subducting slab. *Geophys. J. Int., 111*: 448-464

Shimamura, H., Asada, T. , Suyehiro, K. , Yamada, T. and Inatani, H., 1983. Longshot experiments to study velocity anisotropy in the oceanic lithosphere of the northwestern Pacific. *Phys. Earth Planet Interiors, 31*: 348-362

Shimamura, H. and Asada, T. , 1976. Apparent velocity measurements on an oceanic lithosphere. *Phys. Earth Planet Interiors, 13*: 15-22

Shiono, K., 1974. Travel Time Analysis of Relatively Deep Earthquakes in Southwest Japan with Special Reference to the Underthrusting of the Philippine Sea Plate. *Journal of Geosciences, Osaka City University, 18*: 37-59

Shiono, K., 1977. Focal mechanisms of major earthquakes in southwest Japan and their tectonic significance. *J. Phys. Earth, 25*: 1-26

Shiono, K. and Mikumo, T., 1975. Tectonic Implication of subcrustal, normal, Faulting earthquakes in the western Shikoku Region, Japan. *J. Phys. Earth, 23*: 257-278

Sleep, N.H., 1979. The double seismic zone in downgoing slabs and the viscosity of the mesosphere. *J. Geophys. Res., 84*: 565-4571

Suyehiro, K. and Sacks, I.S., 1979. P- and S-wave velocity anomalies associated with the subducting lithosphere determined from travel-time residuals in the Japan region. *Bull. Seism. Soc. Am., 69*: 97-114

Suzuki, S. and Kasahara, M. , 1996. Unbending and horizontal fracture of the subducting Pacific Plate, as evidenced by the 1993 Kushiro-oki and the 1981 and 1987 intermediate-depth earthquakes in Hokkaido. *Phys. Earth Planet Interiors, 93*: 91-104.

Suzuki, S., Sasatani, T. and Motoya, Y. ,1983. Double seismic zone beneath the middle of Hokkaido, Japan, in the southwestern side of Kurile arc. *Tectonophysics, 96*: 59-76

Tatsumi, Y., Furukawa, Y., Ishikawa, N., Shimoda, H., Torii, M., Sinjoe, H., and Ishizaka, K., 1997, Melting of slab and production of high-Mg andesite magmas: unusual magmatism in SW Japan at 13-15 Ma. *in preparation*

Tsukahara, H., 1980. Physical conditions for double seismic planes of the deep seismic zone. *J. Phys. Earth, 28*: 1-15

Tsumura, K., 1973. Microearthquake activity in the Kanto District, in *Publication for the 50th anniversary of the Great Kanto earthquake, 1923, Earthquake Res. Inst. Univ. Tokyo*: 67-87

Umino, N., Hasegawa, A. and Matsuzawa, T., 1995. sP depth phase at small epicentral distances and estimated subducting plate boundary. *Gephys. Jour. Int. 120*: 356-366

Veith, K., 1974. The relationship of island arc seismicity to plate tectonics. *Ph.D Thesis, South Methodist Univ. Dallas*

Yoshii, T., Ludwig, W. J, . Den, N., Murauchi, S., Ewing, M., Hotta, H., Buhl, P., Asanuma, T. and Sakajiri, N., 1973. Structure of Southwest

Japan Margin off Shikoku. *J. Geophys. Res., 78*: 2517-2525

Yoshii, T., 1979. Compilation of Geophysical Data around the Japanese Islands (1). *Bull. Eartq. Res. Inst., 54*: 75-117 (in Japanese with English abstract)

Zhao, D., and Hasegawa, A., 1993. P Wave Tomographic Imaging of the Crust and Upper Mantle Beneath the Japan Islands. *J. Geophys. Res., 98*: 4333-4353

Figure Captions

Fig. 1-1 Isodepth contours of deep earthquakes caused by subduction of the Pacific plate (after Yoshii, 1979). Solid squares in the rectangular indicate seismic stations used in this study.

Fig. 1-2 Distribution of the earthquakes used in this study in the area bounded by latitudes 34.5°N to 42°N, occurring from July 1985 through December 1988.

Fig. 1-3 An example of seismograms arranged by epicentral distance showing a later arrival of P phase (X phase) for an event located in the upper seismic plane of the double seismic zone.

Fig. 1-4 Epicentral distribution of events whose X phase were observed at the DPRI seismic network (from July 1985 through 1988).

Fig. 1-5 Another example of seismograms arranged by epicentral distance showing X phase for an event located in the upper seismic plane of the double seismic zone.

Fig. 1-6 Particle motions of P and X phases for the same event shown in Fig. 1-3. Up-down, radial and transverse components of seismograms at the AZJ (Δ= 3.05 degree) are also shown. Particle motions of the P and X phases are projected on the U-T plane.

Fig. 1-7 Plot of observed travel time differences of the initial and X phases versus focal depth with error bars.

Fig. 1-8 Possible ray paths for the X phase. Solid and dashed lines denote P- and S-waves, respectively. Triangles and stars indicate stations and hypocenters, respectively.

Fig. 1-9 An example of seismograms arranged by epicentral distance showing a later arrival of P phase (SP phase) for an event located in the lower seismic plane of the double seismic zone.

Fig. 1-10 An example of seismograms arranged by epicentral distance showing a later arrival of P phase (sP phase) for an event located near the Japan trench.

Fig. 1-11 Schematic cross section of the velocity structure model used in the three-dimensional ray tracing. H is the vertical width of the upper layer of the subducting slab.

Fig. 1-12 Shooting points for ray-tracing (stars).

Fig. 1-13 Calculated travel times of P and SP phases assuming starting points at A, B and C in Fig. 1-12.

Fig. 1-14 Synthesized seismograms for a case with a starting point located at B in Fig. 1-12 with a depth of 41km. H is assumed to be 50 km. The double-couple mechanism for the Gaussian Beam method is projected on to the lower hemisphere. Parameters of Gaussian Beam are as follows: Initial beam width (L_0) is 20. Source wavelet is a ricker wavelet with f=2 Hz, γ =4, and φ=0 which is expressed as $f(t)=\exp(-(2\pi f/\gamma)^2)\cos(2\pi ft+\varphi)$.

Fig. 1-15 Synthesized seismograms for a case with a starting point located at C in Fig. 1-12 with a depth of 126 km. H is also assumed to be 50 km. The double-couple mechanism for the Gaussian Beam method is shown. The same Gaussian Beam parameters for Fig. 1-14 were used.

Fig. 1-16 Synthesized seismograms for case B assuming that the velocity difference between the upper and the lower layers of the plate is 10%. H is assumed to be 50 km. The double-couple mechanism for the Gaussian Beam method is shown. The same Gaussian Beam parameters for Fig. 1-14 were used.

Fig. 1-17 Synthesized seismograms in the model with a flat interface. An assumed shooting point is B in Fig. 1-12, but the radiation pattern used in the Gaussian Beam method is slightly different from that shown in Fig. 1-14. The same Gaussian Beam parameters for Fig. 1-14 were used.

Fig. 1-18 Schematic cross section of the model with an irregular internal discontinuity used in the Gaussian Beam method.

Fig. 1-19 Synthesized seismograms in the model with the irregular interface shown in Fig. 1-18. The assumed shooting point is B in Fig. 1-12. The double-couple mechanism for the Gaussian Beam method is also shown. The same Gaussian Beam parameters for Fig. 1-14 were used.

Fig. 1-20 A schematic view of the two layered slab which best explains

the observed X phase.

Fig. 2-1 Map of southwest Japan. N.T. and J.T represent Nankai Trough and Japan trench, respectively. EU, PH and PA in the insert represent Eurasia Plate, Philippine Sea plate and Pacific plate, respectively.

Fig. 2-2 Epicentral distribution of the so-called upper mantle earthquakes and seismic stations used in this study. Solid squares and triangles indicate stations of TMO and KEO, respectively. Solid line indicate the depth contours of the top of the seismic zone (From west to east: Miura et al. 1991; Okano et al. 1985; and Mizoue et al. 1983).

Fig. 2-3 An example of three-component seismograms associated with distinct later arrivals. The initial and later arrivals are indicated by triangles and circles, respectively. The solid and open symbols denote P and S waves, respectively. The hypocenter is listed in Table 1 as Eq. 10.

Fig. 2-4 An example of vertical-component seismograms assembled in order of epicentral distances for the same event in Fig. 2-3.

Fig. 2-5 An example of three-component seismograms without later arrivals. The hypocenter is listed in Table 1 as Eq. 18.

Fig. 2-6 Distribution of events associated with later phases. Solid symbols show events for which later arrivals can be observed in the Tottori region. Open symbols show events without later

arrivals in the Tottori region.

Fig. 2-7 A plot of composite travel time of the initial and later phases. Open and solid symbols indicate the initial and later arrivals, respectively.

Fig. 2-8 Possible ray paths for the initial and the later phase projected on the vertical section. Solid and dashed lines denote P- and S-wave, respectively. Triangles and stars indicate stations and hypocenters, respectively.

Fig. 2-9 An example of three-component seismograms at stations of KEO associated with distinct later arrivals. The hypocenter is listed in Table 1 as Eq. 7.

Fig. 2-10 Distribution of events associated with later arrivals. Solid and open symbols indicate the events with and without later arrivals at the stations in Shikoku, respectively.

Fig. 2-11 A plot of composite travel times of the initial and later phases. Open and solid symbols indicate the initial and later arrivals, respectively.

Fig. 2-12 An example of vertical-component seismograms, which shows distinct later arrivals, assembled in order of epicentral distances. The hypocenter is listed in Table 2 as Eq. 12.

Fig. 2-13 Distribution of events with later phases. Solid and open symbols indicate the events with and without later arrivals at the stations

of TMO, respectively.

Fig. 2-14 An example of vertical-component seismograms for an event occurring in the continental upper crust, assembled in order of epicentral distances. The apparent velocity of the later phase is smaller than that of later phase which appeared in Fig. 2-12. The hypocenter is located at 134.149°E, 33.430°N and 12 km occurring on June 6, 1984.

Fig. 2-15 (a) The isodepth contours of the top of the Philippine Sea Plate used in three-dimensional ray tracing and Gaussian-beam method. A and B (stars) are the shooting points. Solid line indicates the vertical cross section of Fig. 2-15c.

(b) The velocity structure of the crust and overlying mantle used in three-dimensional ray tracing and Gaussian-beam method.

(c) A cross section showing the velocity structure across A and TTT station.

Fig. 2-16 Calculated travel times for case A shown in Fig. 2-15a. Crosses indicate calculated travel times and solid circles shows the observed travel times from all the events with a depth of 40~50 km. Calculated travel times are plotted for rays which reached in a range of 10km from stations of TMO.

Fig. 2-17 Synthesized seismograms in order of epicentral distance. An assumed hypocenter is located at A in Fig. 2-15a with a depth of 45 km. The double-couple source mechanism is also shown.

Parameters of Gaussian Beam are as follows: Initial beam width (L_0) is 15. Source wavelet is a ricker wavelet with f=2 Hz, γ =4, and φ=0 which is expressed as $f(t)=\exp(-(2\pi f/\gamma)^2)\cos(2\pi ft+\varphi)$.

Fig. 2-18 Synthesized seismograms in order of epicentral distance. An assumed hypocenter is located at A in Fig. 2-15a with a depth of 45 km. The double-couple source mechanism is also shown. The same Gaussian Beam parameters for Fig. 2-17 were used.

Fig. 2-19 Synthesized seismograms in order of epicentral distance. An assumed hypocenter is located at B in Fig. 2-15a with a depth of 54 km. The double-couple source mechanism is also shown. The same Gaussian Beam parameters for Fig. 2-17 were used.

Fig. 2-20 Synthesized seismograms in order of epicentral distance. An assumed hypocenter is located at B in Fig. 2-15a with a depth of 54 km. The double-couple source mechanism is also shown. The same Gaussian Beam parameters for Fig. 2-17 were used.

Fig. 2-21(a) The velocity structure of the crust and overlying mantle used in the three-dimensional ray tracing are shown. This structure is based on Okano et al. (1986).

(b) A cross section which shows the velocity structure beneath Shikoku.

Fig. 2-22 Calculated and observed travel times for case A. Pluses indicate calculated travel times and solid circles indicate the observed

travel time for the events with a depth of 40~50 km. Calculated travel times are plotted for rays which reached in a range of 10km from stations of KEO.

Fig. 2-23 Calculated and observed travel times for case B. Pluses indicate calculated travel times and solid circles indicate the observed travel time for the events with a depth of 50~60 km. Calculated travel times are plotted for rays which reached in a range of 10km from stations of KEO.

Fig. 2-24 Isodepth lines (Miura et al. 1991) and epicenters. Solid and open symbols show events with and without later arrivals in Tottori region, respectively. Eq.9 and Eq.20 show the events with later phases in Shikoku but not in the Tottori region.

Fig. 2-25 Schematic illustrations showing ray paths from Eq. 9 to the stations of (a) TMO and (b) KEO, respectively.

Fig. 2-26 Vertical sections velocity structure beneath Shikoku. MTL represents the Median Tectonic Line.

(a) After from Kimura and Okano (1991).

(b) Our interpretation based on the later phase analysis. Earthquakes take place in the subducting oceanic crust, but not in the mantle. And there is no mantle wedge between PHS and overriding crust beneath the central and western part of Shikoku.

Fig. 2-27Hatched area shows the place where the oceanic crust is in contact with the continental crust. Stars shows locations where

HMAs (high-Mg andesites) were produced at 13 -15 Ma after Tatsumi et al. (1997). No HMA is found to the south of the solid line.

Figures and Tables

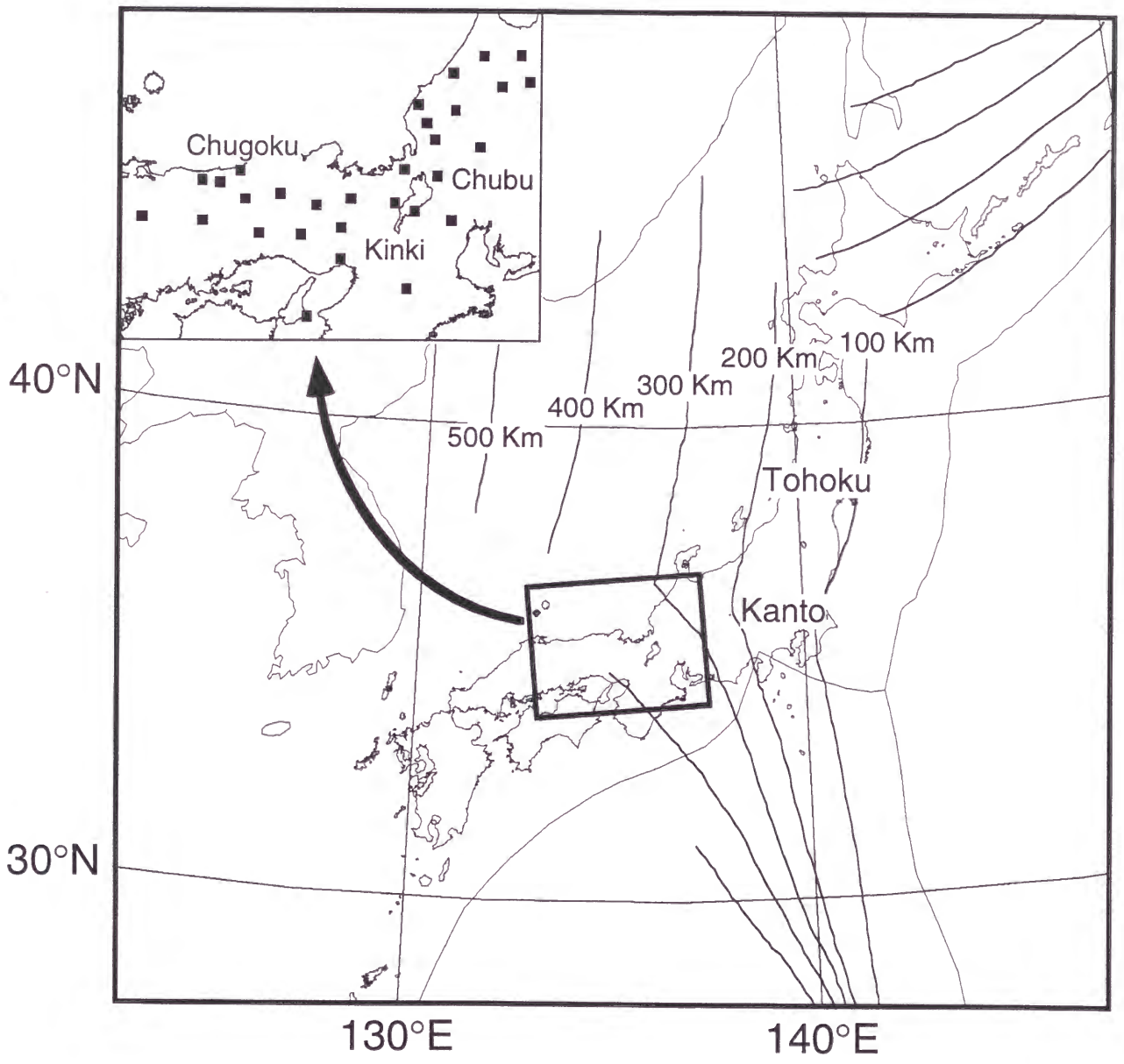
Chugoku
Chubu
Kinki
100 Km
200 Km
300 Km
400 Km
500 Km
Tohoku
Kanto
40°N
30°N
130°E
140°E

Fig. 1-1

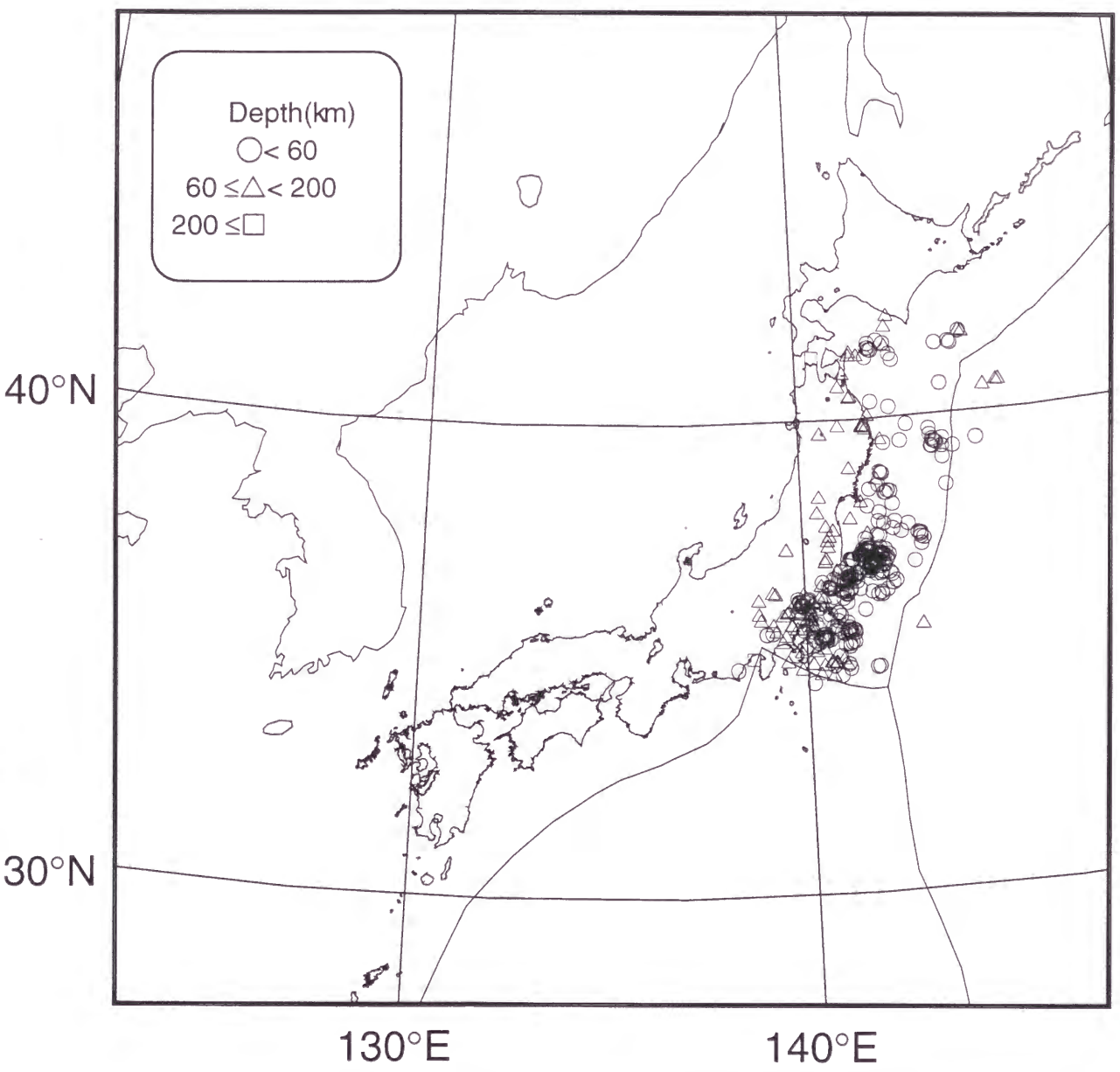

Fig. 1-2

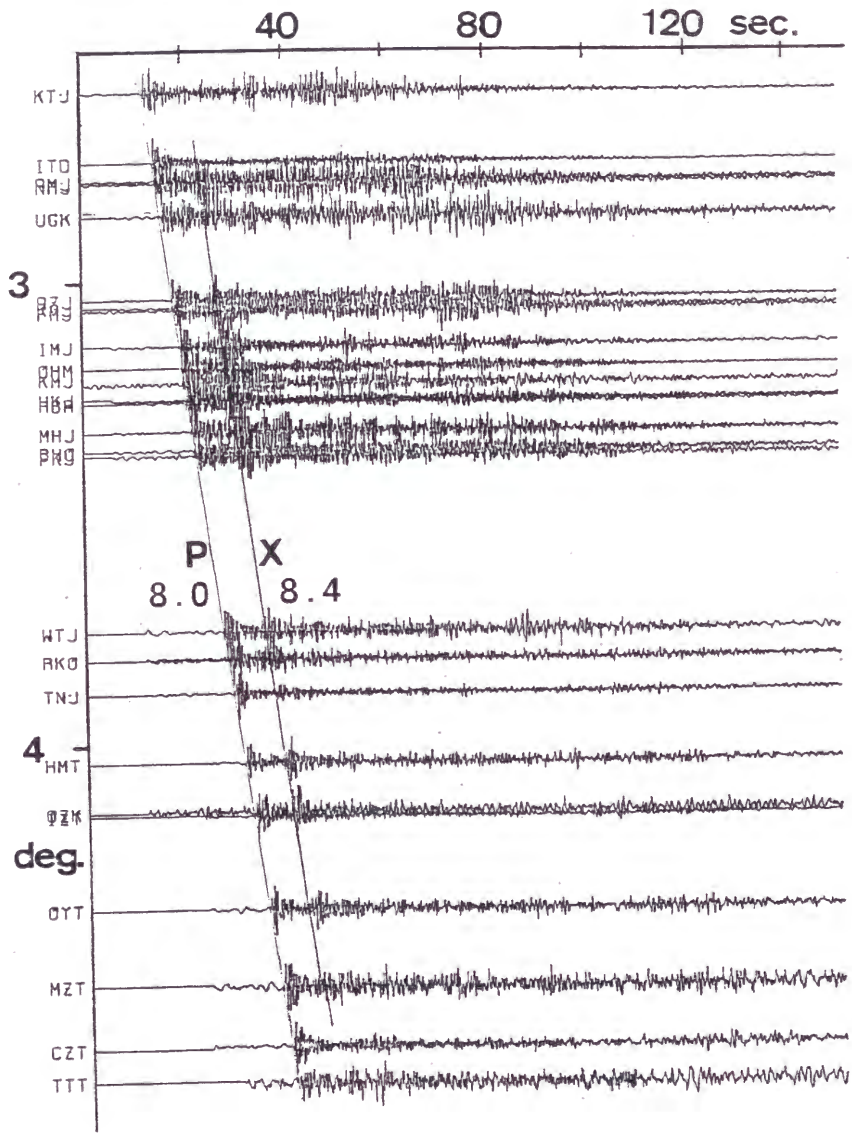

1987-2-13 01:34 34.747°N 139.086°E 88km M4.4

Fig. 1-3

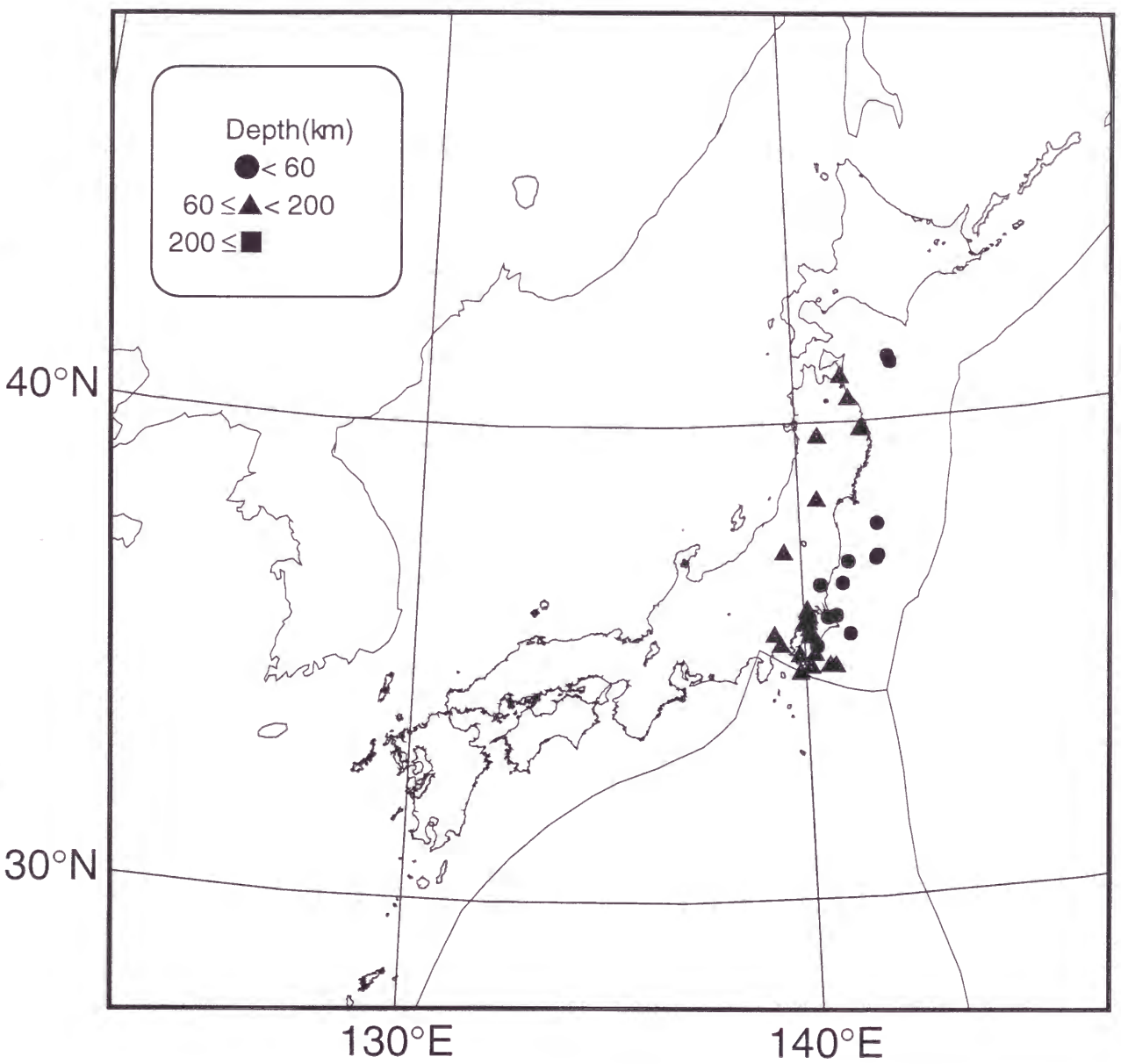

Fig. 1-4

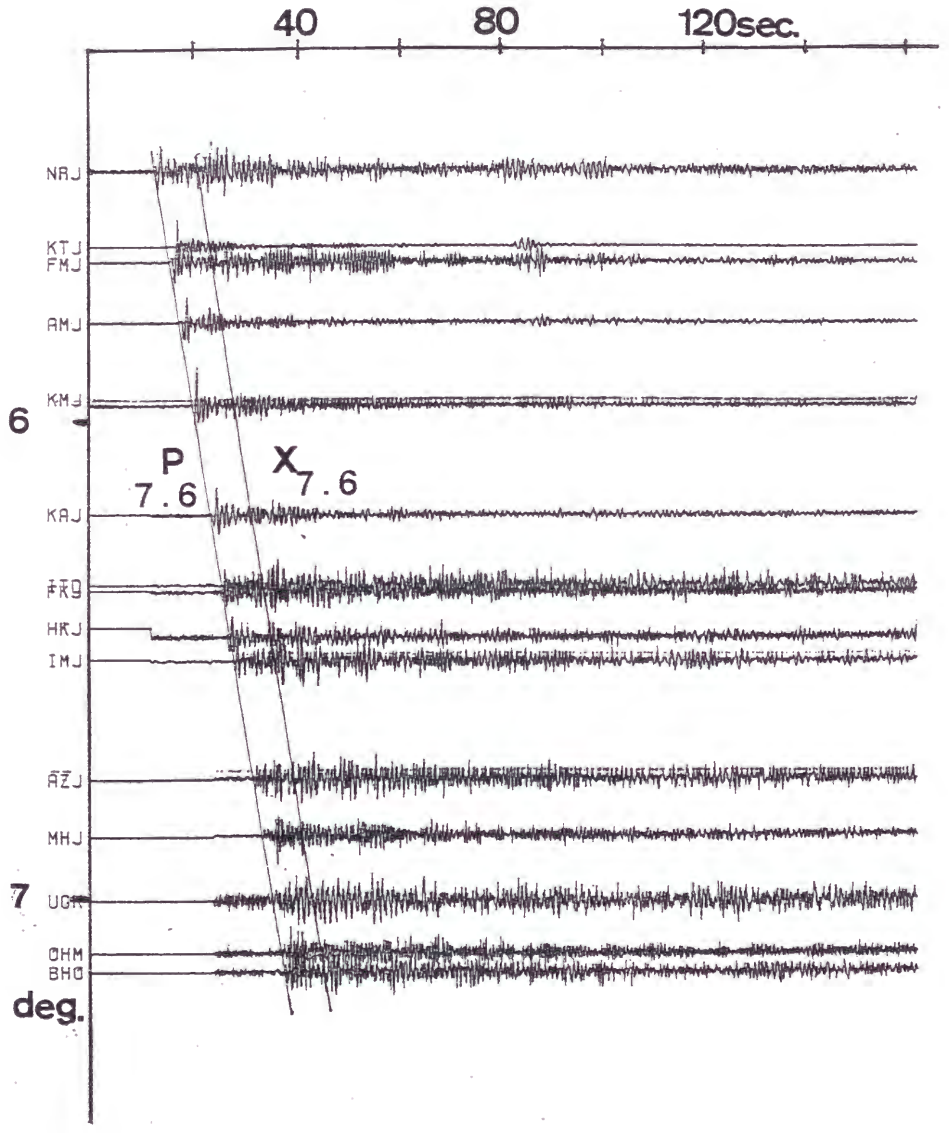

1987-4-15 11:43 40.948°N 141.302°E 89km M4.5

Fig. 1-5

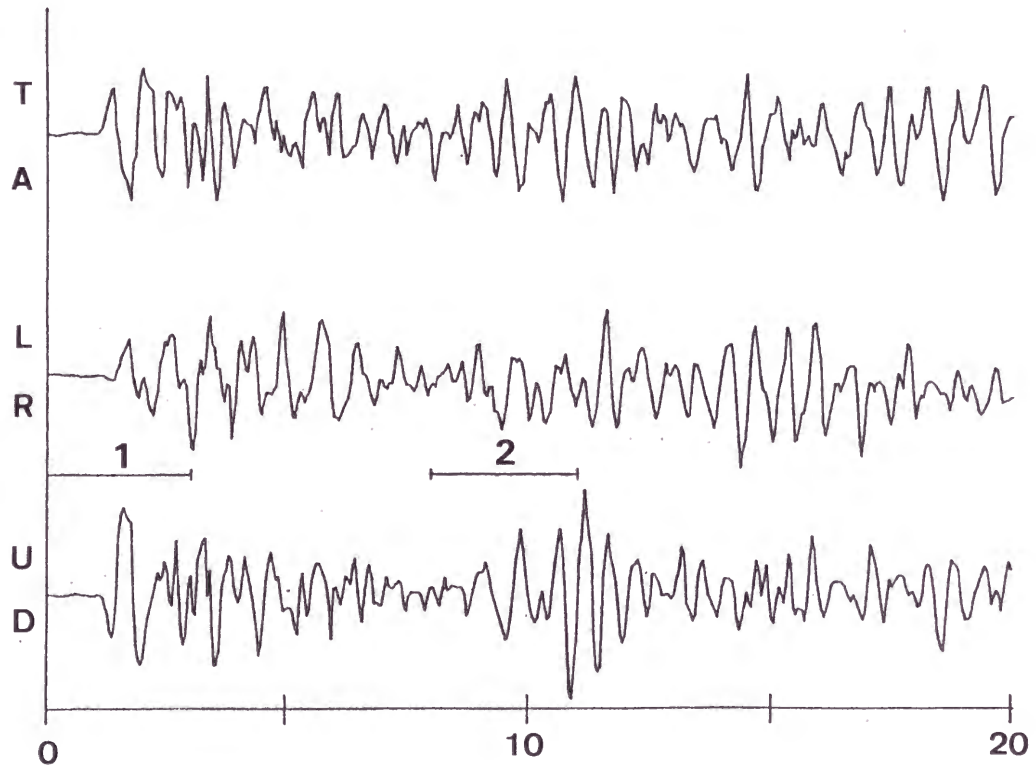

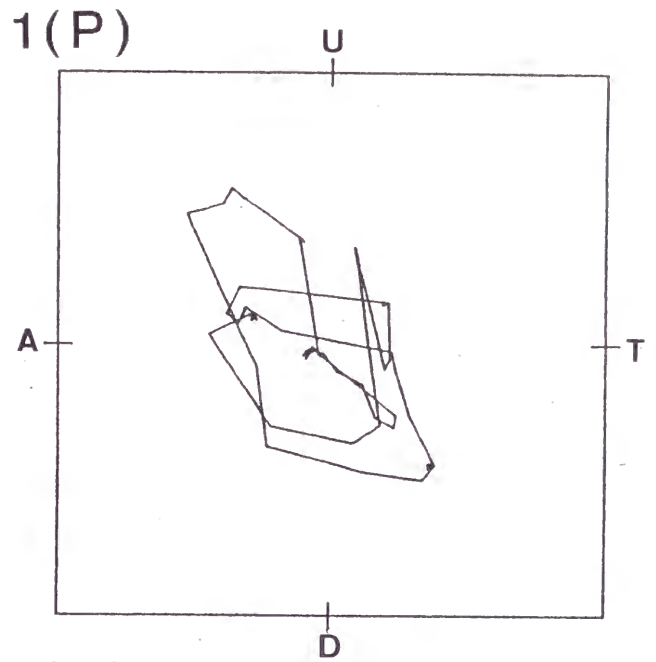

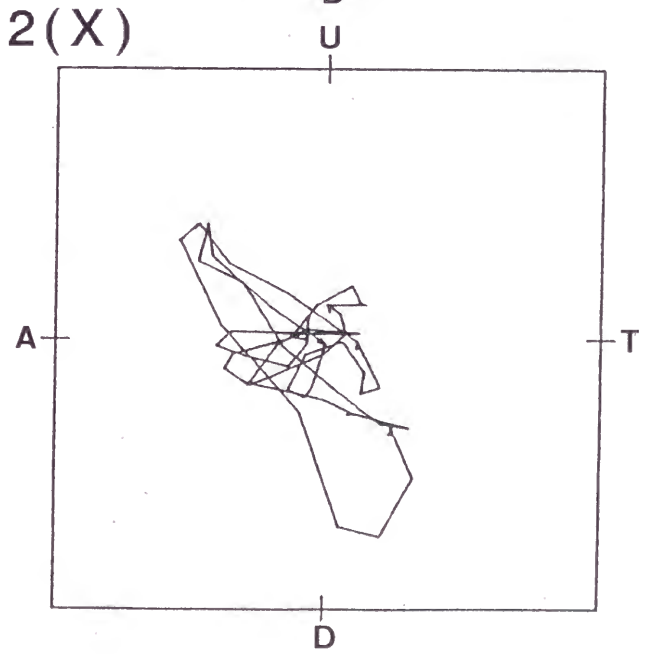

Fig. 1-6

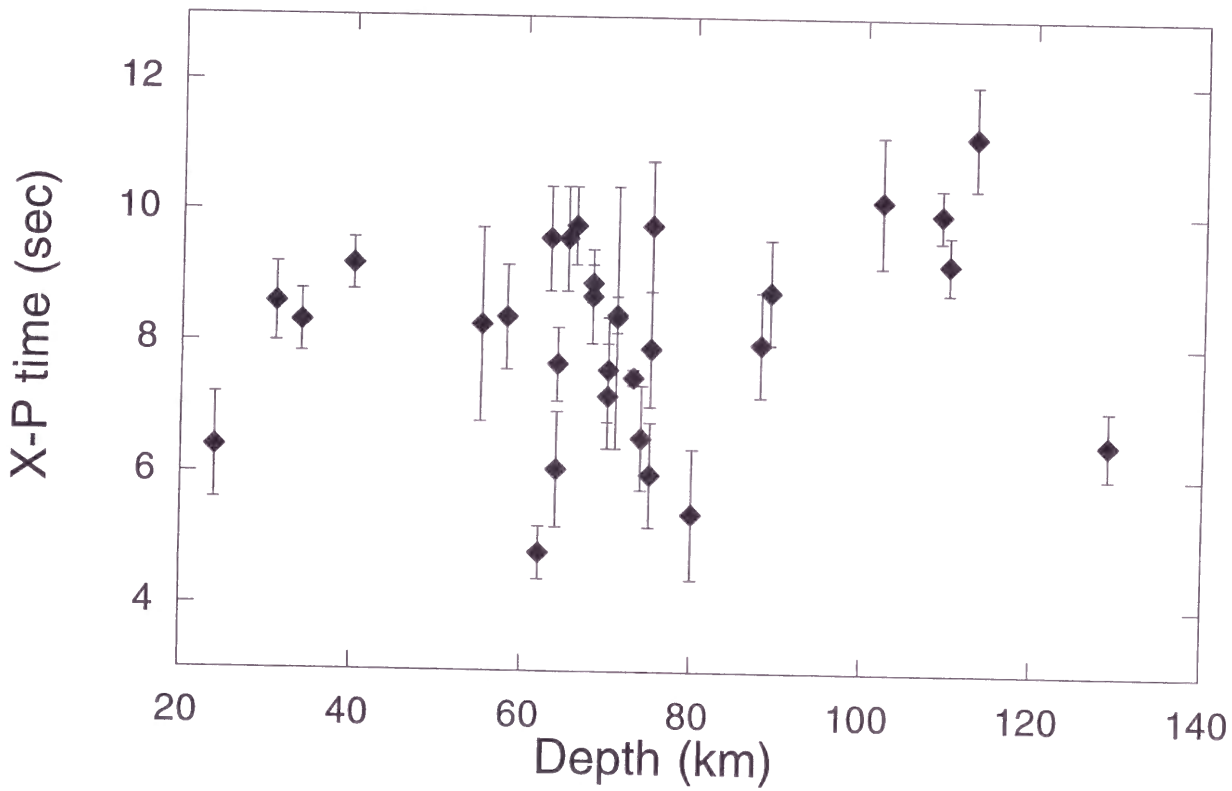

Fig. 1-7

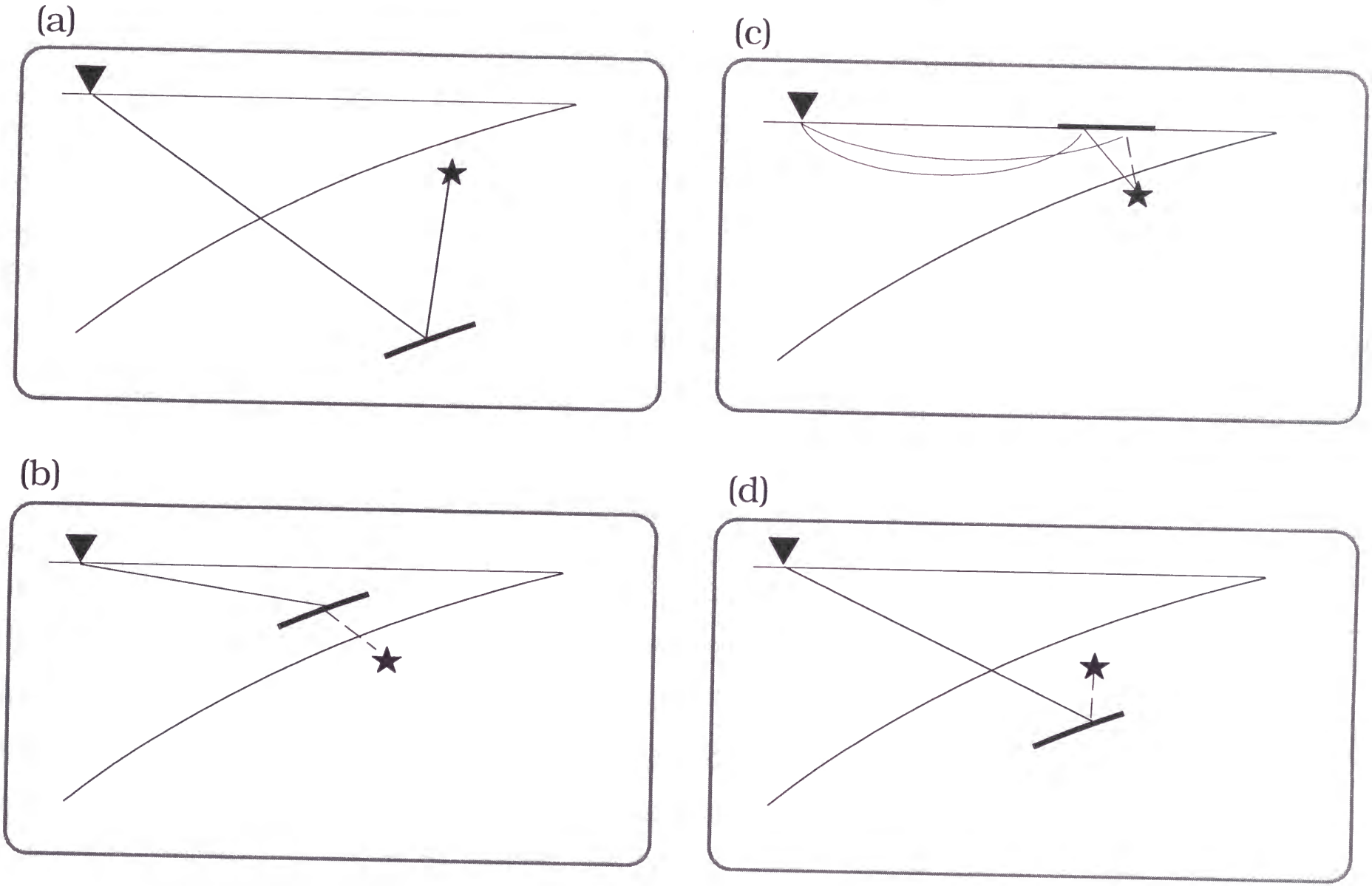

Fig. 1-8

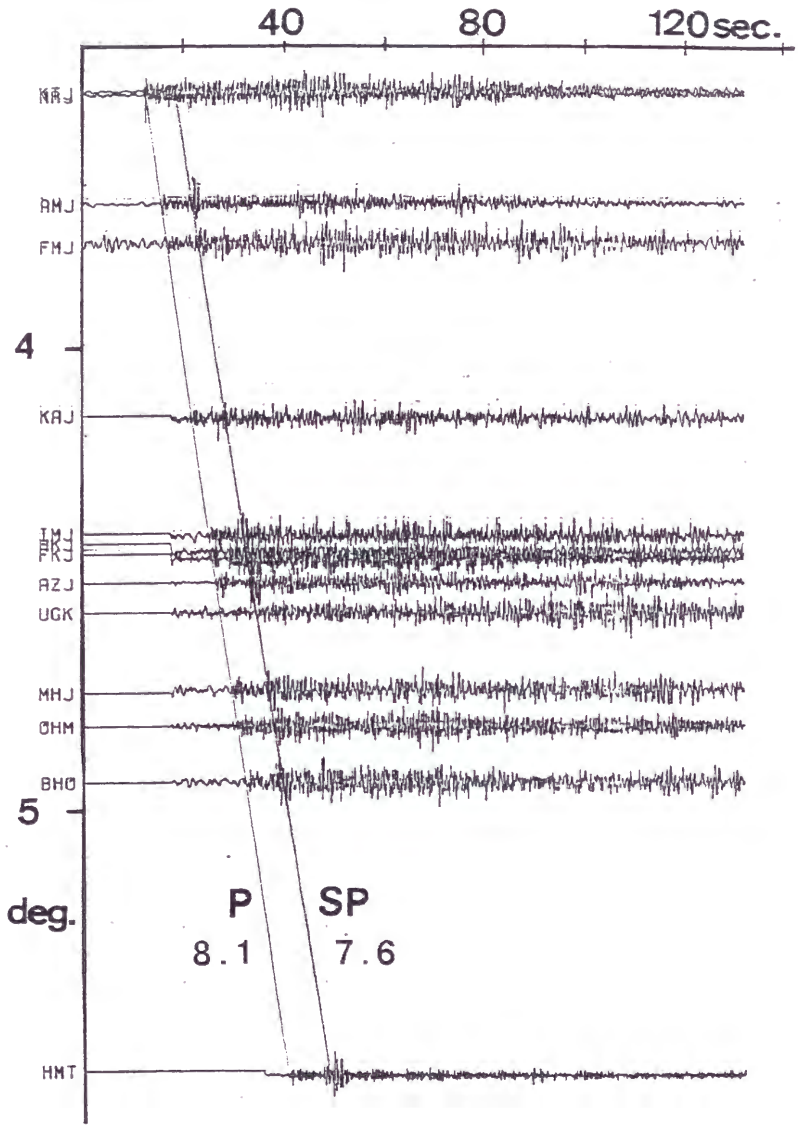

1986-9-28 17:12 37.232°N 141.48°E 82km M4.8

Fig. 1-9

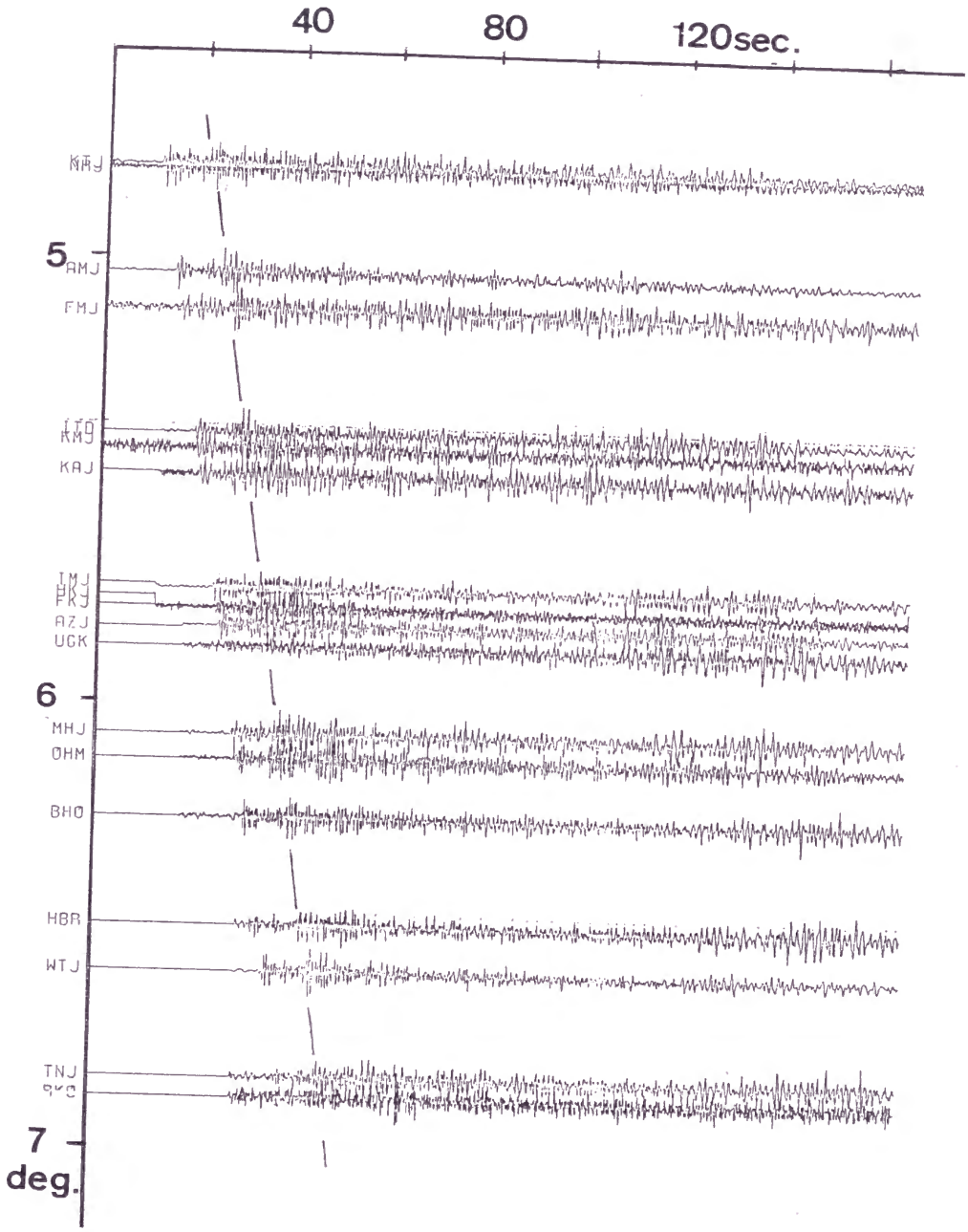

1986-4-3 11:56 37.442°N 143.158°E 49km M4.2

Fig. 1-10

Two Layered Slab Model for 3-D ray tracing

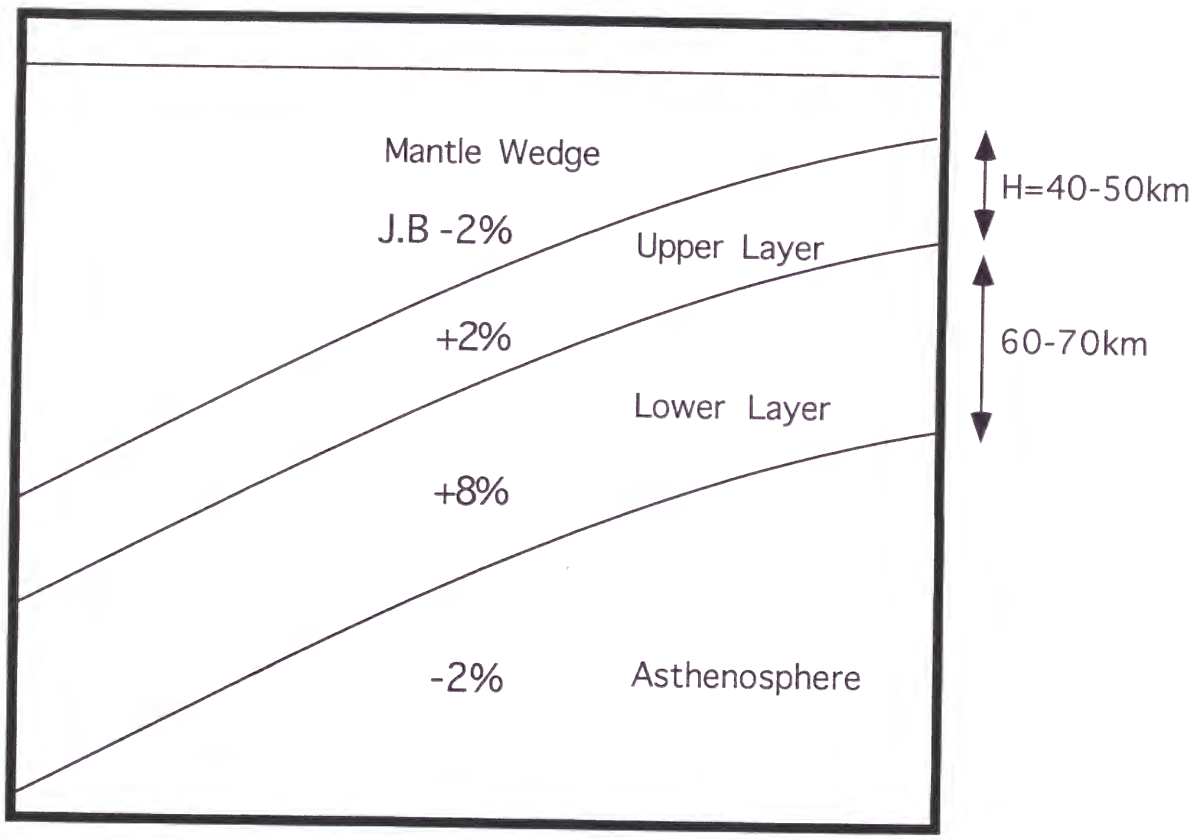

Fig. 1-11

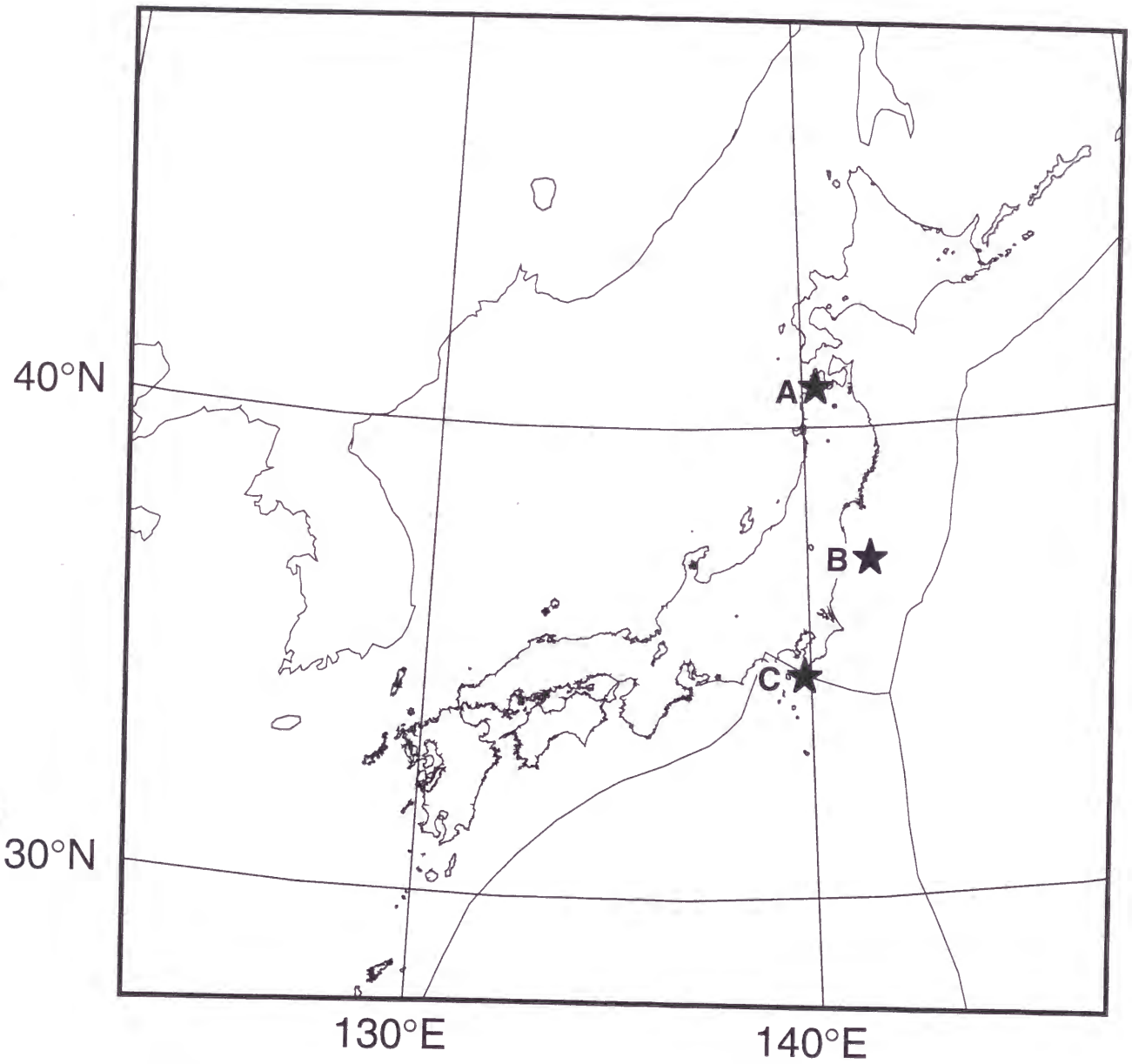

Fig. 1-12

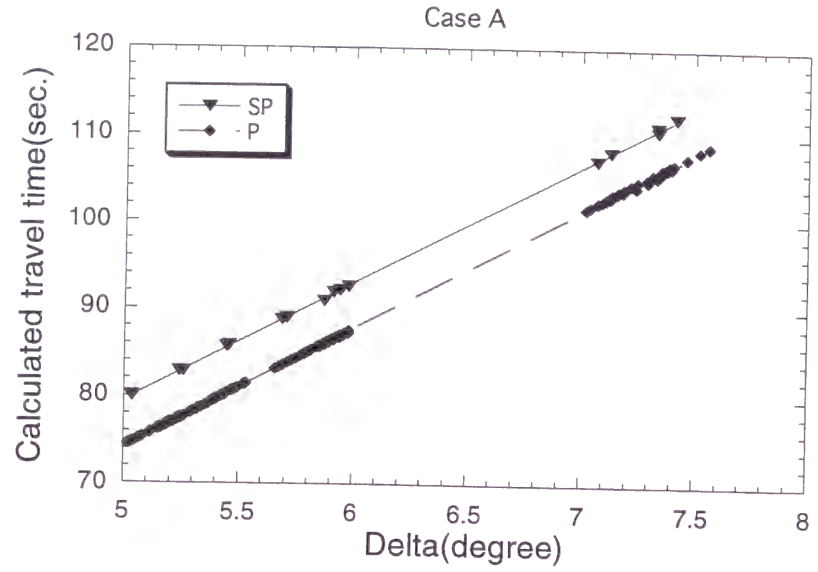
Case A
Calculated travel time(sec.)
120
110
100
90
80
70
SP
P
5
5.5
6
6.5
7
7.5
8
Delta(degree)

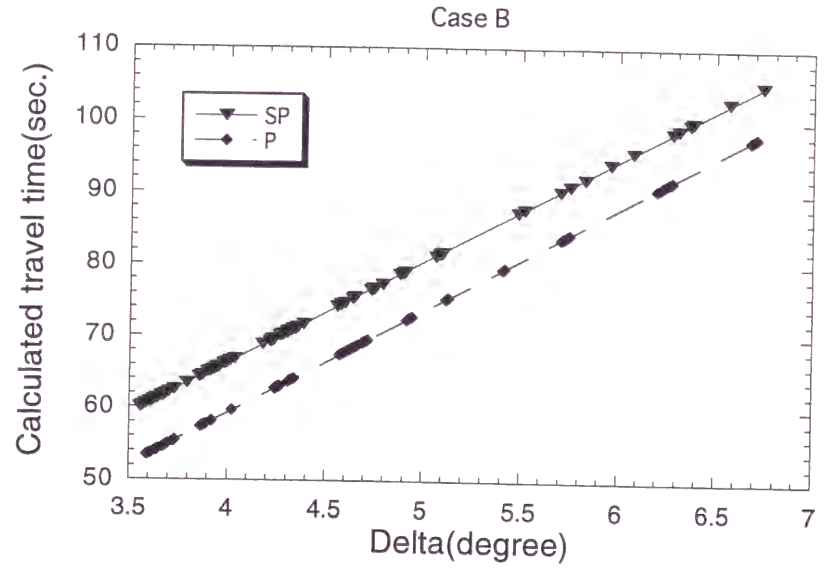
Case B
Calculated travel time(sec.)
110
100
90
80
70
60
50
SP
P
3.5
4
4.5
5
5.5
6
6.5
7
Delta(degree)

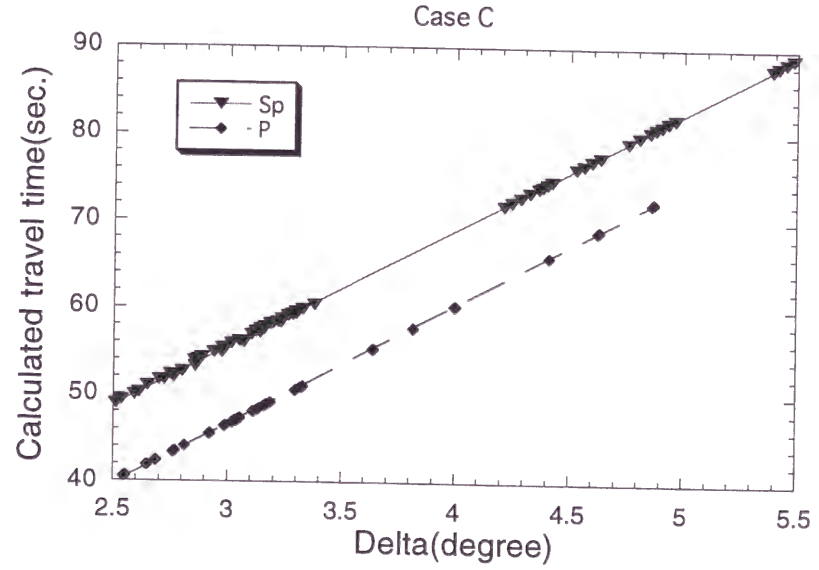
Case C
Calculated travel time(sec.)
90
80
70
60
50
40
Sp
P
2.5
3
3.5
4
4.5
5
5.5
Delta(degree)

Fig.1-13

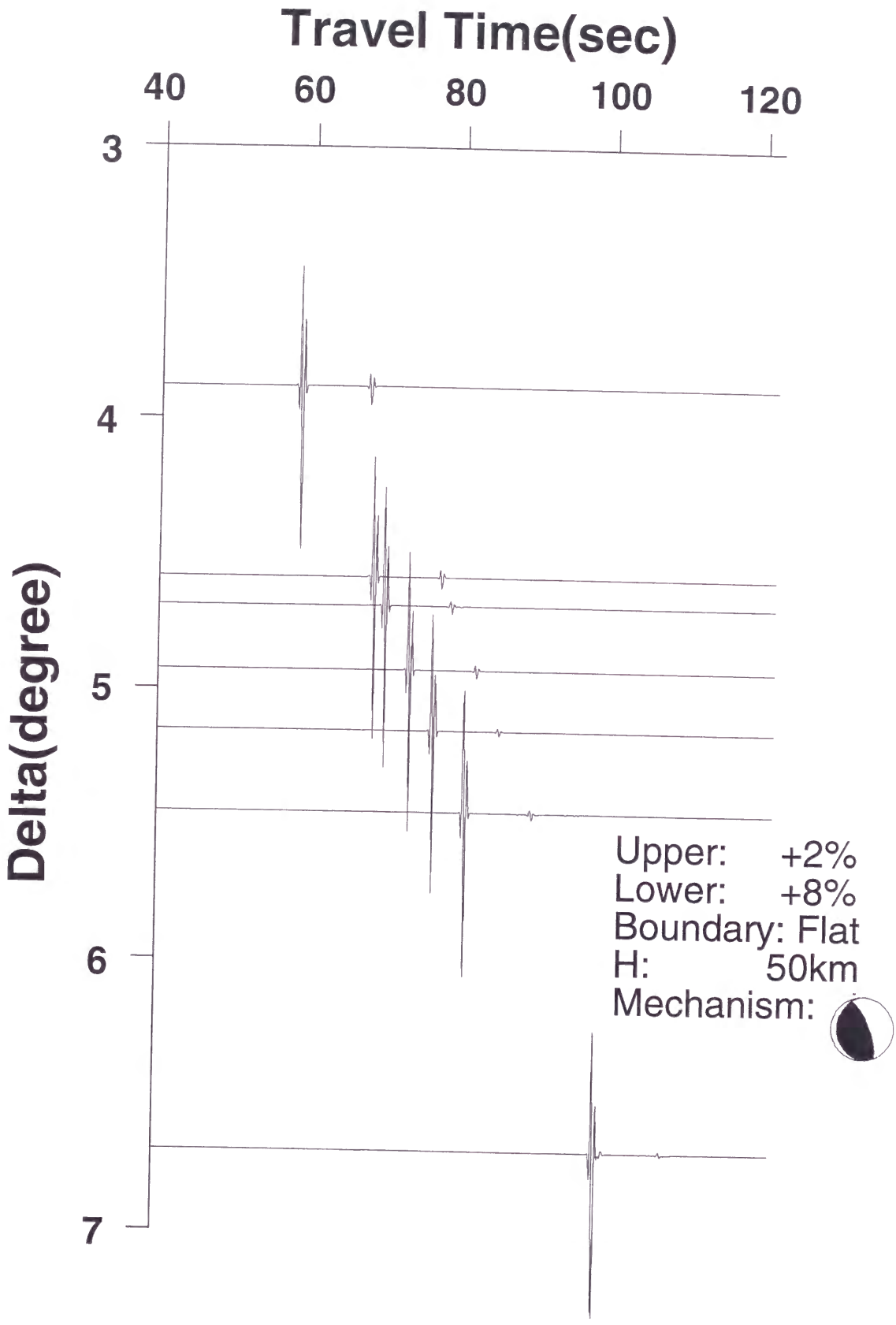
Travel Time(sec)
40
60
80
100
120
3
4
5
6
7
Delta(degree)
Upper: +2%
Lower: +8%
Boundary: Flat
H: 50km
Mechanism:

Fig. 1-14

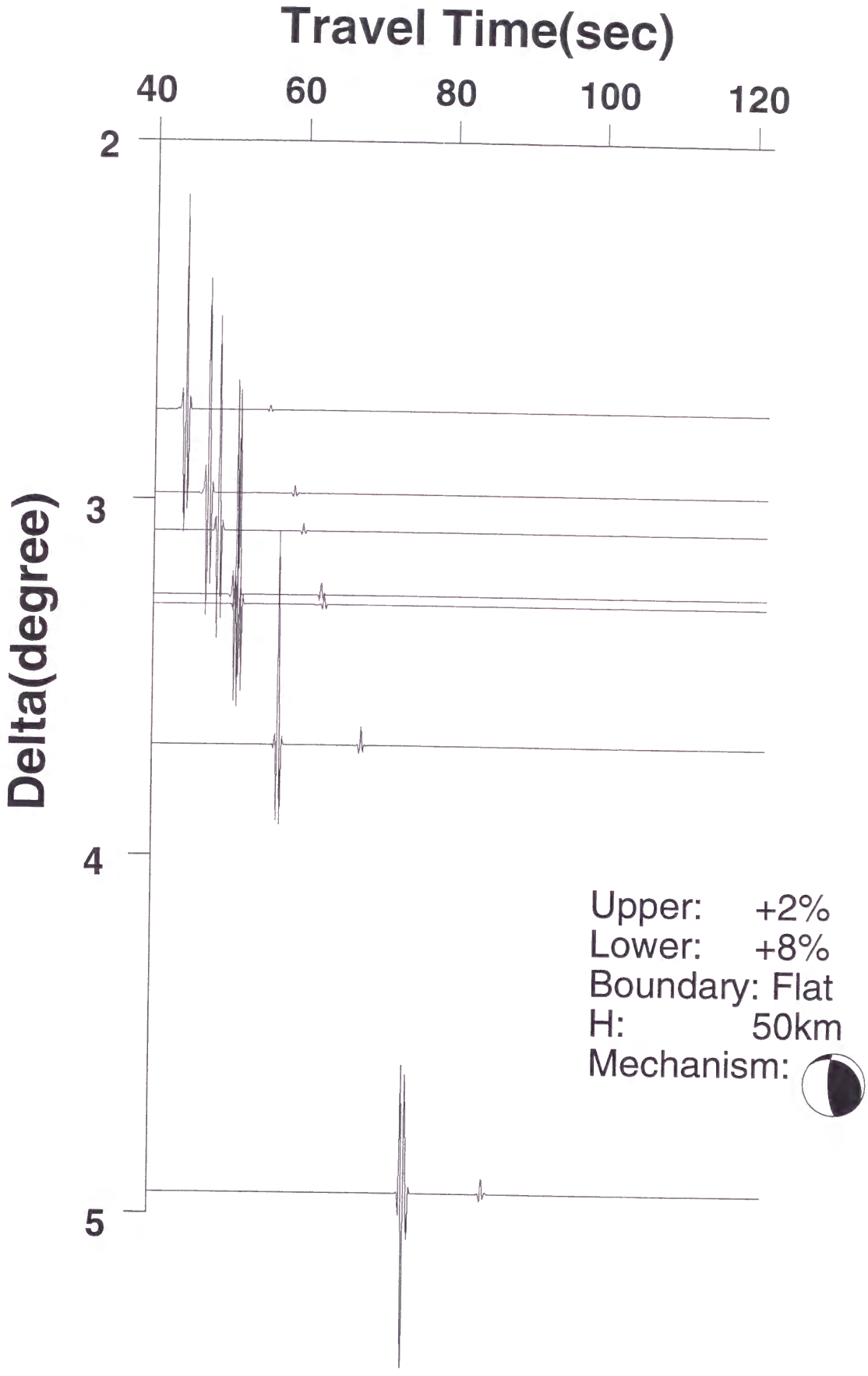
Travel Time(sec)
40
60
80
100
120
2
3
4
5
Delta(degree)
Upper: +2%
Lower: +8%
Boundary: Flat
H: 50km
Mechanism:

Fig. 1-15

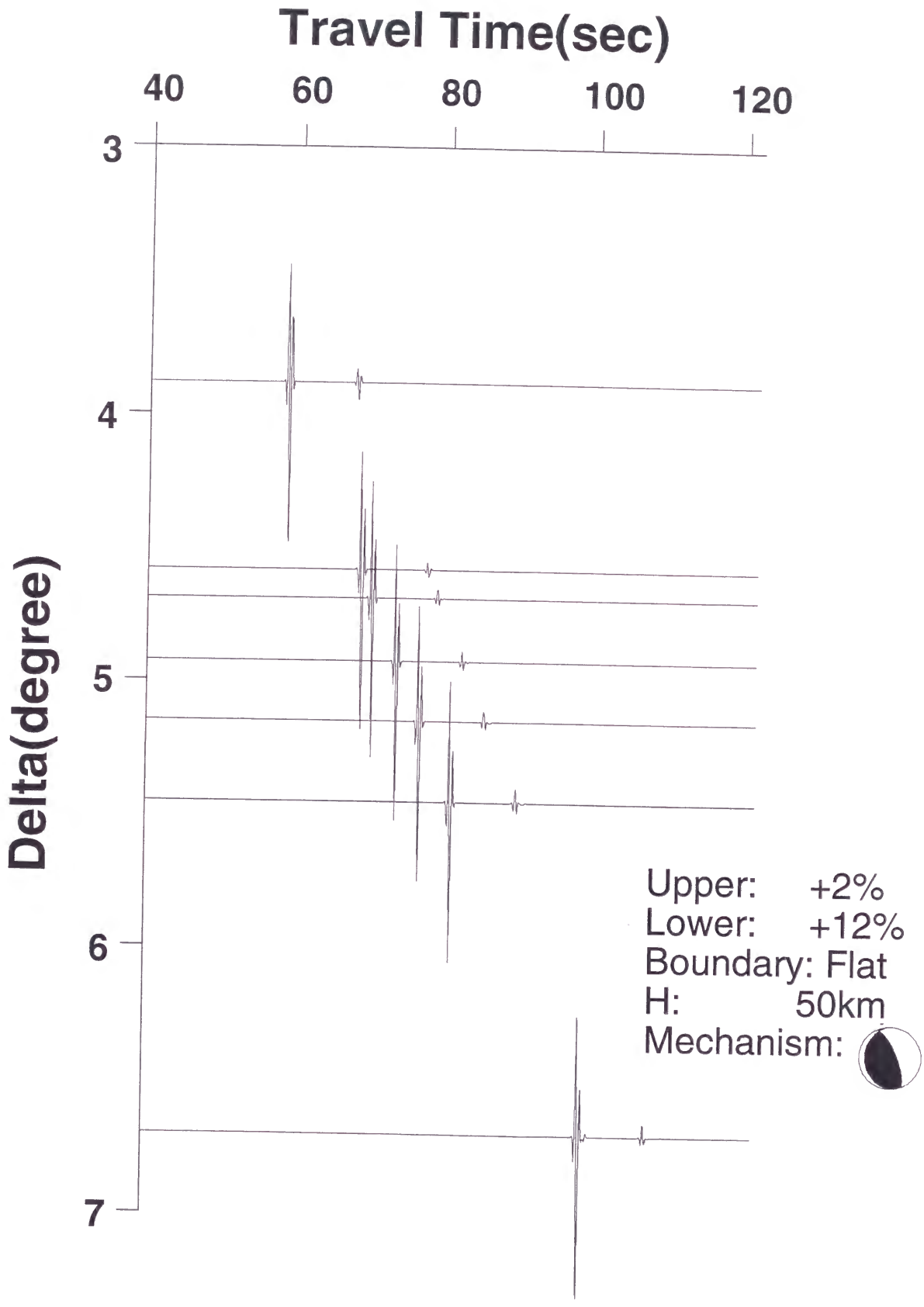
Travel Time(sec)
40
60
80
100
120
3
4
5
6
7
Delta(degree)
Upper: +2%
Lower: +12%
Boundary: Flat
H: 50km
Mechanism:

Fig.1-16

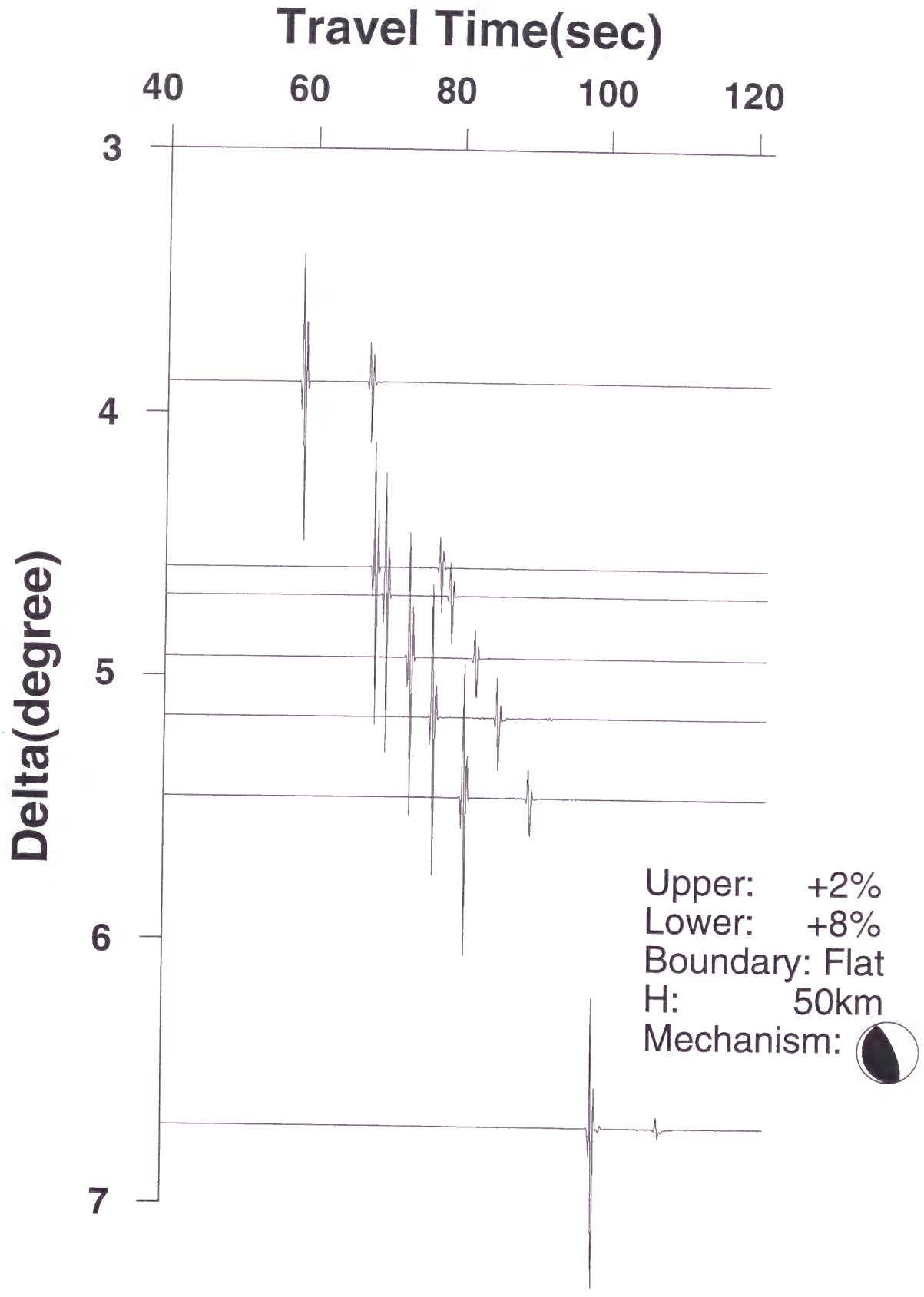
Travel Time(sec)
40
60
80
100
120
3
4
5
6
7
Delta(degree)
Upper: +2%
Lower: +8%
Boundary: Flat
H: 50km
Mechanism:

Fig. 1-17

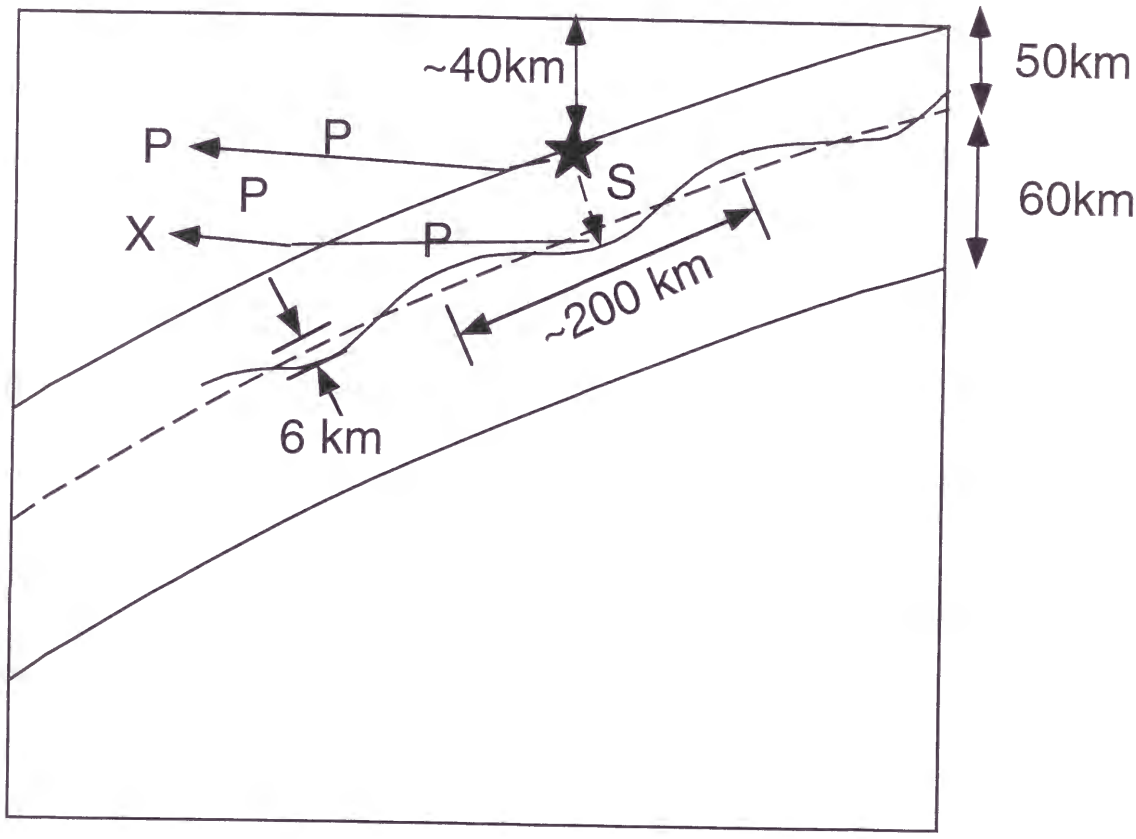

Fig. 1-18

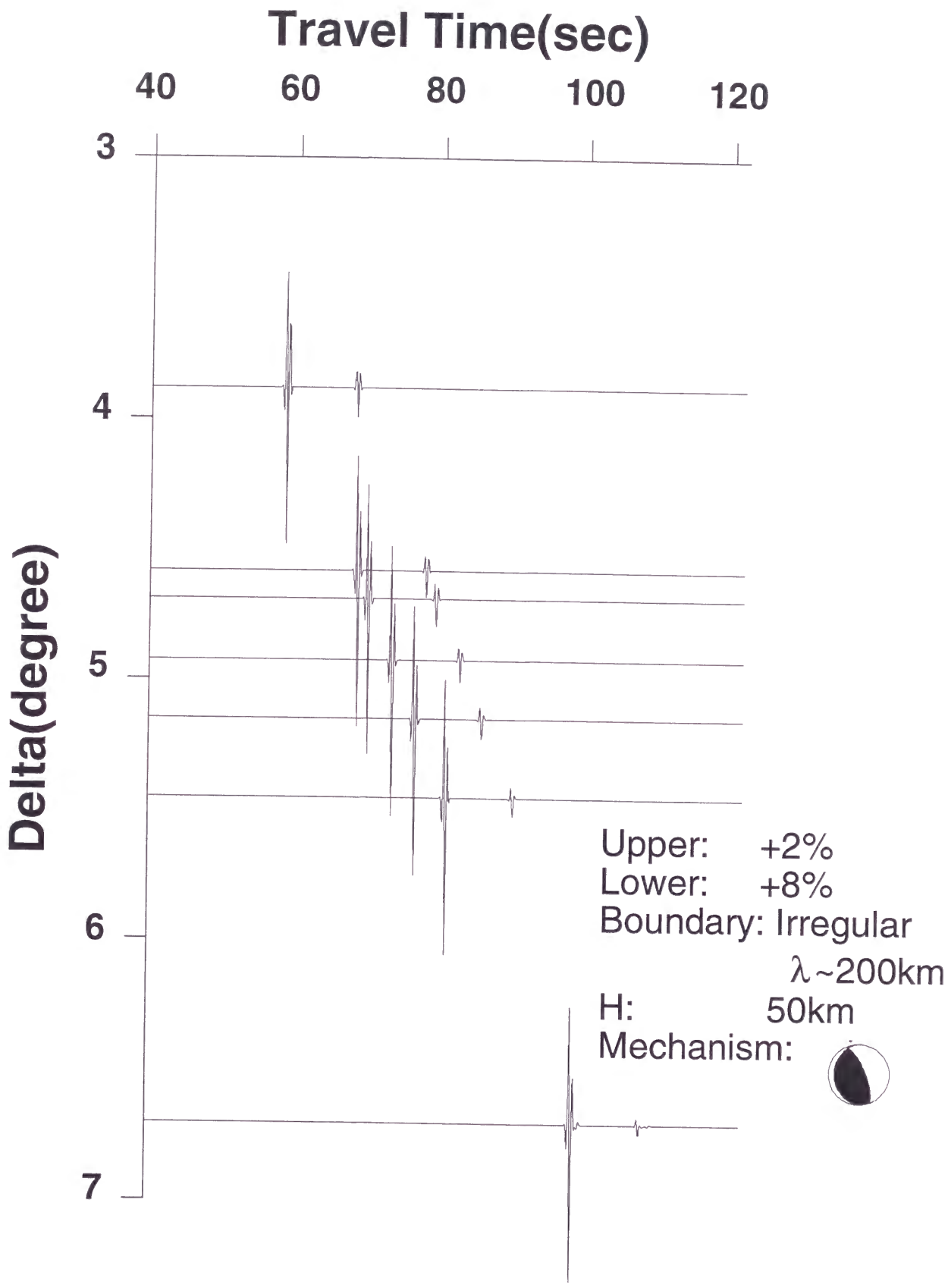
Travel Time(sec)
40
60
80
100
120
3
4
5
6
7
Delta(degree)
Upper: +2%
Lower: +8%
Boundary: Irregular
λ~200km
H: 50km
Mechanism:

Fig. 1-19

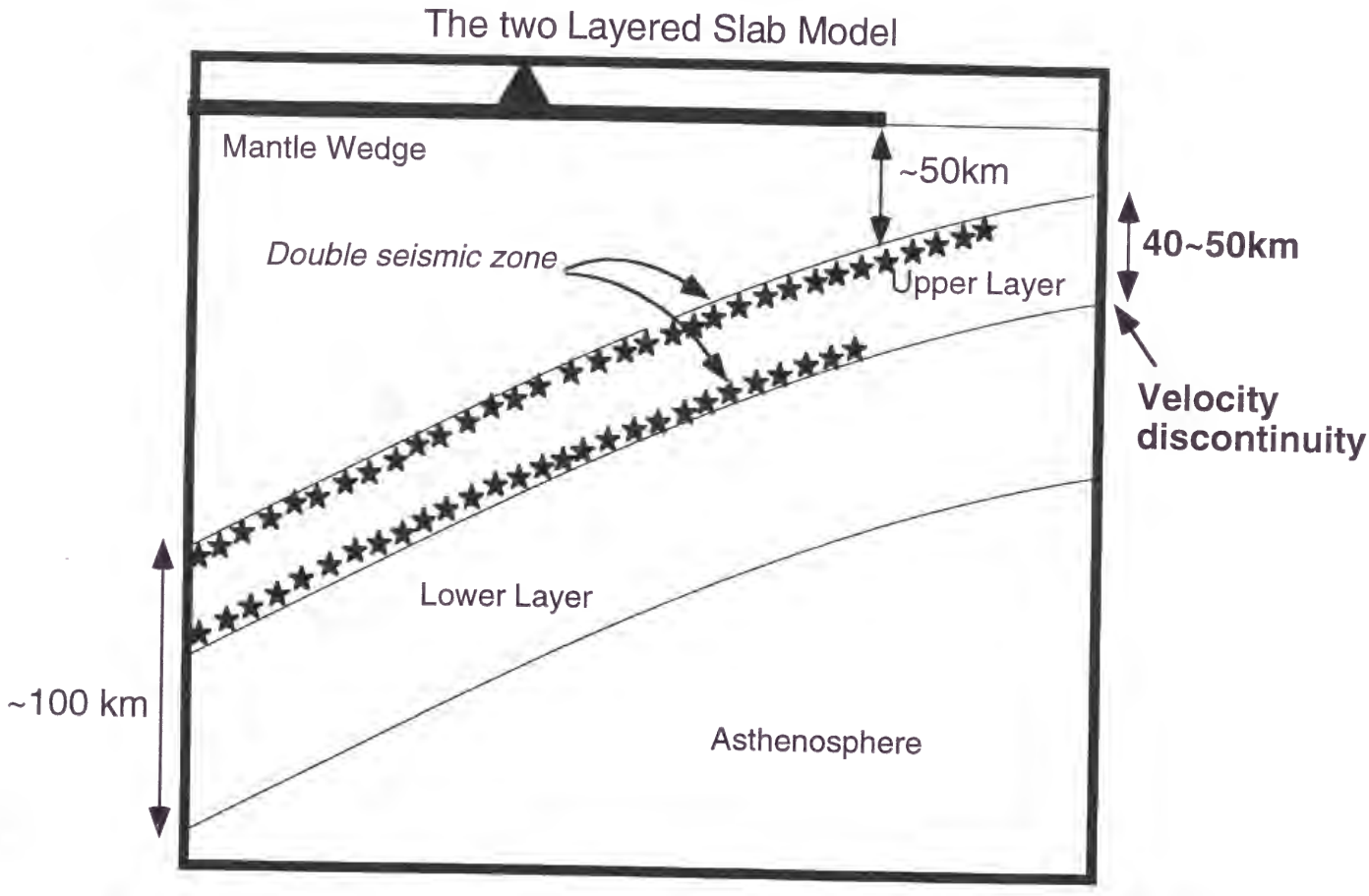
The two Layered Slab Model
Mantle Wedge
~50km
40~50km
Double seismic zone
Upper Layer
Velocity
discontinuity
Lower Layer
~100 km
Asthenosphere

Fig. 1-20

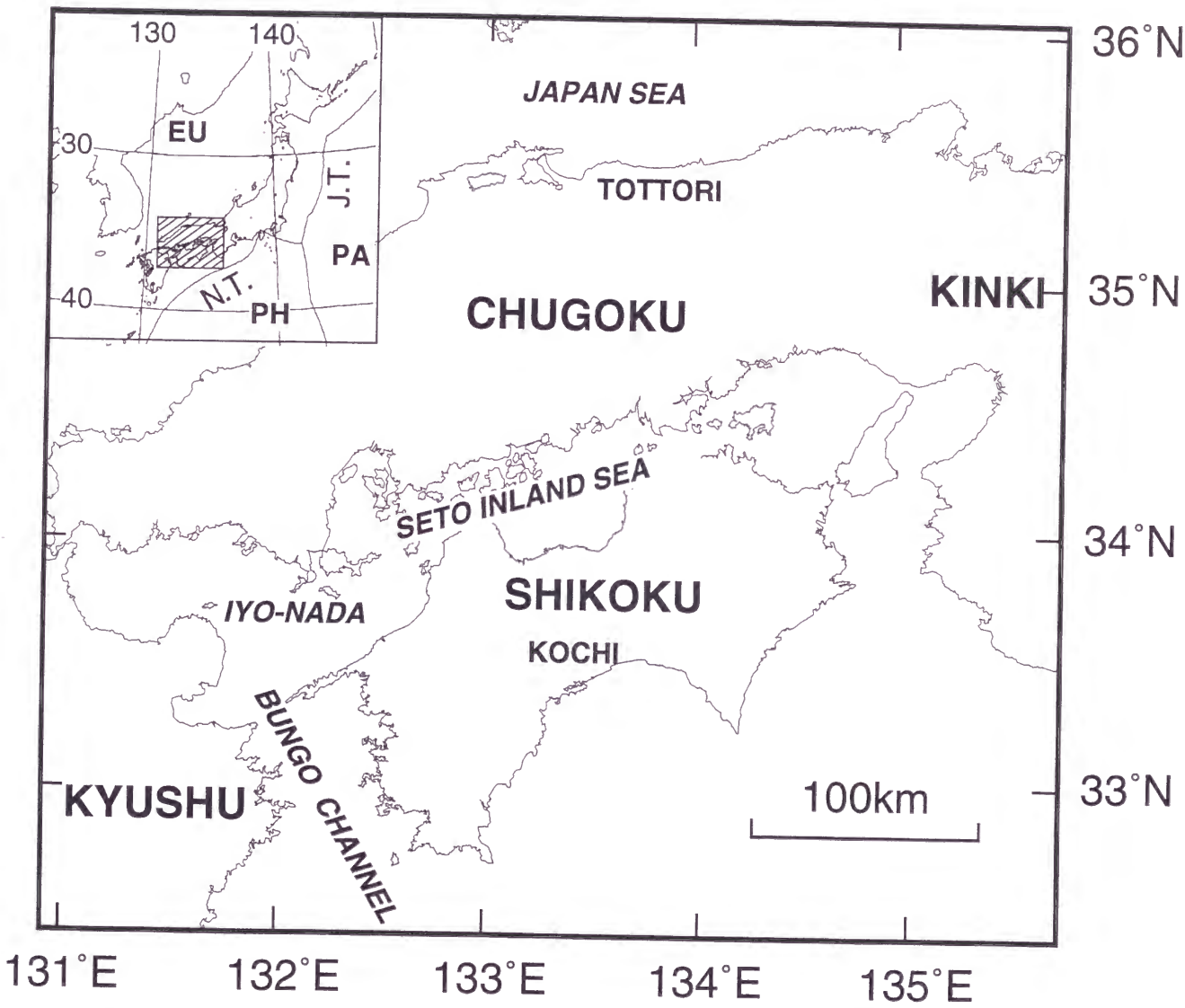
130
140
30
40
EU
J.T.
PA
N.T.
PH
JAPAN SEA
TOTTORI
KINKI
CHUGOKU
SETO INLAND SEA
IYO-NADA
SHIKOKU
KOCHI
BUNGO CHANNEL
KYUSHU
100km
36°N
35°N
34°N
33°N
131°E
132°E
133°E
134°E
135°E

Fig.2-1

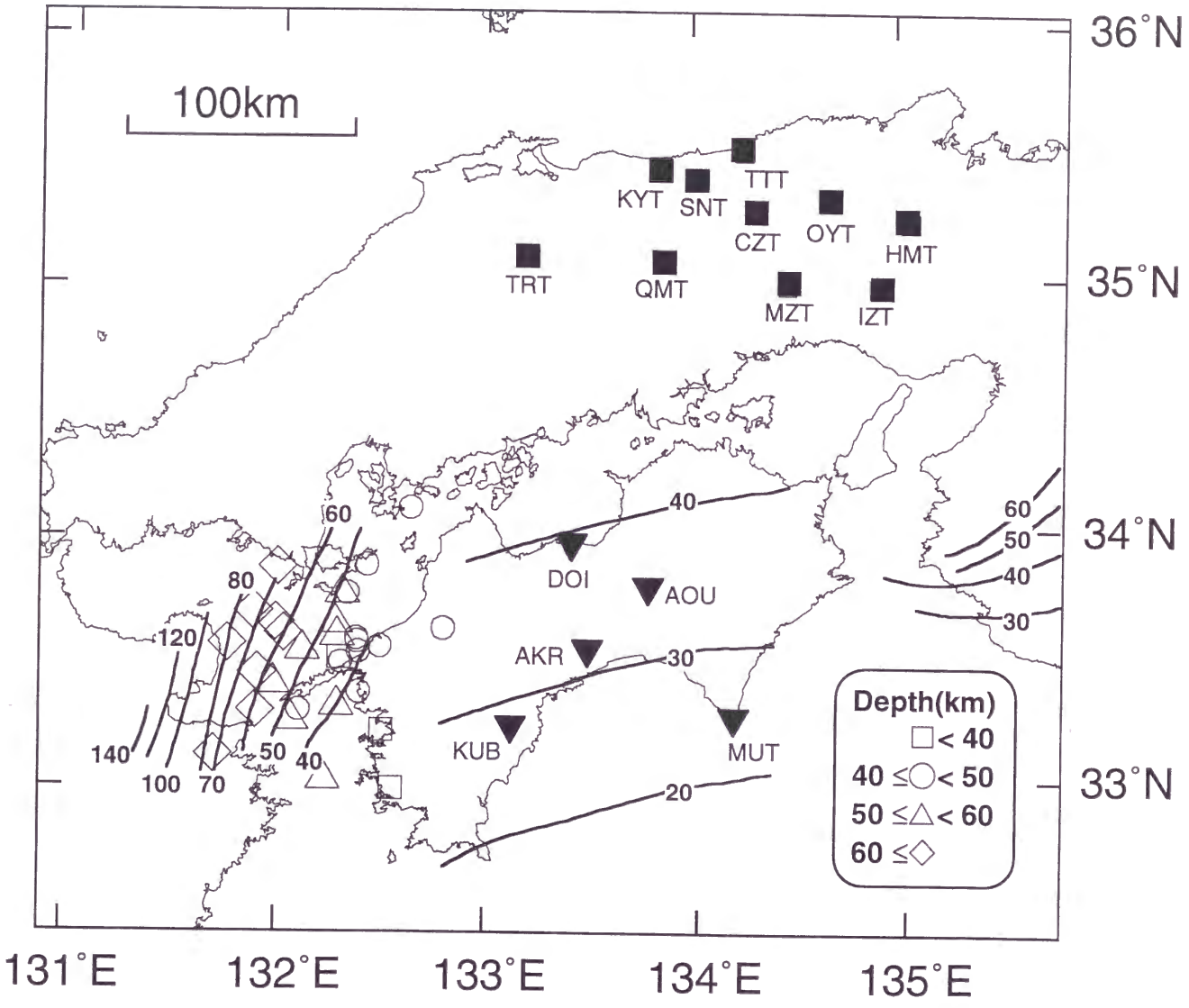
100km
KYT
SNT
TTT
CZT
OYT
HMT
TRT
QMT
MZT
IZT
DOI
AOU
AKR
KUB
MUT
40
60
80
120
140
100
70
50
40
30
20
60
50
40
30
Depth(km)
□< 40
40 ≤○< 50
50 ≤△< 60
60 ≤◇
36°N
35°N
34°N
33°N
131°E
132°E
133°E
134°E
135°E

Fig.2-2

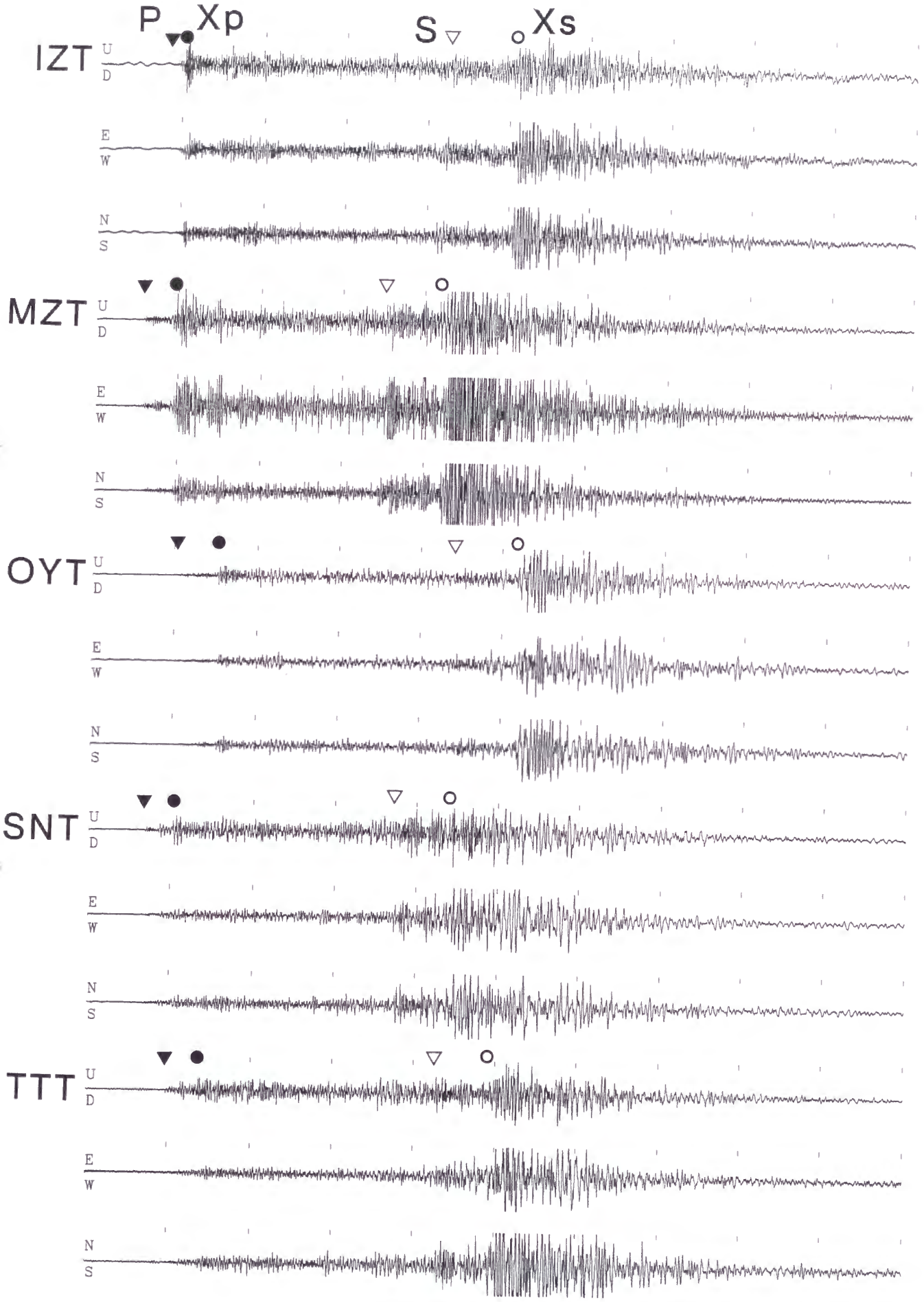

Fig.2-3

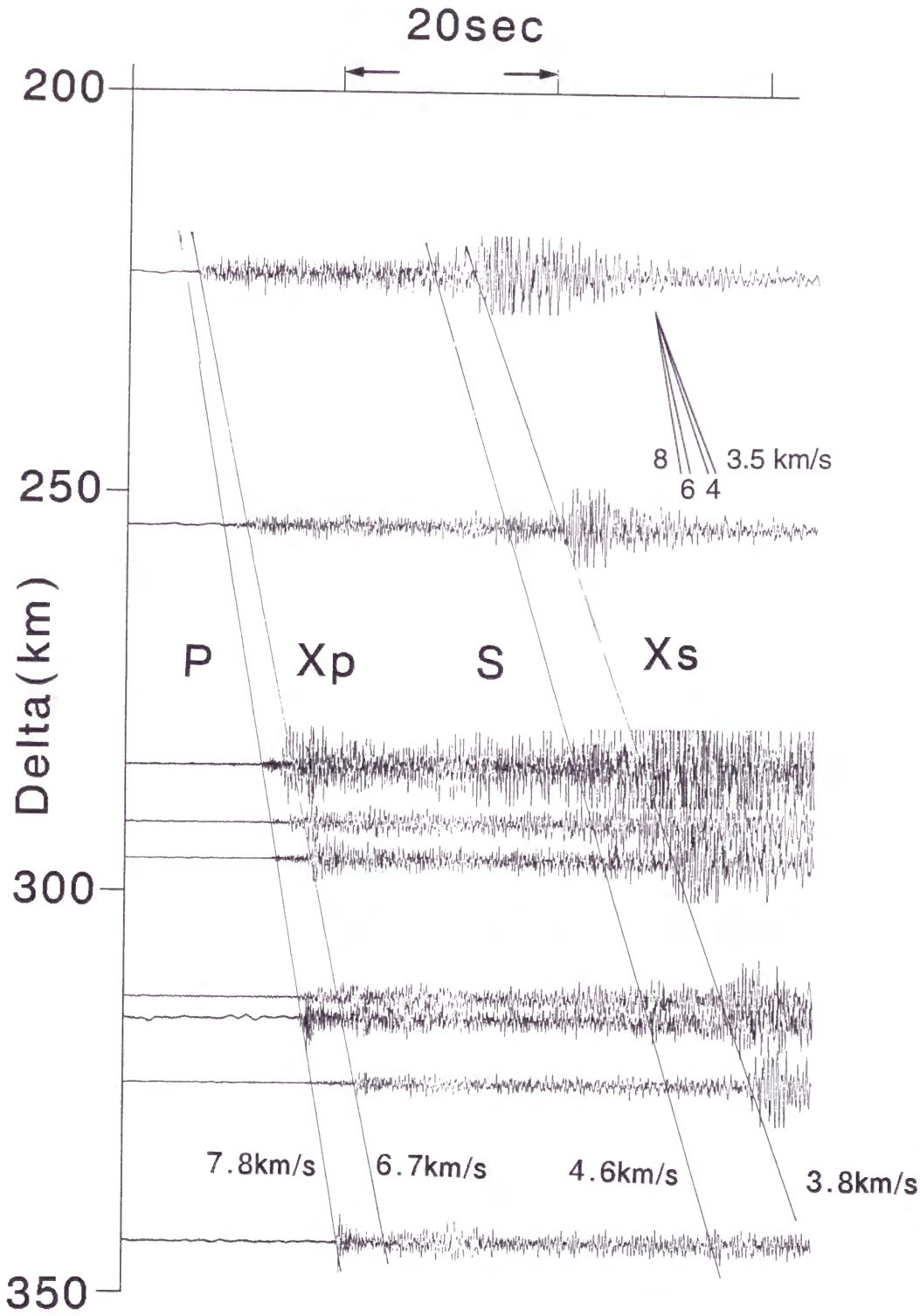
20sec
200
250
300
350
Delta(km)
8
6
4
3.5 km/s
P
Xp
S
Xs
7.8km/s
6.7km/s
4.6km/s
3.8km/s

Fig.2-4

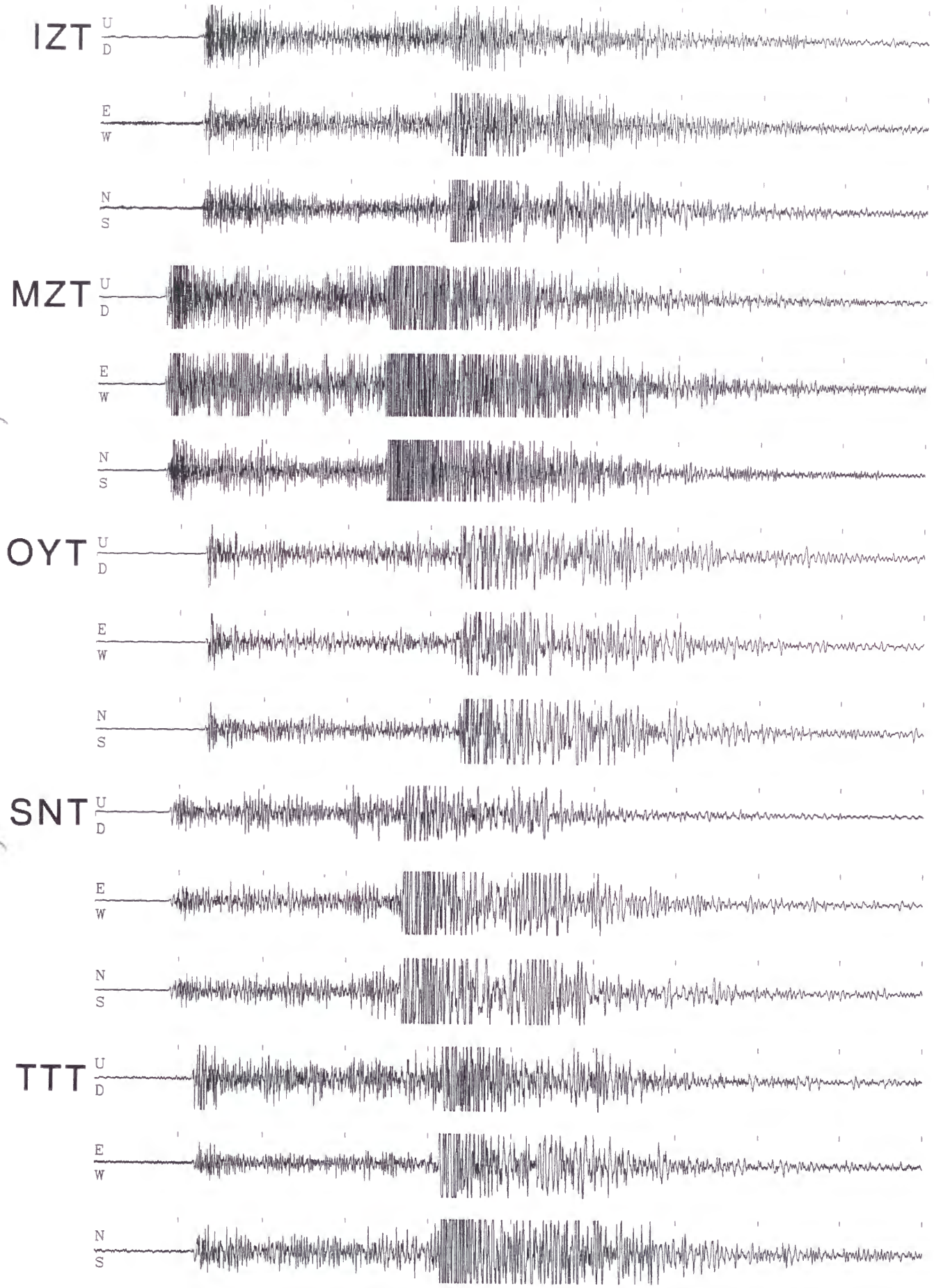

Fig. 2-5

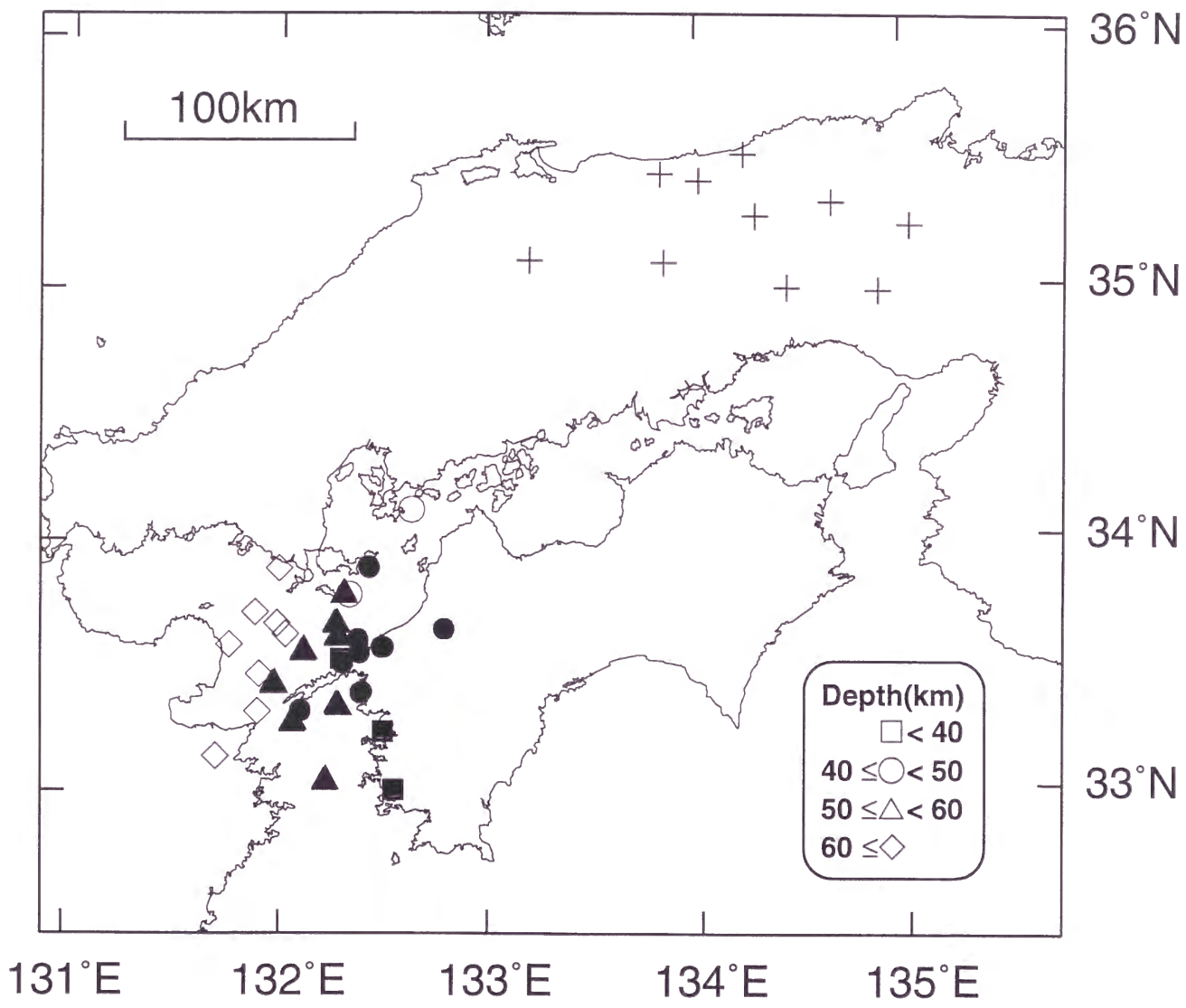
100km
36°N
35°N
34°N
33°N
131°E
132°E
133°E
134°E
135°E
Depth(km)
□< 40
40 ≤○< 50
50 ≤△< 60
60 ≤◇

Fig.2-6

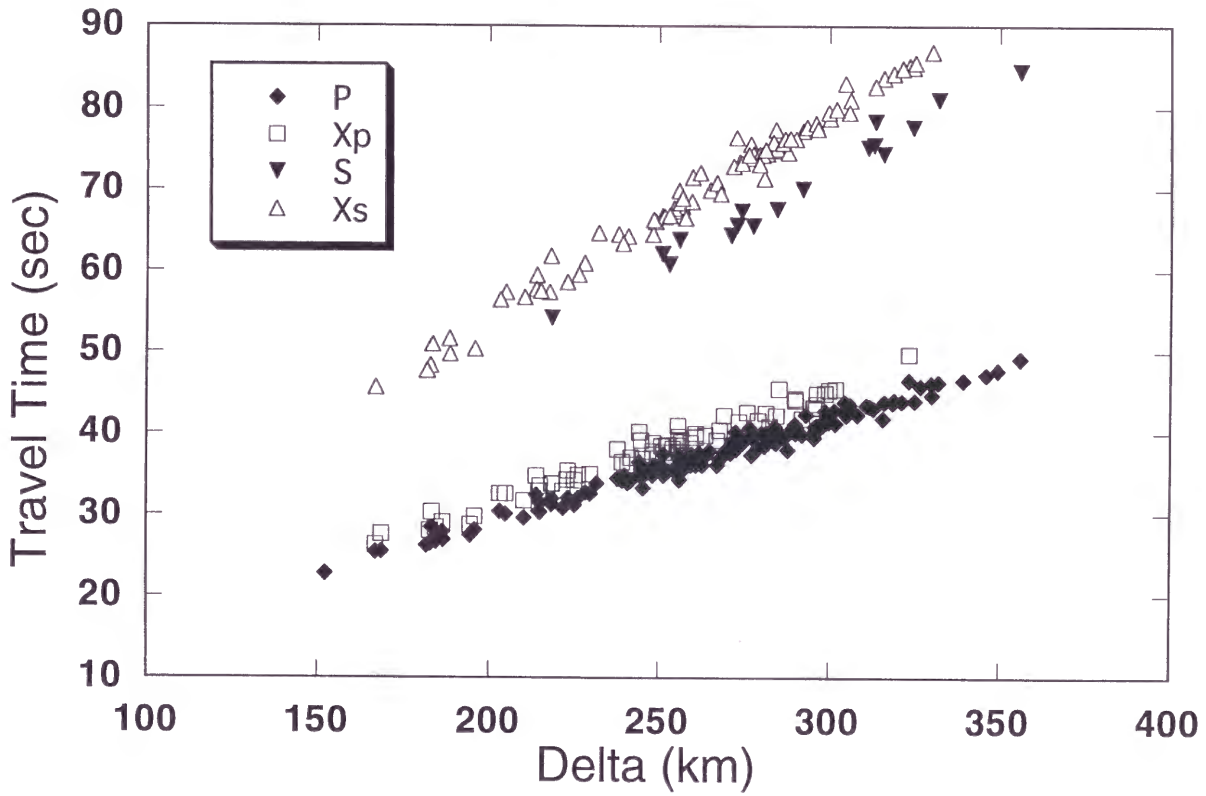
P
Xp
S
Xs
Travel Time (sec)
Delta (km)
10
20
30
40
50
60
70
80
90
100
150
200
250
300
350
400

Fig. 2-7

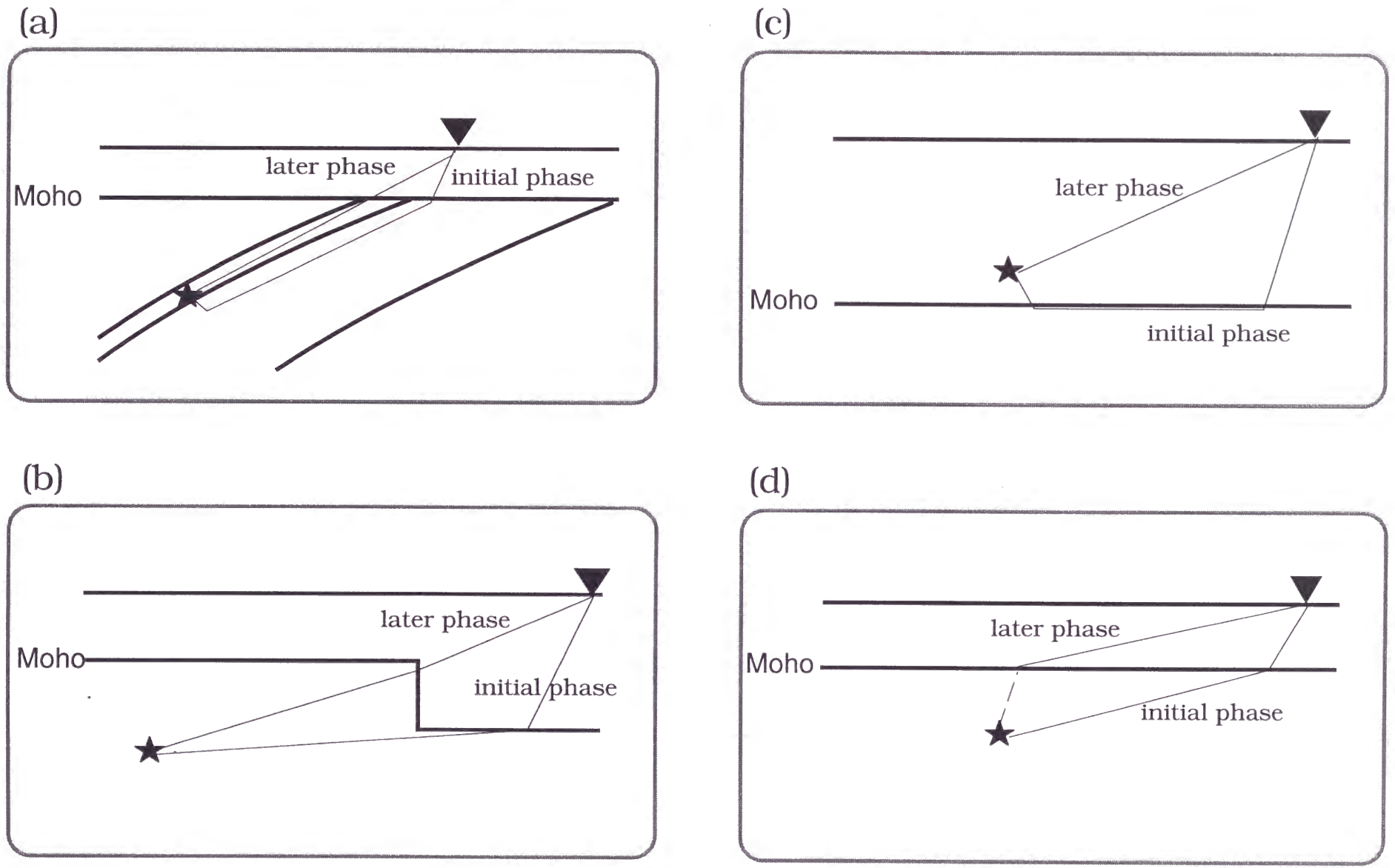
(a)
later phase
initial phase
Moho
(c)
later phase
Moho
initial phase
(b)
later phase
Moho
initial phase
(d)
later phase
Moho
initial phase

Fig.2-8

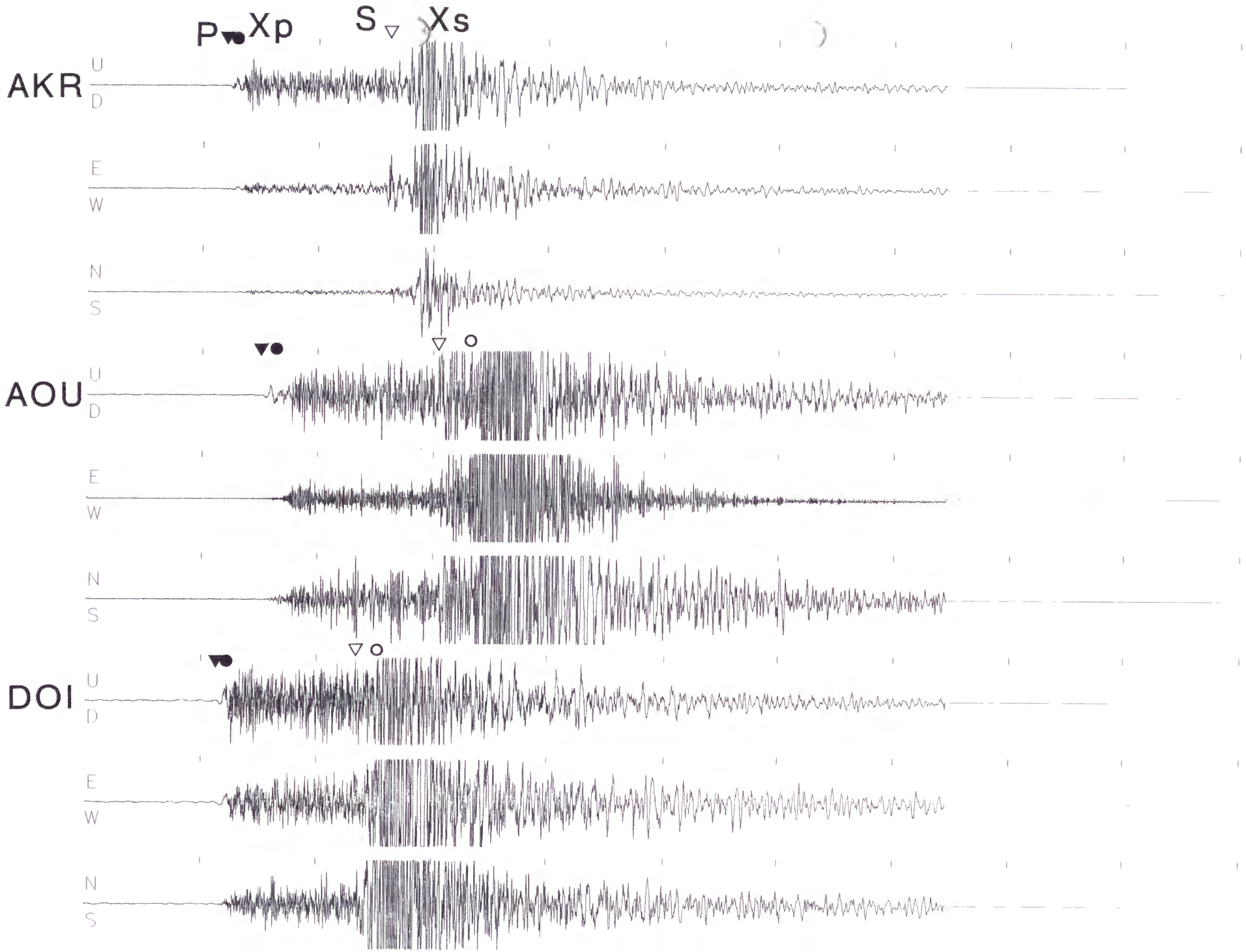

Fig. 2-9

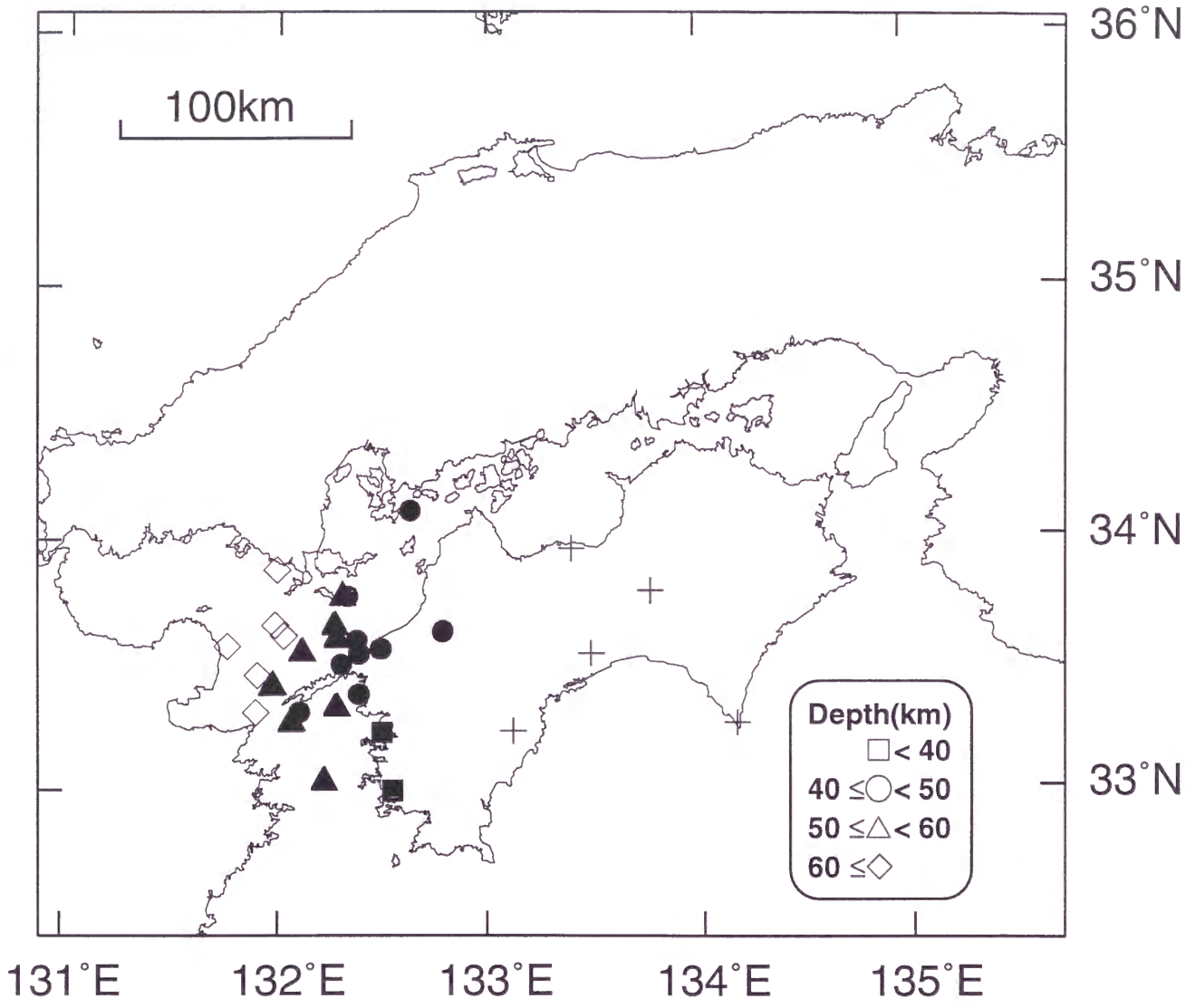
100km
36°N
35°N
34°N
33°N
131°E
132°E
133°E
134°E
135°E
Depth(km)
□< 40
40 ≤○< 50
50 ≤△< 60
60 ≤◇

Fig. 2-10

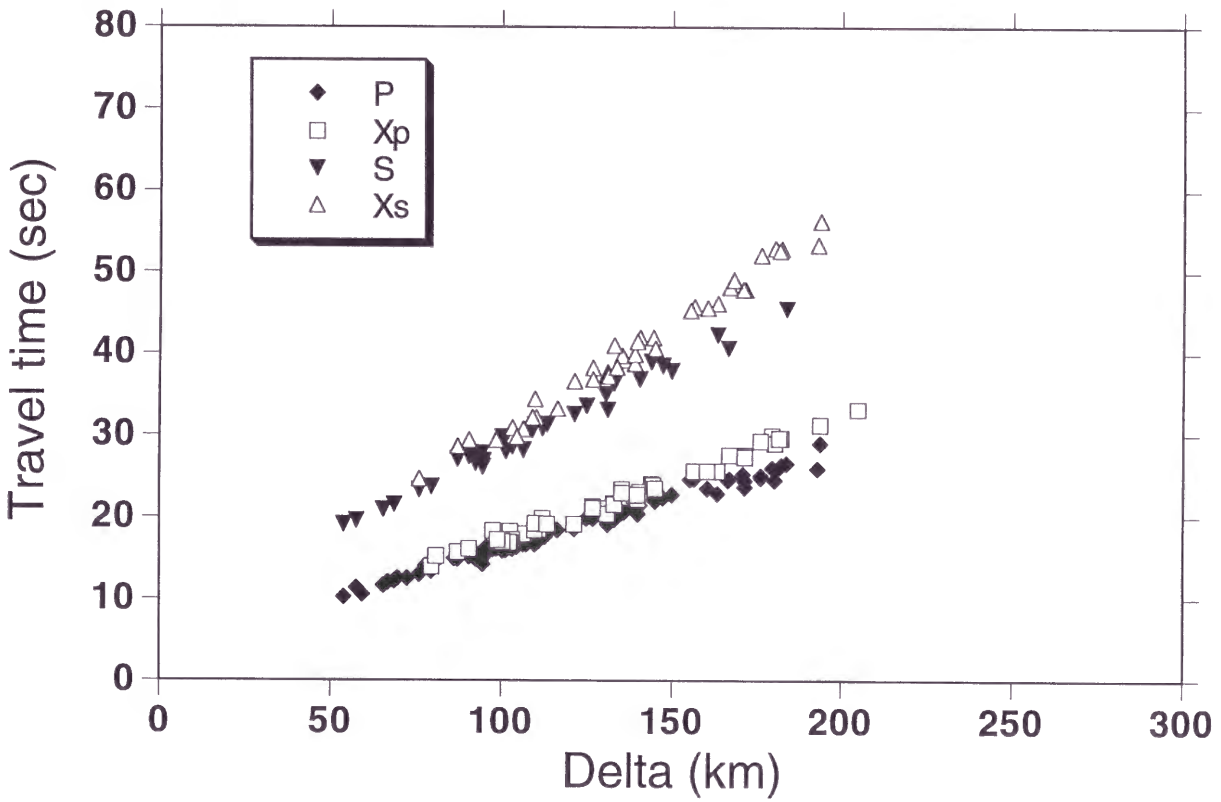
Travel time (sec)
Delta (km)
P
Xp
S
Xs
0
10
20
30
40
50
60
70
80
0
50
100
150
200
250
300

Fig.2-11

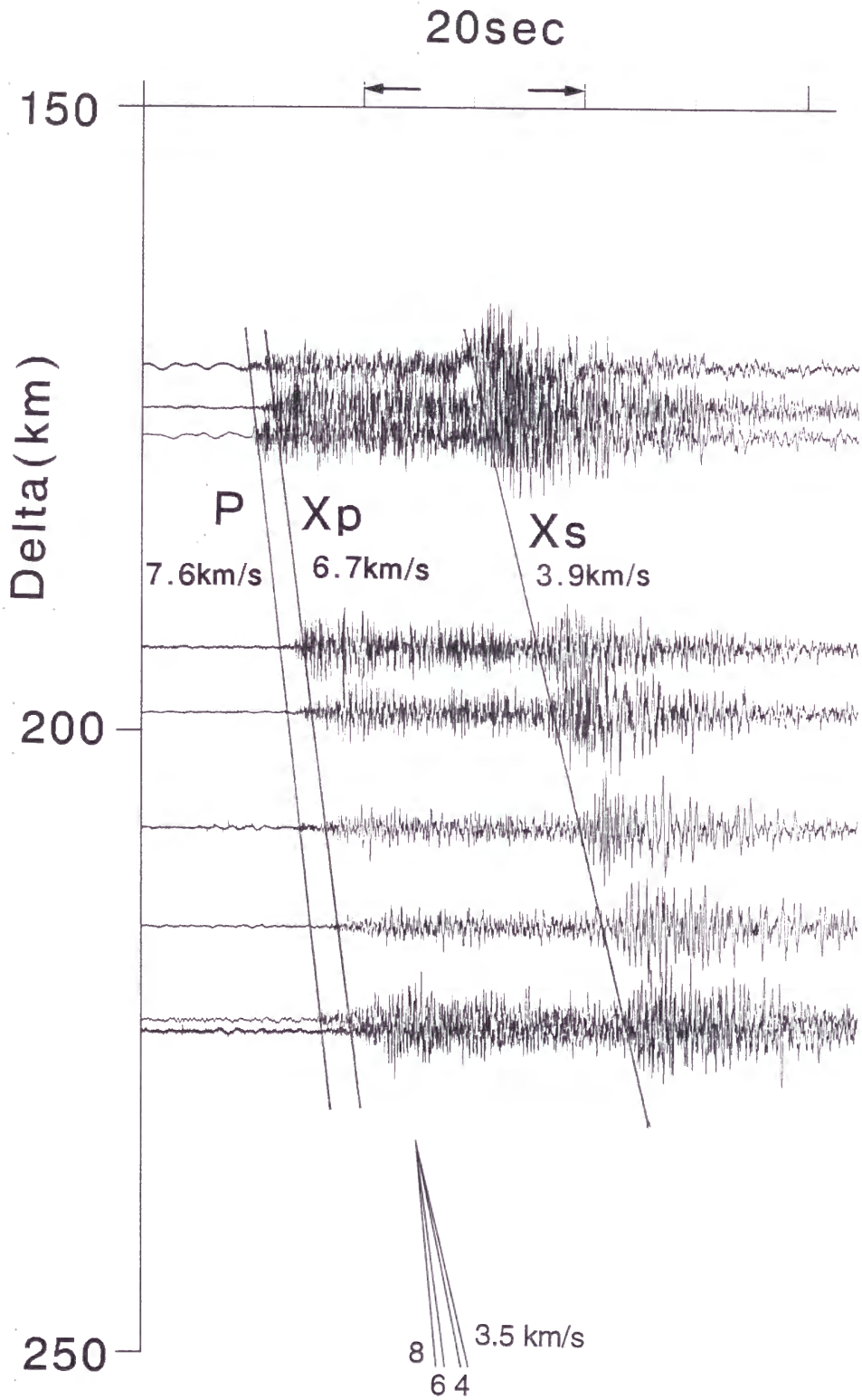

Fig.2-12

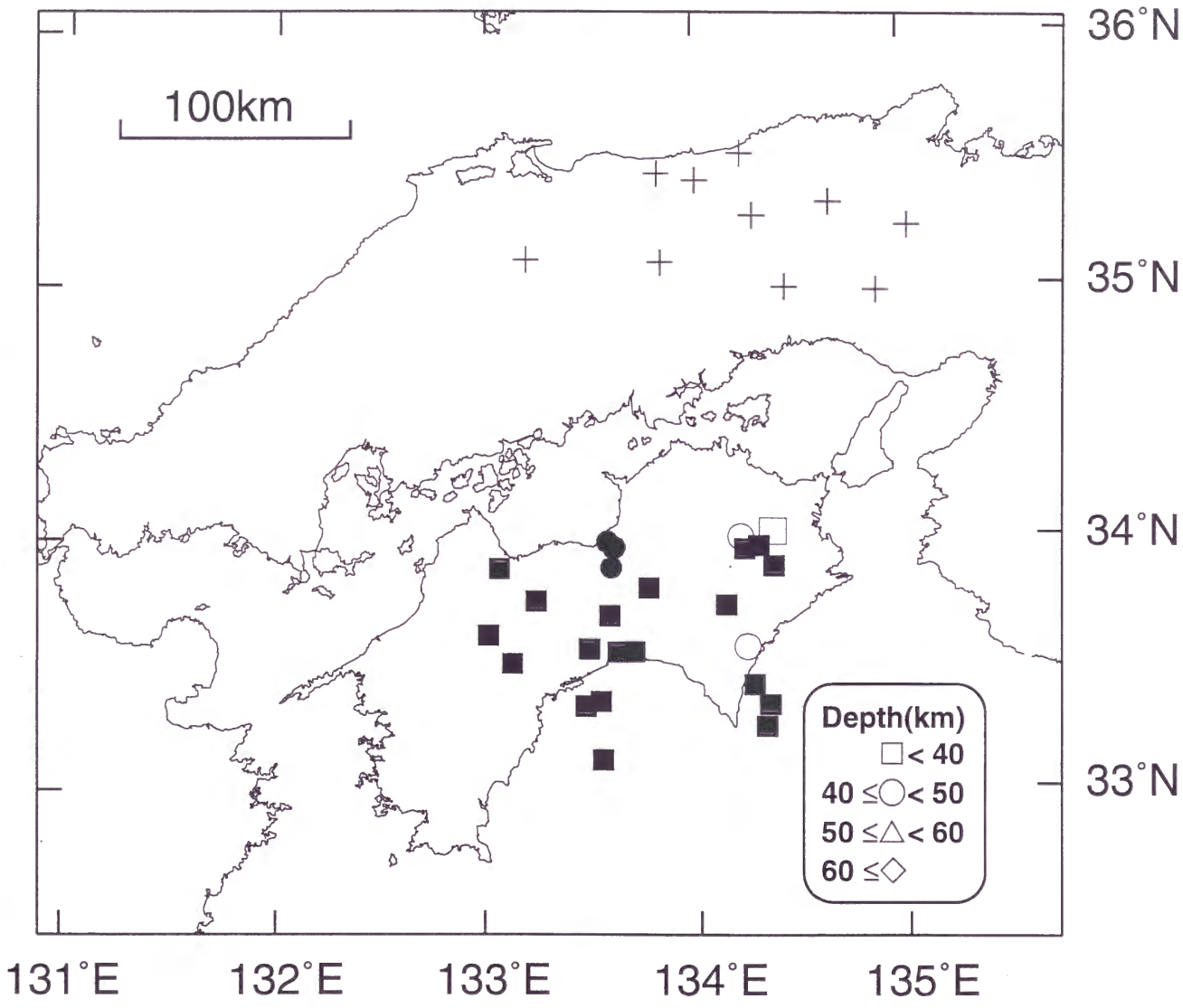
100km
36°N
35°N
34°N
33°N
131°E
132°E
133°E
134°E
135°E
Depth(km)
□< 40
40 ≤○< 50
50 ≤△< 60
60 ≤◇

Fig.2-13

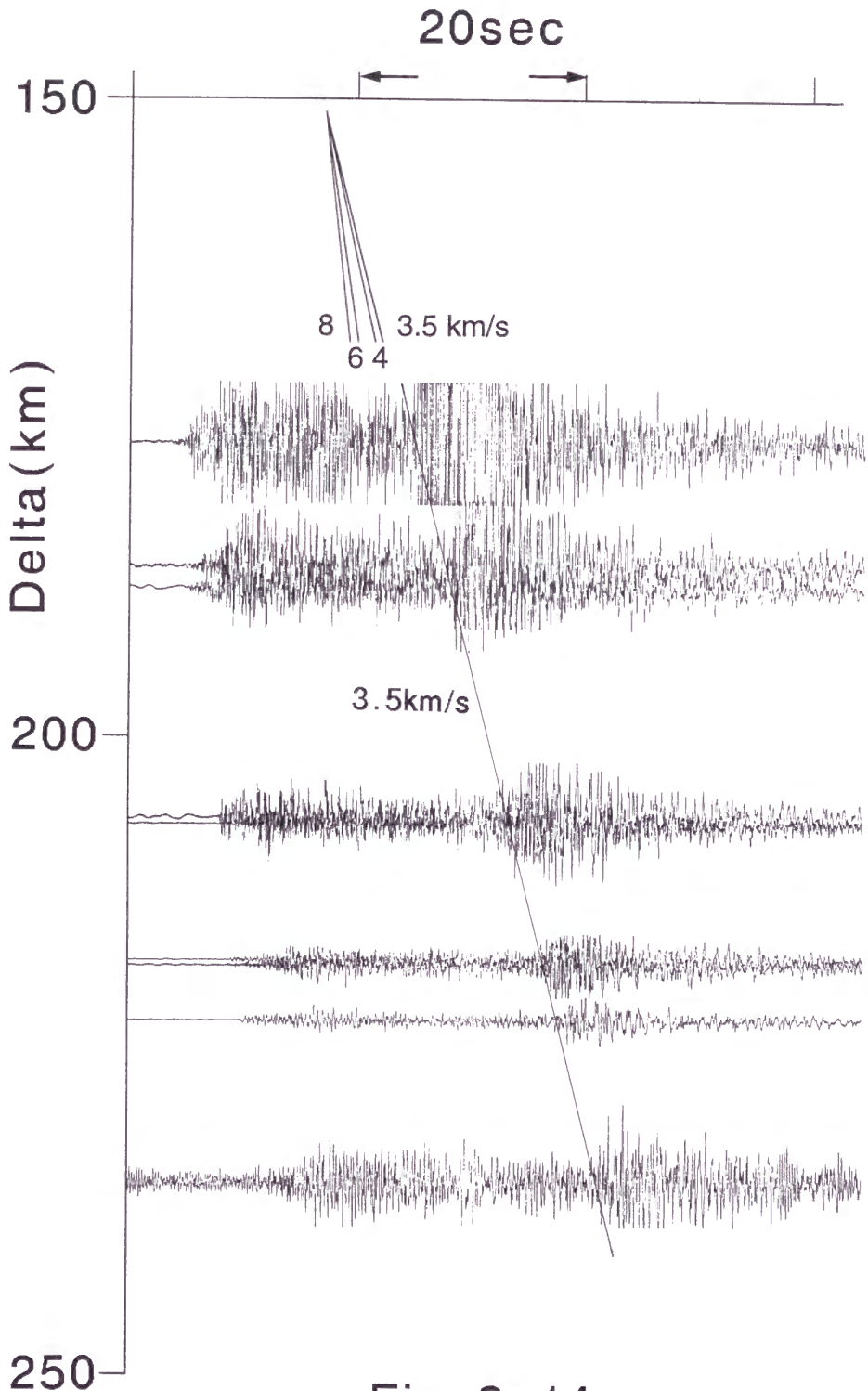

Fig. 2-14

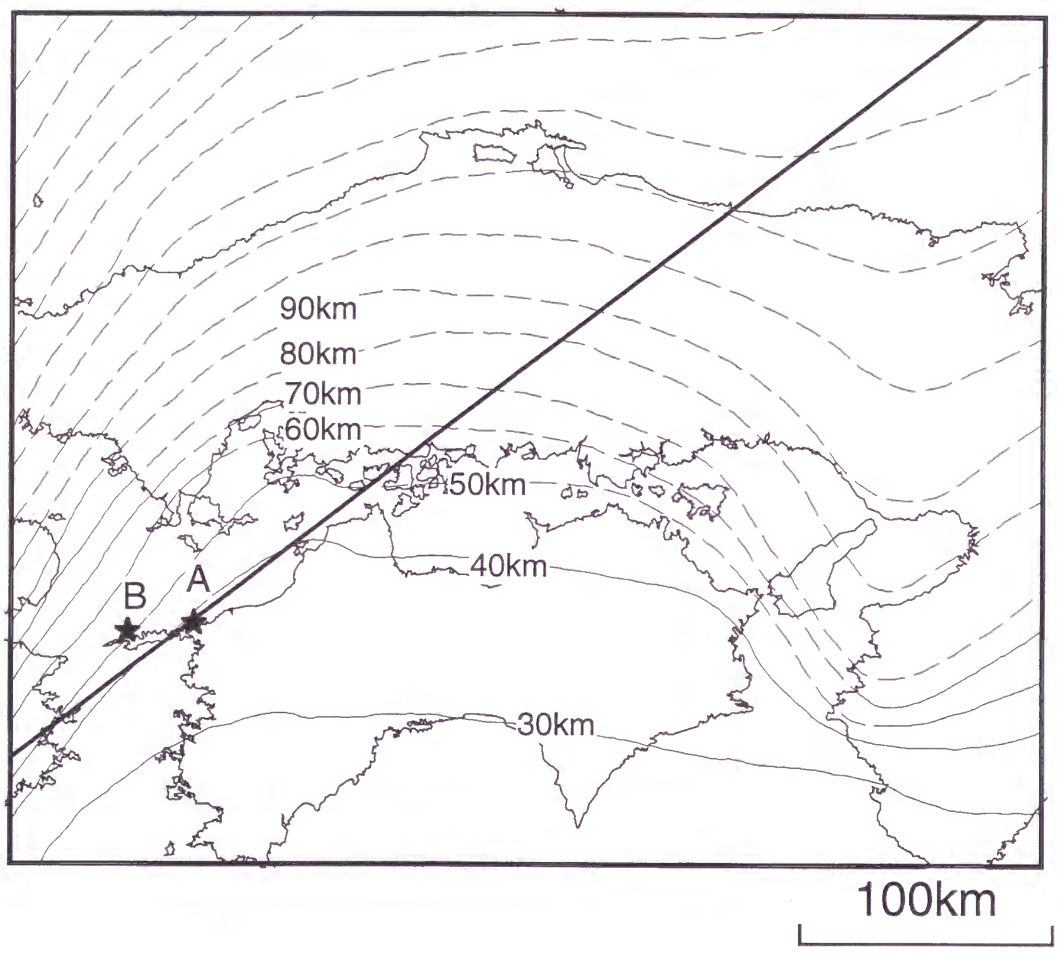

Fig.2-15a

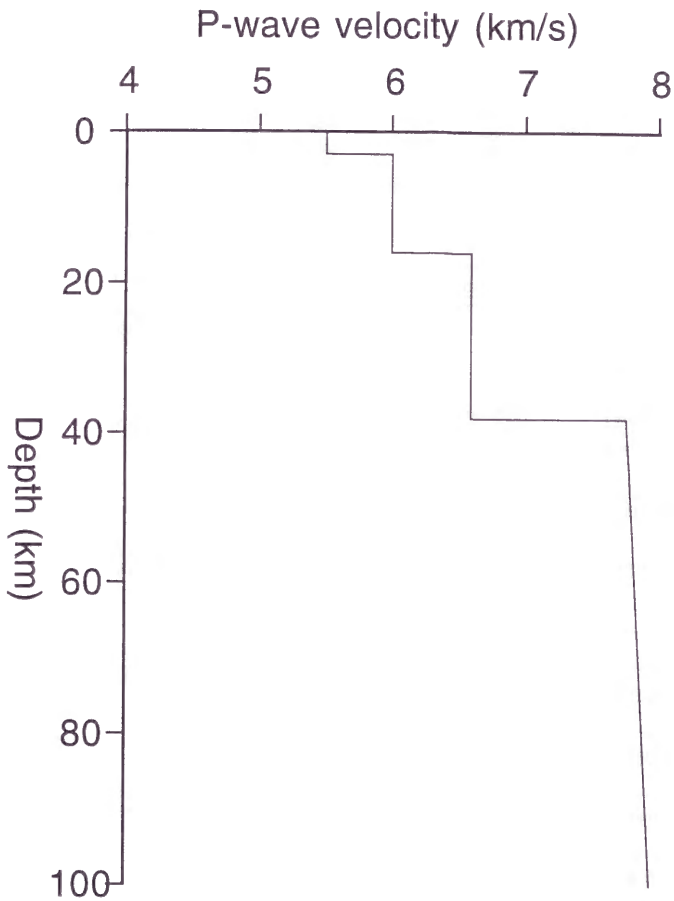

Fig. 2-15b

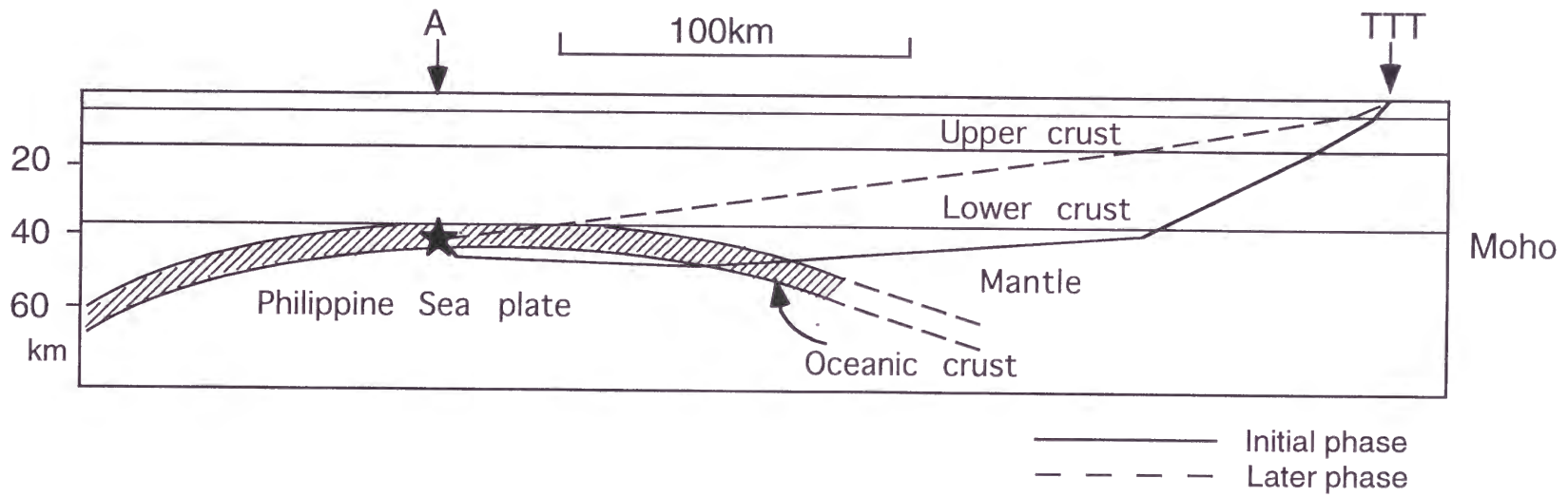
A
100km
TTT
Upper crust
Lower crust
Moho
20
40
60
km
Philippine Sea plate
Mantle
Oceanic crust
Initial phase
Later phase

Fig.2-15c

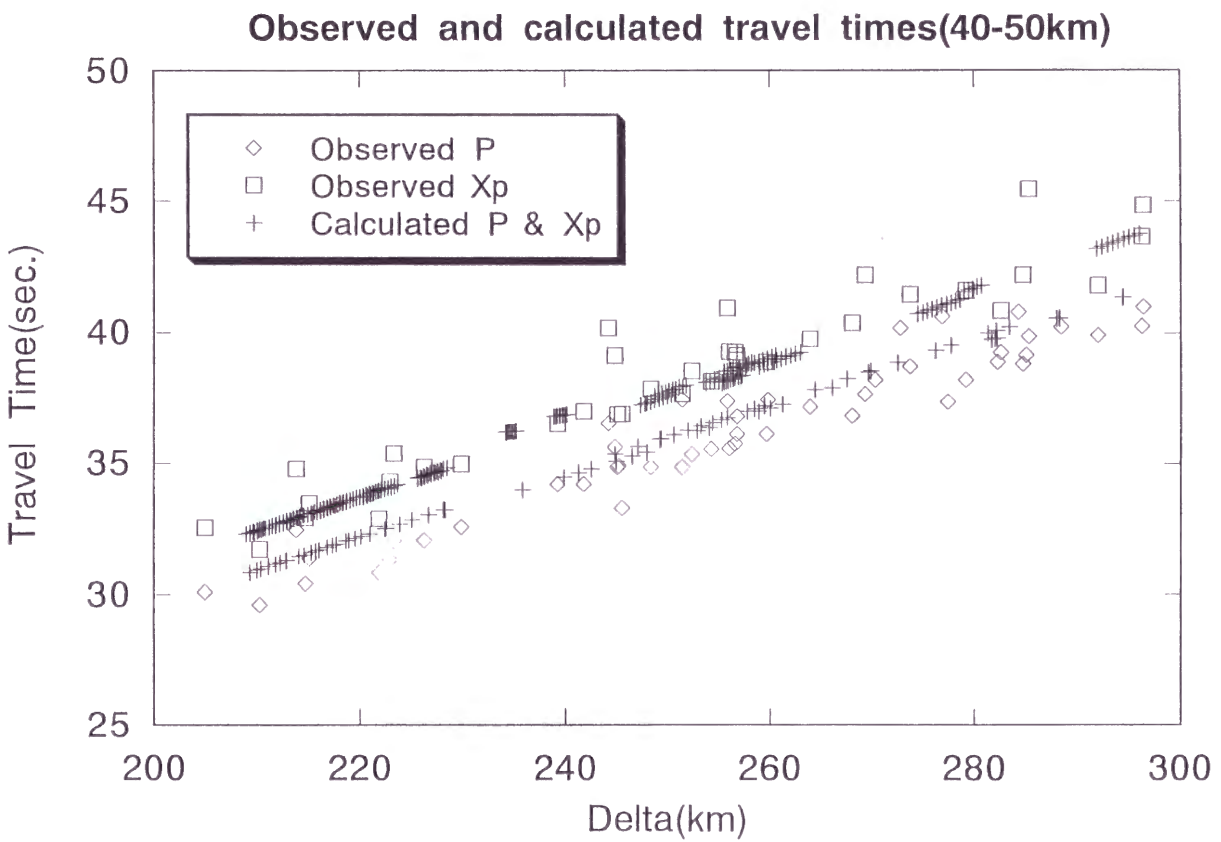
Observed and calculated travel times(40-50km)
Observed P
Observed Xp
Calculated P & Xp
Travel Time(sec.)
Delta(km)
50
45
40
35
30
25
200
220
240
260
280
300

Fig. 2-16

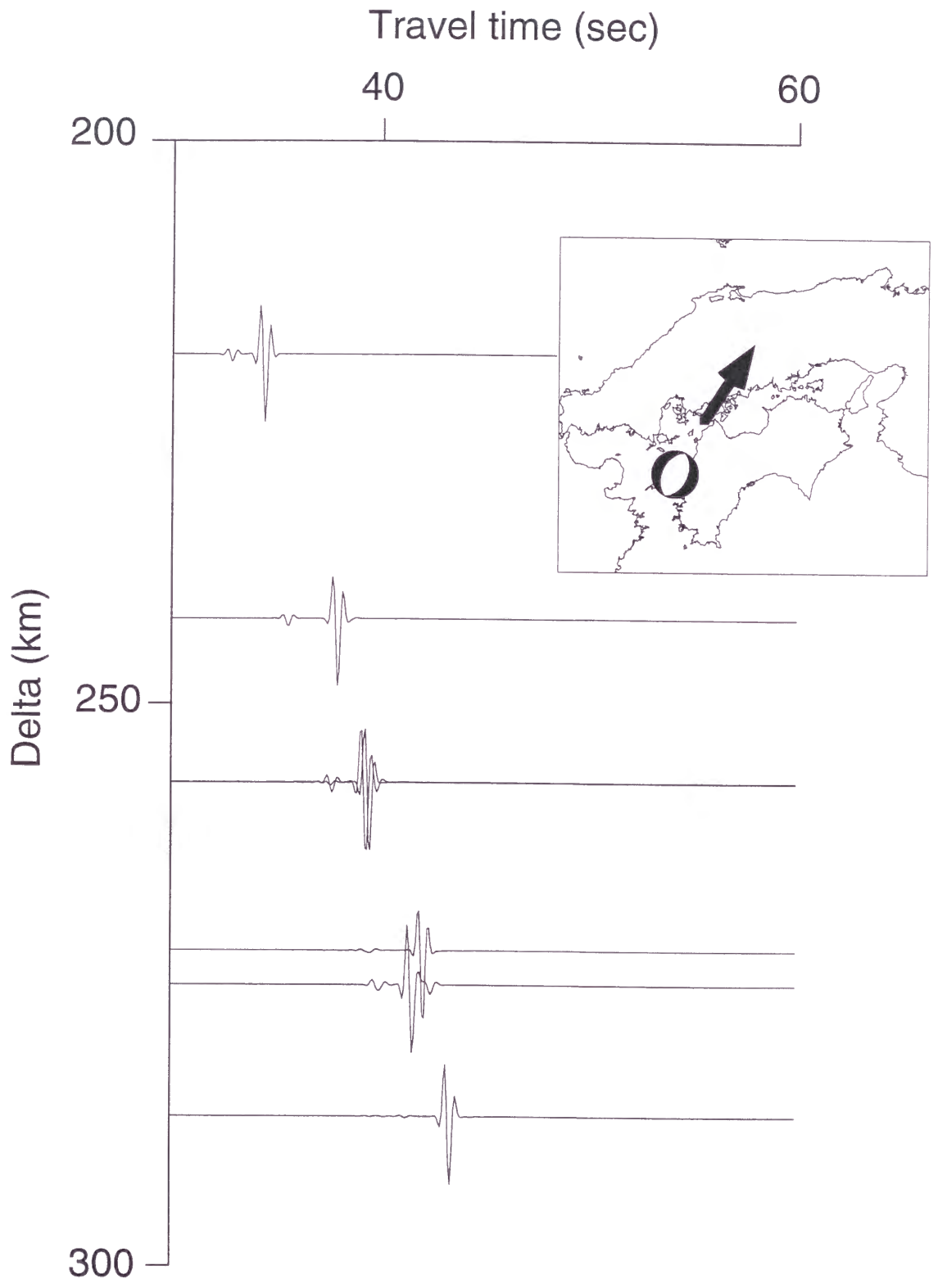

Fig. 2-17

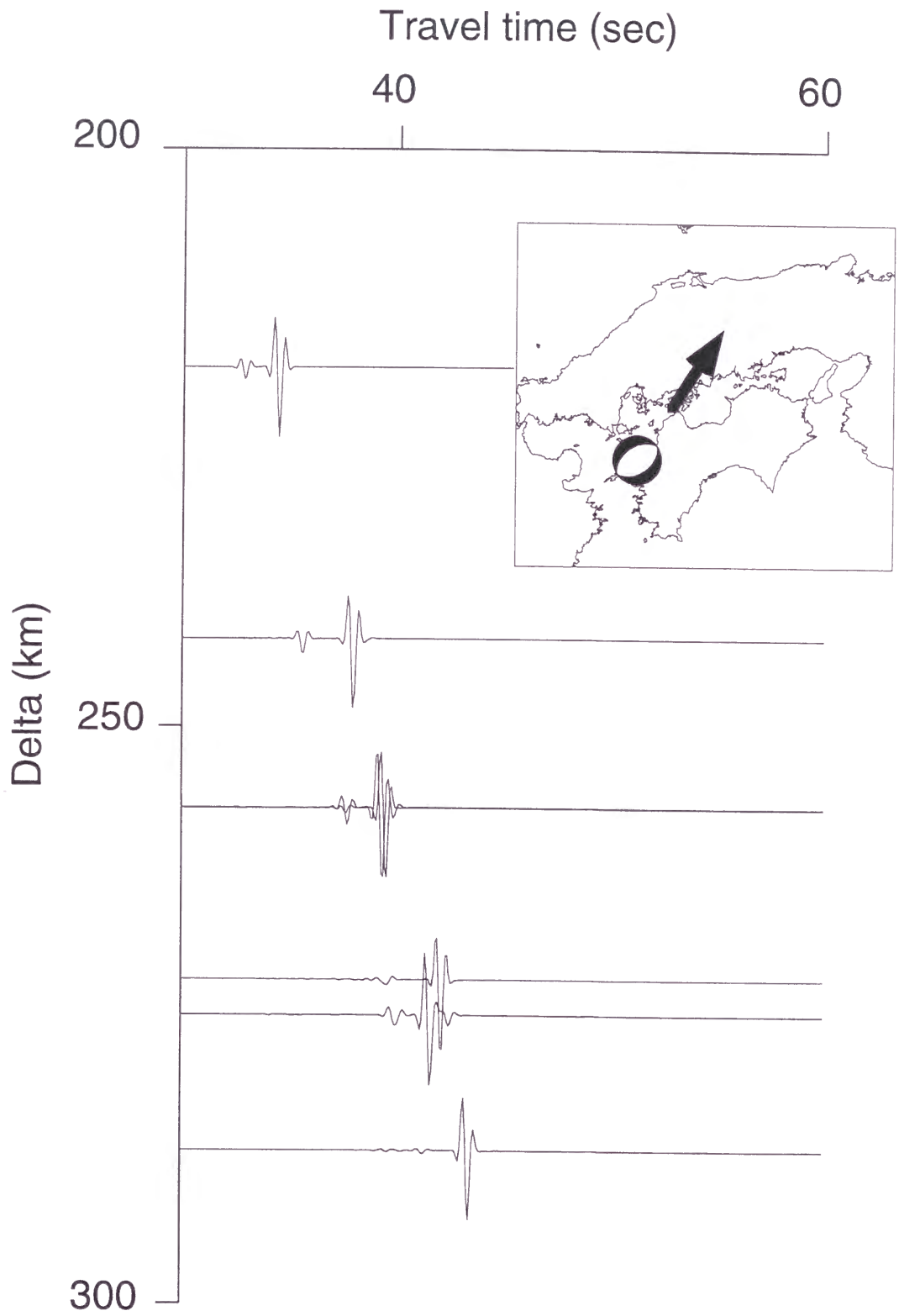

Fig. 2-18

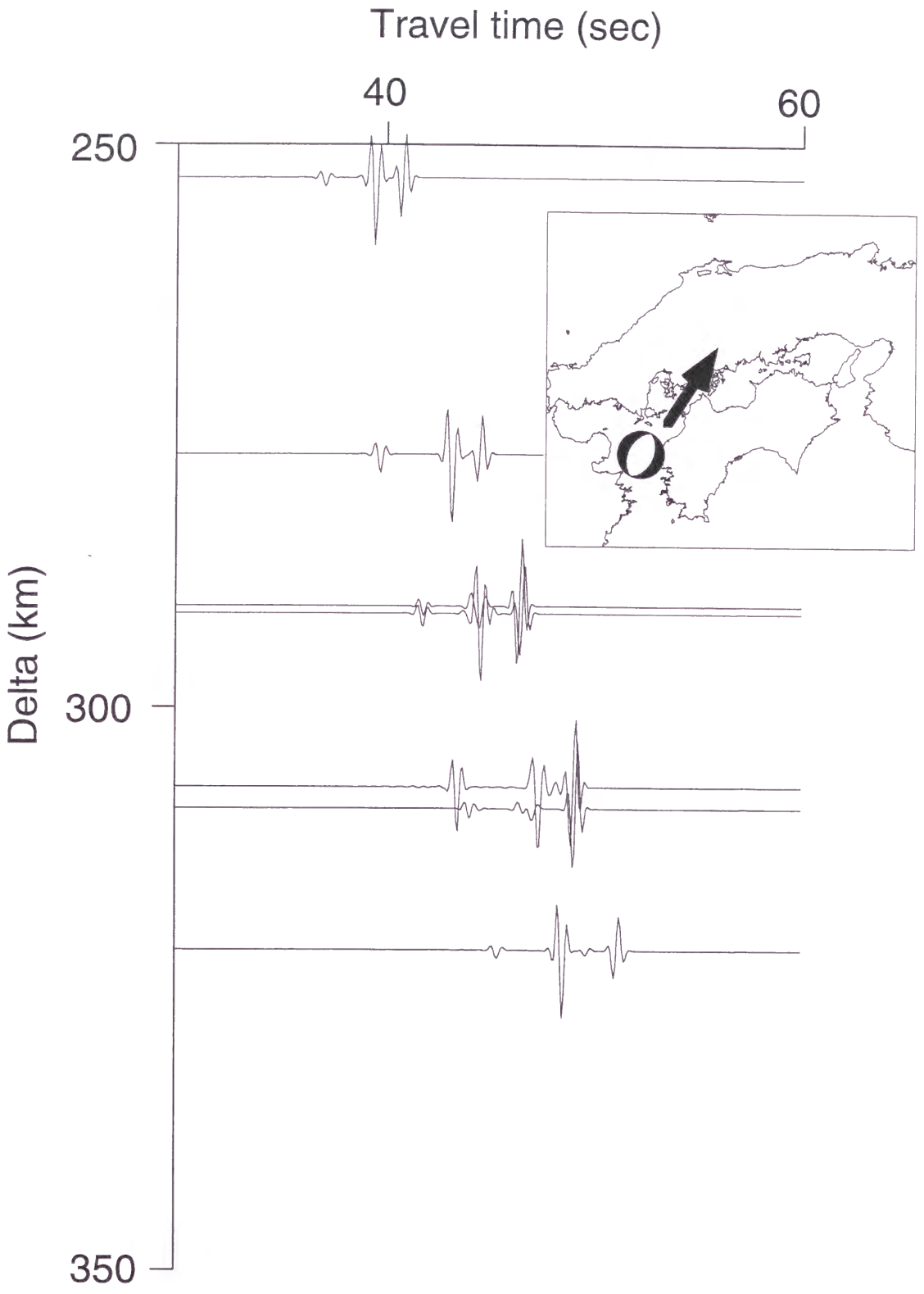

Fig. 2-19

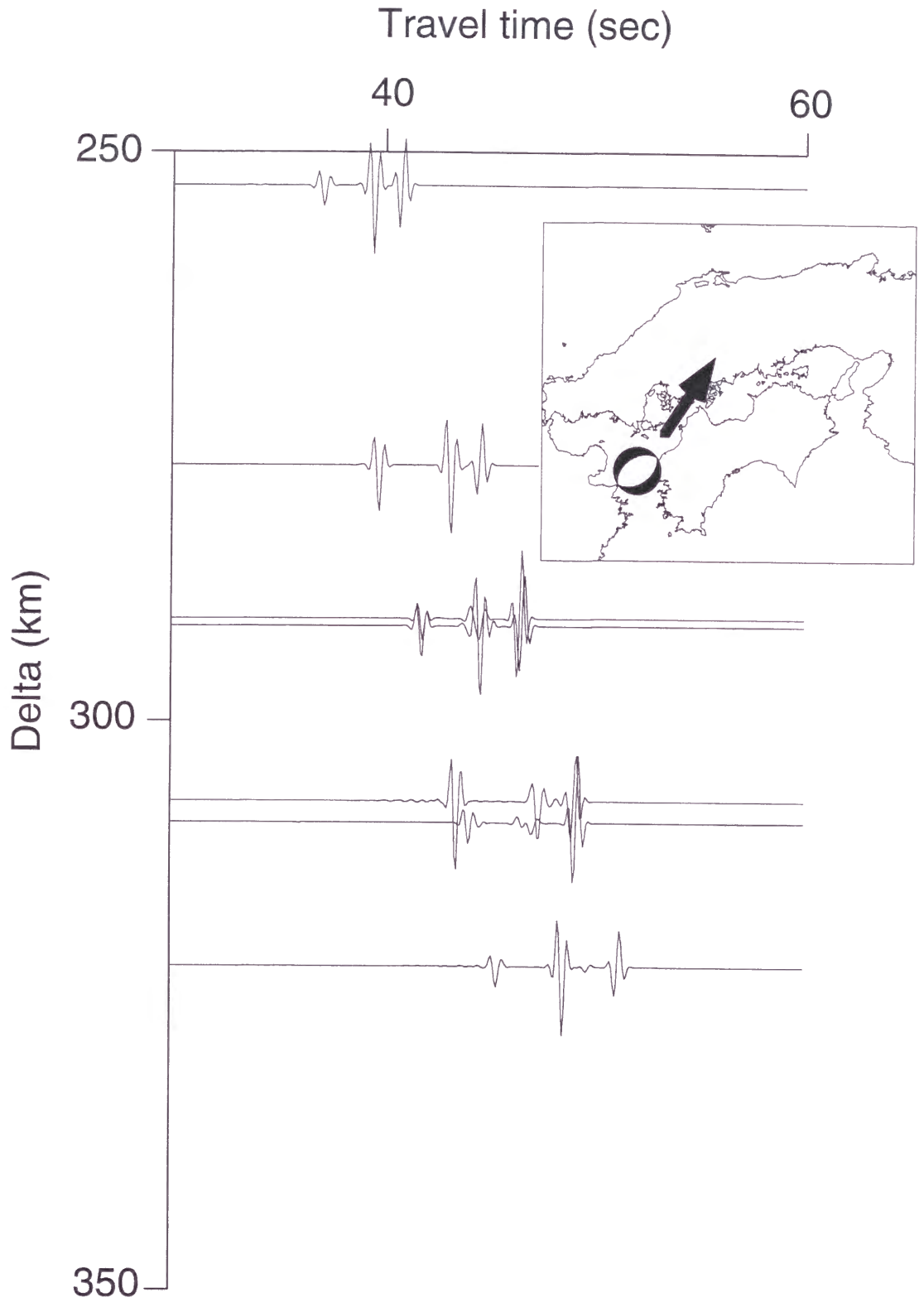

Fig. 2-20

Fig.2-21a

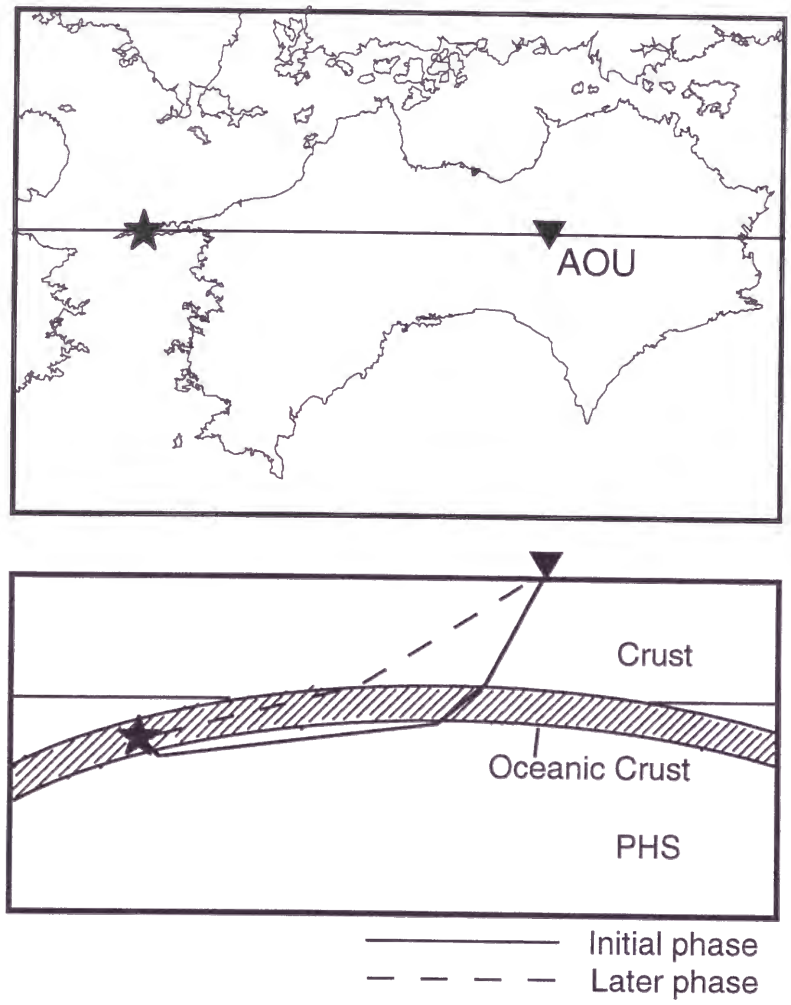

Fig. 2-21b

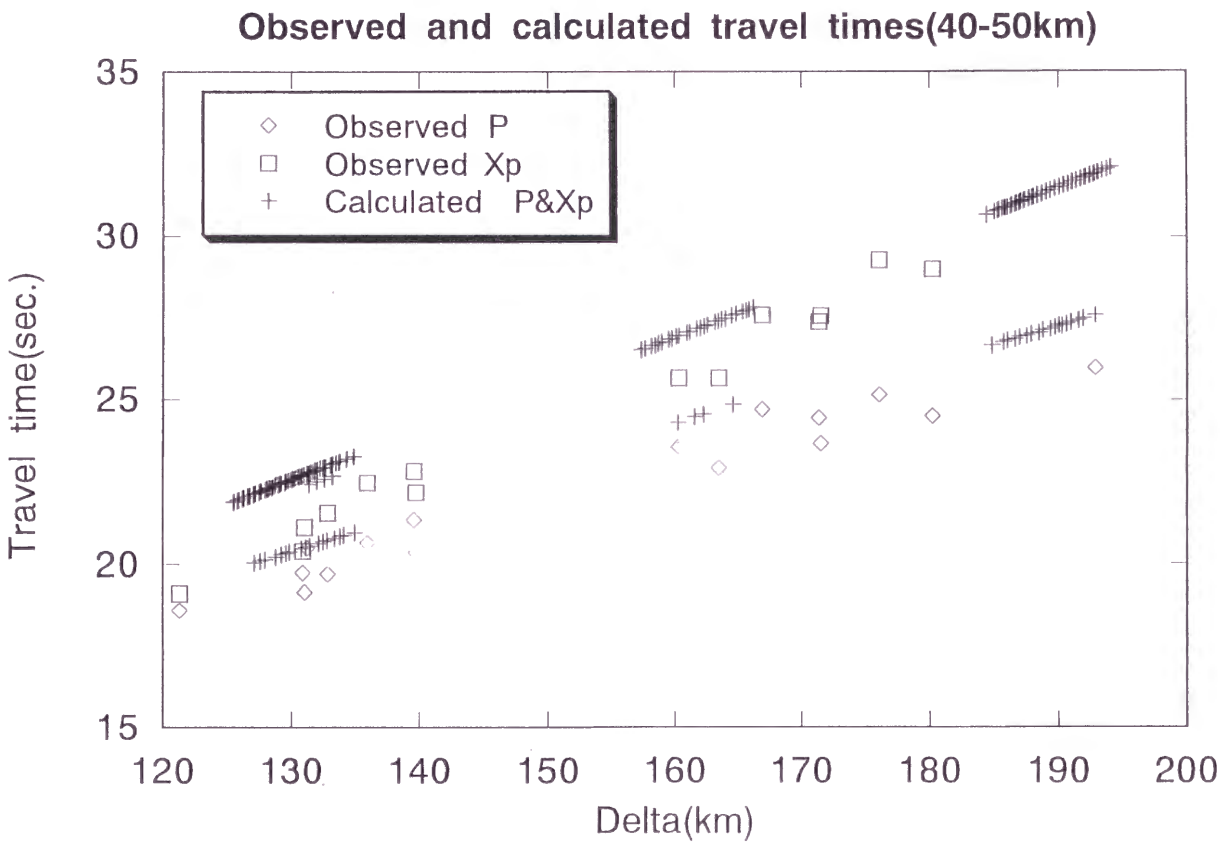
Observed and calculated travel times(40-50km)
Observed P
Observed Xp
Calculated P&Xp
Travel time(sec.)
Delta(km)
35
30
25
20
15
120
130
140
150
160
170
180
190
200

Fig.2-22

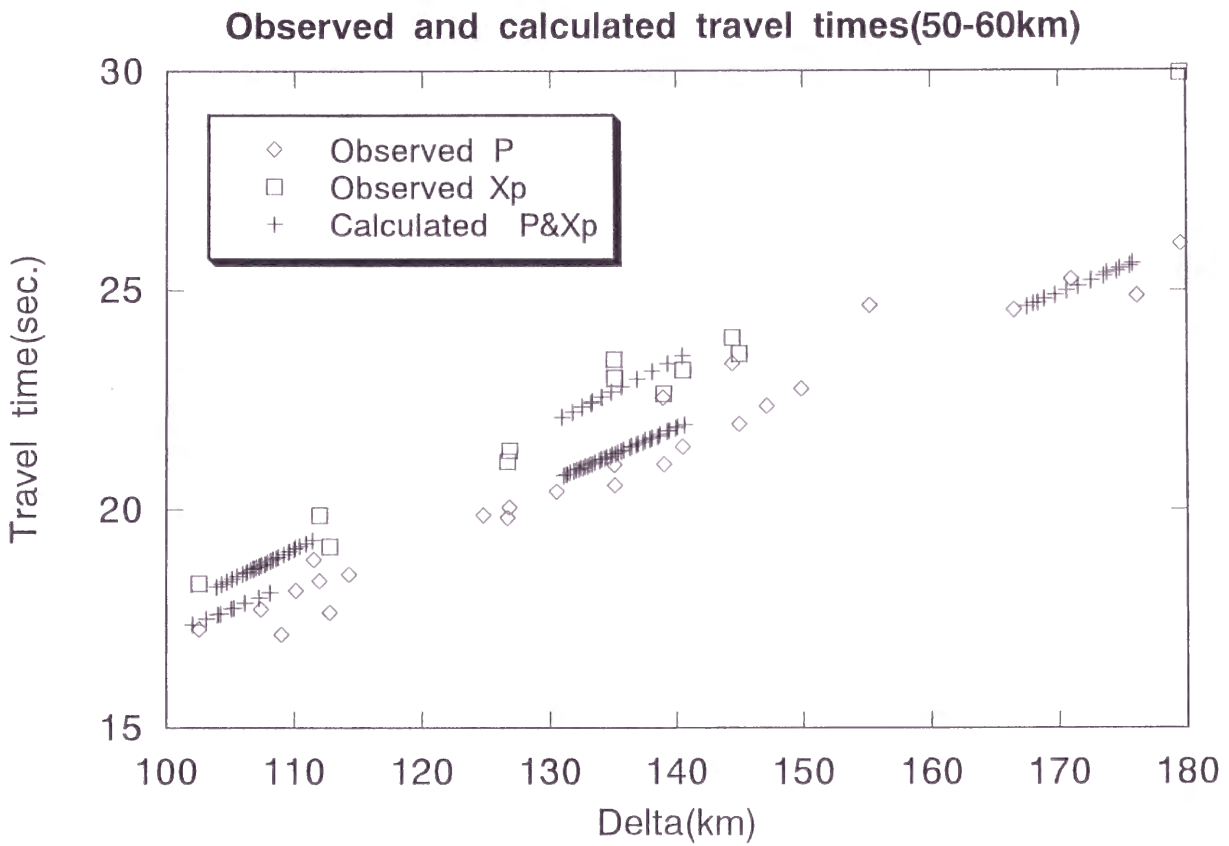
Observed and calculated travel times(50-60km)
Observed P
Observed Xp
Calculated P&Xp
Travel time(sec.)
Delta(km)
30
25
20
15
100
110
120
130
140
150
160
170
180

Fig.2-23

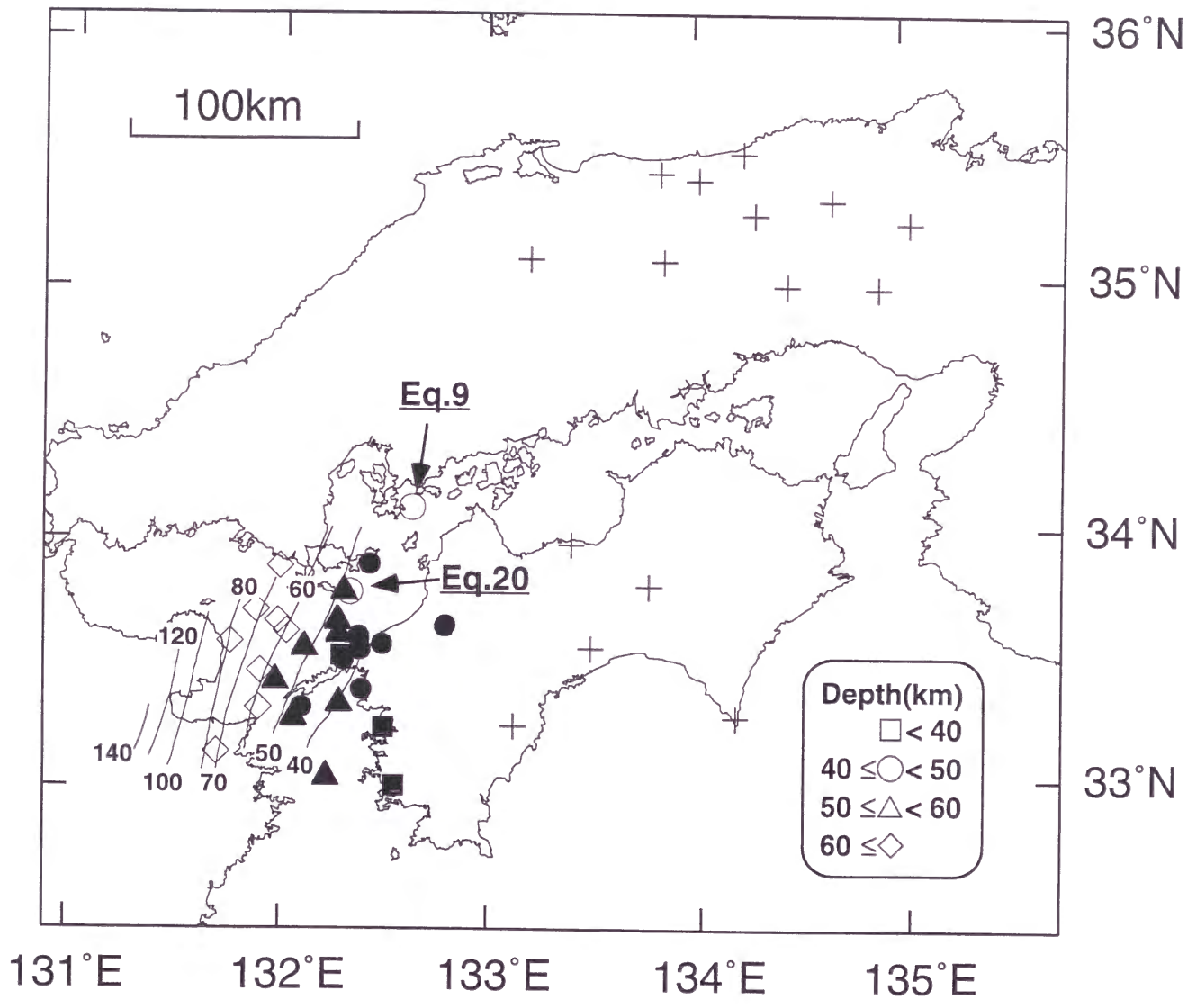
100km
36°N
35°N
34°N
33°N
131°E
132°E
133°E
134°E
135°E
Eq.9
Eq.20
80
60
120
140
100
70
50
40
Depth(km)
□< 40
40 ≤○< 50
50 ≤△< 60
60 ≤◇

Fig. 2-24

(a)

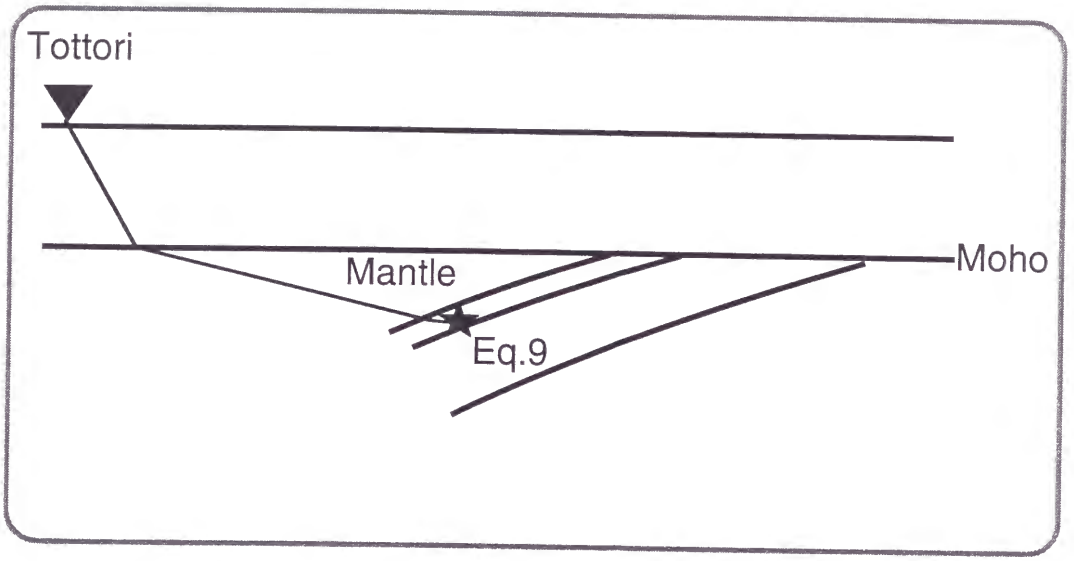
Tottori
Mantle
Moho
Eq.9

(b)

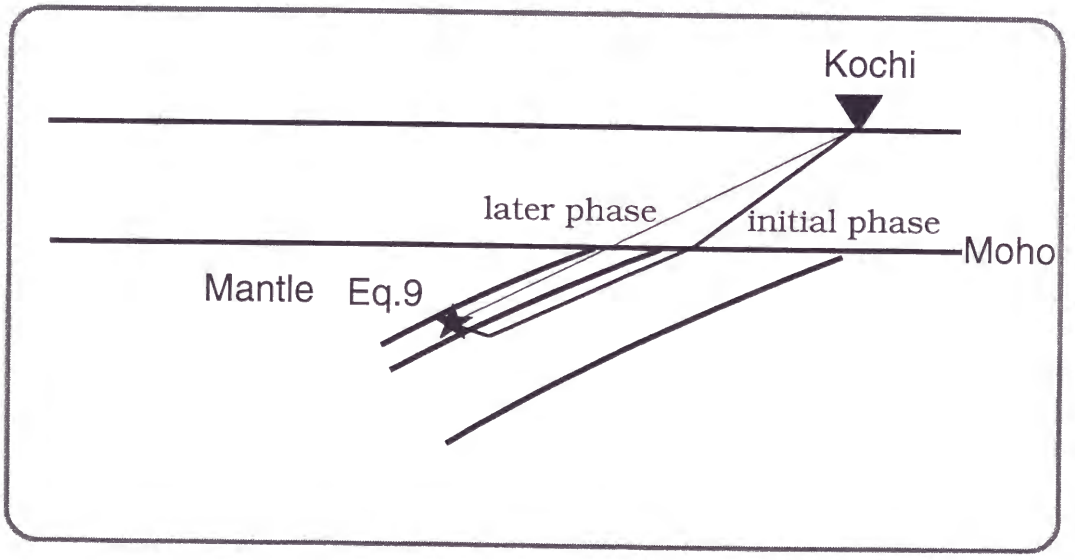
Kochi
later phase
initial phase
Moho
Mantle
Eq.9

Fig.2-25

(a)

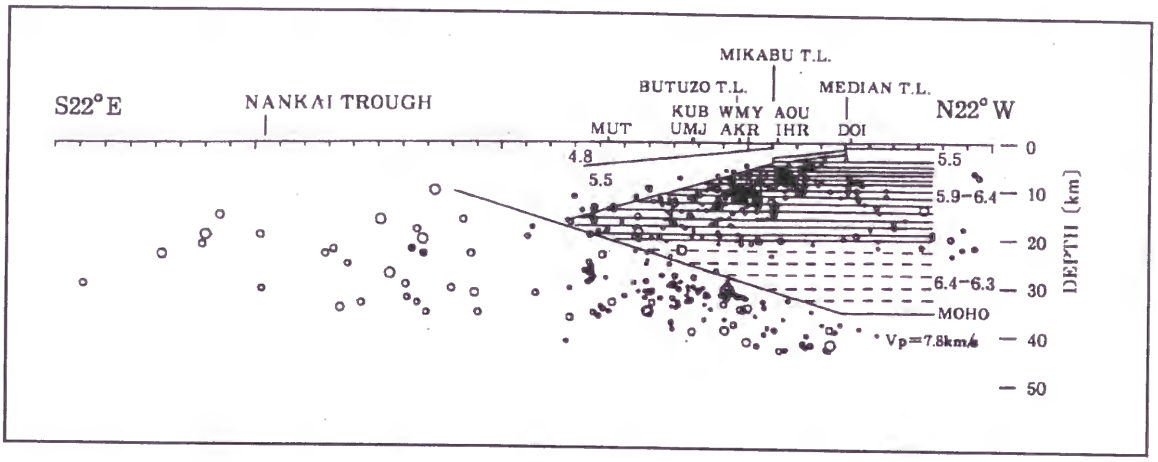
MIKABU T.L.
BUTUZO T.L.
MEDIAN T.L.
S22° E
NANKAI TROUGH
KUB WMY AOU
MUT UMJ AKR IHR DOI
N22° W
4.8
5.5
5.5
5.9–6.4
6.4–6.3
MOHO
Vp=7.8km/s
0
10
20
30
40
50
DEPTH (km)

(b)

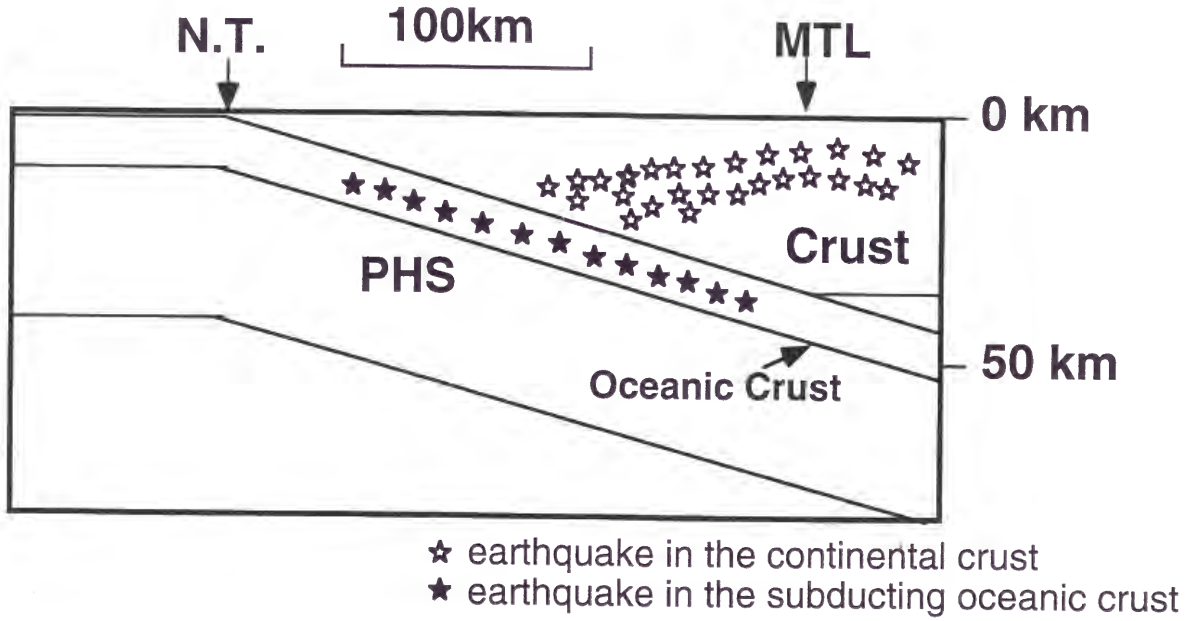
N.T.
100km
MTL
0 km
Crust
PHS
50 km
Oceanic Crust
☆ earthquake in the continental crust
★ earthquake in the subducting oceanic crust

Fig. 2-26

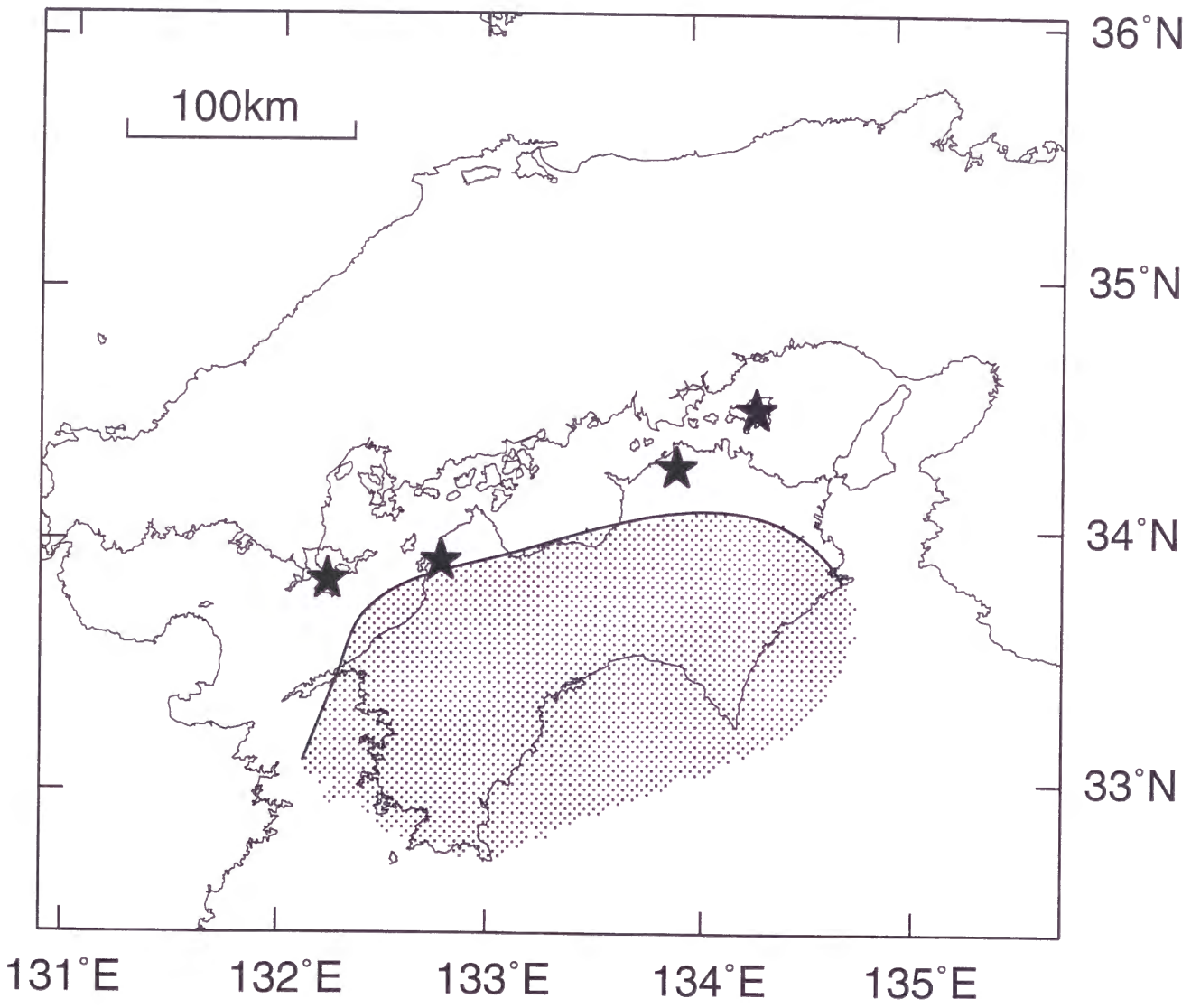

Fig. 2-27

Table 1. Earthquake list used in sections 2.2.1 and 2.2.2

Eq.	Origin time (JST)					Hypocenter			Mag.
	Y	*M*	*D*	*h*	*m*	*Lon.(°E)*	*Lat.(°N)*	*Depth(km)*	
1	1983	8	18	16	58	132.288	33.326	53.96	3.8
2	1983	10	1	0	20	132.005	33.878	69.98	4.4
3	1984	1	26	5	47	132.036	33.616	66.74	4.0
4	1984	2	10	23	2	132.391	33.383	44.63	3.7
5	1984	4	4	14	3	131.771	33.574	81.18	3.9
6	1984	4	14	9	47	131.710	33.132	98.68	4.5
7	1984	10	4	23	7	132.313	33.771	52.82	4.3
8	1984	12	26	10	0	132.228	33.032	51.35	4.2
9	1985	3	5	18	36	132.634	34.113	43.75	4.0
10	1985	5	12	23	9	132.108	33.311	41.04	4.2
11	1985	5	23	8	14	132.549	32.999	26.14	4.2
12	1985	5	30	21	18	132.430	33.886	43.39	4.5
13	1985	5	31	11	1	132.382	33.584	47.25	4.3
14	1985	6	1	18	11	132.379	33.596	46.26	4.1
15	1985	8	11	12	26	132.790	33.636	42.41	3.6
16	1985	11	20	7	38	132.290	33.601	51.17	4.1
17	1985	11	22	7	35	132.388	33.543	46.19	4.0
18	1986	5	28	18	18	131.996	33.658	74.20	4.3
19	1986	8	27	9	26	132.499	33.230	34.50	4.1
20	1986	8	28	11	52	132.337	33.774	40.19	4.2
21	1986	11	9	8	32	132.492	33.564	41.50	4.3
22	1987	4	18	9	3	131.893	33.702	79.26	4.5
23	1987	4	20	0	40	131.913	33.458	71.29	4.2
24	1987	6	6	14	6	131.986	33.413	59.84	4.2
25	1987	12	22	18	14	132.281	33.652	50.46	4.0
26	1988	1	1	4	3	132.298	33.519	39.33	4.8
27	1988	1	31	15	19	131.906	33.309	63.36	4.4
28	1988	2	8	2	9	132.074	33.268	55.33	3.9
29	1988	2	8	22	0	132.124	33.547	53.92	4.0
30	1988	3	3	5	28	132.307	33.501	48.10	4.3

Table 2. Earthquake list used in section 2.2.3

Eq.	Origin time (JST)					Hypocenter			Mag.
	Y	*M*	*D*	*h*	*m*	*Lon.(°E)*	*Lat.(°N)*	*Depth(km)*	
1	1983	02	08	13	50	33.9615	134.3078	38.93	3.5
2	1983	07	18	14	29	33.5589	134.2490	42.65	3.4
3	1984	02	27	22	15	33.3270	133.4781	26.68	3.0
4	1984	07	07	21	10	33.2400	134.3339	29.69	3.1
5	1984	07	28	18	34	33.5557	133.4966	32.65	3.5
6	1984	12	22	02	58	34.0189	134.3748	36.81	2.6
7	1985	02	28	08	41	33.5422	133.6307	28.81	3.1
8	1985	03	27	00	33	33.6875	133.5936	19.46	2.9
9	1985	03	30	05	52	33.8805	133.6027	42.87	2.9
10	1985	04	17	19	22	33.5001	133.1303	31.15	4.6
11	1985	04	25	04	40	33.6122	133.0162	37.63	3.8
12	1985	05	20	21	52	33.5429	133.7114	31.79	3.2
13	1986	01	03	22	47	33.8806	134.3763	34.04	3.2
14	1986	01	05	22	02	33.3450	133.5496	22.11	3.5
15	1986	05	02	20	02	33.7261	134.1514	30.42	5.2
16	1986	05	02	21	21	33.7267	134.1498	30.38	4.5
17	1986	06	06	19	40	33.9603	133.6191	41.66	4.0
18	1987	05	12	17	32	33.9495	134.2411	38.93	2.8
19	1987	06	28	22	13	33.9824	133.5830	40.56	3.6
20	1988	01	01	10	54	33.7968	133.7809	35.65	2.7
21	1988	01	23	14	16	33.9981	134.2228	40.77	3.0
22	1988	03	05	14	01	33.3265	134.3509	26.07	2.7
23	1988	04	30	02	51	33.4062	134.2792	27.32	2.5
24	1988	08	26	00	32	33.7484	133.2454	37.20	3.1
25	1988	10	26	11	40	33.1139	133.5584	25.37	4.0
26	1988	11	16	07	43	33.8785	133.0688	37.63	2.7

Table 3. Q-structure used in Gaussian Beam method

Layer	Q_p	Q_s
Surface layer	1000	450
Upper crust	1000	450
Lower crust	1000	450
Mantle	130	60
Oceanic crust	1000	450
Slab	1200	550